1	Title: Cnidarian hair cell development illuminates an ancient role for the class IV POU
2	transcription factor in defining mechanoreceptor identity
3	
4	Authors:
5	Ethan Ozment ¹ (<u>etozment@uark.edu</u>)
6	Arianna N. Tamvacakis ¹ (<u>ariannat@uark.edu</u>)
7	Jianhong Zhou ¹ (jxz011@uark.edu)
8	Pablo Yamild Rosiles-Loeza ² (<u>pablo.rosiles@cinvestav.mx</u>)
9	Esteban Elías Escobar-Hernandez ² (<u>esteban.escobar@cinvestav.mx</u>)
10	Selene L. Fernandez-Valverde ² (<u>selene.fernandez@cinvestav.mx</u>)
11	Nagayasu Nakanishi ^{1*} (<u>nnakanis@uark.edu</u>)
12	
13	¹ Department of Biological Sciences, University of Arkansas, 850 West Dickson St. Fayetteville
14	Arkansas, 72701
15	² Unidad de Genómica Avanzada (Langebio), Centro de Investigación y de Estudios Avanzados
16	del IPN, Irapuato, México
17	
18	* Correspondence:
19	Nagayasu Nakanishi
20	nnakanis@uark.edu
21	
22	Running title: Cnidarian mechanoreceptor evo-devo
23	
24	Key words: Cnidaria, mechanoreceptor, evo-devo, cell differentiation, Nematostella
25	
26	
27	
28	
29	
30	
31	

Abstract: Although specialized mechanosensory cells are found across animal phylogeny, early evolutionary histories of mechanoreceptor development remain enigmatic. Cnidaria (e.g. sea anemones and jellyfishes) is the sister group to well-studied Bilateria (e.g. flies and vertebrates), and has two mechanosensory cell types – a lineage-specific sensory-effector known as the cnidocyte, and a classical mechanosensory neuron referred to as the hair cell. While developmental genetics of cnidocytes is increasingly understood, genes essential for cnidarian hair cell development are unknown. Here we show that the class IV POU homeodomain transcription factor (POU-IV) – an indispensable regulator of mechanosensory cell differentiation in Bilateria and cnidocyte differentiation in Cnidaria – controls hair cell development in the sea anemone cnidarian Nematostella vectensis. N. vectensis POU-IV is postmitotically expressed in tentacular hair cells, and is necessary for development of the apical mechanosensory apparatus, but not of neurites, in hair cells. Moreover, it binds to deeply conserved DNA recognition elements, and turns on a unique set of effector genes – including the transmembrane-receptor-encoding gene polycystin 1 – specifically in hair cells. Our results suggest that POU-IV directs differentiation of cnidarian hair cells and cnidocytes via distinct gene regulatory mechanisms, and support an evolutionarily ancient role for POU-IV in defining the mature state of mechanosensory neurons.

Introduction:

One of the most fundamental sensory cell types that emerged in animal evolution is the mechanosensory cell – the specialized sensory epithelial cell that transduces mechanical stimuli (e.g. water vibration) into internal signals. These signals are then communicated, usually via the nervous system, to effector cells (e.g. muscle cells) to elicit behavioral and/or physiological responses of the organism. Indeed, specialized mechanosensory cells are found across diverse animal lineages, from vertebrate hair cells, cephalopod angular acceleration receptors, to statocyst cells of enidarian jellyfish and etenophores. Typically, a mechanosensory cell bears an apical mechanosensory apparatus consisting of a single non-motile cilium surrounded by a circle of rigid microvilli with actin rootlets (i.e. stereovilli, or stereocilia), and extends basal neuronal processes that connect to the nervous system (reviewed in (Beisel et al., 2008, Budelmann, 1989, Manley and Ladher, 2008)).

The structure of animal mechanosensory cells is not uniform, however (reviewed in (Bezares-Calderon et al., 2020)). For instance, insect and cephalopod mechanosensory cells lack stereovilli (Jarman, 2002, Budelmann, 1989), while the apical mechanosensory apparatus of vertebrate hair cells is differently shaped, having a cilium on one side of a group of stereovilli of graded lengths, with the stereovilli next to the cilium being the longest (Fain, 2003). The observed morphological diversity in mechanosensory cells of distantly related animals has led to a fundamental question in animal mechanoreceptor evolution: whether the diversity evolved by divergence from a common ancestral form (Beisel et al., 2008, Jørgensen, 1989, Schlosser, 2020), or by independent evolution (Coffin et al., 2004, Holland, 2005). Addressing this question requires an understanding of the mechanisms of mechanoreceptor development across disparate groups of animals.

Developmental genetics of mechanosensory cells has been extensively studied in bilaterian models such as vertebrates and flies (reviewed in (Schlosser, 2020, Boekhoff-Falk, 2005, Beisel et al., 2008). Yet, relatively little is known about the genetics of mechanoreceptor development in non-bilaterian, early-evolving animal groups such as Cnidaria (e.g. jellyfish, corals and sea anemones), Ctenophora (combjellies), Placozoa and Porifera (sponges), the knowledge of which is key to defining the ancestral conditions for mechanoreceptor development basal to Bilateria. This baseline knowledge, in turn, is necessary for reconstructing how mechanoreceptors diversified in each lineage. In this paper, we focus on investigating the

development of a fundamental, yet understudied, mechanosensory cell type of Cnidaria – the concentric hair cell.

Cnidaria is the sister group to Bilateria (Medina et al., 2001, Putnam et al., 2007, Hejnol et al., 2009, Erwin et al., 2011), and has two broad classes of mechanosensory cells – cnidocytes (Brinkmann et al., 1996)) and concentric hair cells ((Arkett et al., 1988, Oliver and Thurm, 1996, Holtman and Thurm, 2001); not to be confused with vertebrate hair cells) - that are characterized by an apical mechanosensory apparatus consisting of a single cilium surrounded by a ring of stereovilli. The cnidocyte is the phylum-defining stinging cell type, and additionally contains a cnidarian-specific exocytotic organelle called the cnida (plural: cnidae) which is made up of a capsule enclosing a coiled tubule (reviewed in (Thomas and Edwards, 1991, Lesh-Laurie and Suchy, 1991, Fautin and Mariscal, 1991)). Cnidocytes are abundant in the ectodermal epithelium of cnidarian tentacles, and, upon perceiving mechanical stimuli, discharge cnidae by rapidly everting the coiled tubule to pierce nearby animals for defense and/or prey capture. There is no structural or functional evidence that the cnidocyte transmits sensory information to other cells, but firing of cnidae is thought to be modulated by neurons that innervate cnidocytes through chemical synapses (Westfall, 2004). Thus, the cnidocyte is a cnidarian-specific mechanosensory cell type that – uniquely among animal mechanosensory cells – functions as an effector cell.

The cnidarian hair cell, on the other hand, represents the classical mechanosensory cell type with dedicated sensory-neuronal function. Hair cells are integrated within the ectodermal epithelium of mechanosensory structures, such as gravity-sensors of jellyfishes and tentacles of hydroids and corals (Horridge, 1969, Lyons, 1973, Tardent and Schmid, 1972, Singla, 1975, Hundgen and Biela, 1982). Structurally, the cnidarian hair cell exhibits the stereotypical mechanosensory neuron-like morphology described above, including the apical mechanosensory apparatus and basal neurites that become part of the basiepithelial nerve plexus (Horridge, 1969, Singla, 1975, Singla, 1983, Hundgen and Biela, 1982). Upon stimulation, the hair cells communicate mechanosensory information to other cells by converting mechanical stimuli into internal electrical signals (Arkett et al., 1988, Oliver and Thurm, 1996), and are thought to generate highly coordinated response behaviors such as righting and feeding. Similar to vertebrate hair cells, hair cells of jellyfish gravity-sensors are sensitive to sound and can be lost due to noise trauma (Sole et al., 2016). Cnidarian hair cells show morphological and functional

characteristics that parallel those of mechanosensory cells in other animal lineages, consistent with a deep evolutionary origin or convergent origins.

124

125

126

127

128

129

130

131

132

133

134

135

136

137

138

139

140

141

142

143

144

145

146

147

148

149

150

151

152

153

154

Although genetics of cnidocyte development is increasingly understood (e.g. (Babonis and Martindale, 2017, Richards and Rentzsch, 2015, Richards and Rentzsch, 2014, Wolenski et al., 2013)), that of cnidarian hair cell development remains poorly known. This knowledge gap severely limits our ability to reconstruct the evolutionary histories of mechanoreceptor development within Cnidaria and across the basal branches of the animal tree. A previous study has shown that the class IV POU homeodomain transcription factor (POU-IV or Brn-3)-encoding gene is expressed in the hair-cell-bearing mechanosensory organ called the touch plate in moon jellyfish Aurelia sp. 1 (Nakanishi et al., 2010), consistent with a role in cnidarian hair cell development. Yet, the function of POU-IV in chidarian hair cell development, if any, remains undefined. As the first step towards elucidating the genetic mechanism of cnidarian hair cell development, here we dissect the role of POU-IV in the development of mechanosensory hair cells using the genetically tractable sea anemone cnidarian model Nematostella vectensis. POU-IV is shared by all extant animal groups except for Ctenophora (comb jellies), indicative of early emergence in animal evolution (Gold et al., 2014). POU-IV is absent in choanoflagellates, although the class II POU-like gene has been reported to be present in Mylnosiga fluctuans indicative of a premetazoan origin of POU transcription factors (Lopez-Escardo et al., 2019). As in other POU proteins, POU-IV is characterized by having a bipartite DNA binding domain consisting of the N-terminal POU-specific domain and the C-terminal POU homeodomain (reviewed in (Herr and Cleary, 1995)). In Bilateria, POU-IV-binding DNA elements are POU-IV-class-specific and conserved; mammalian POU-IV proteins Brn3.0 (Brn-3a or POU4F1) and Brn3.2 (Brn-3b or POU4F2) and C. elegans POU-IV protein Unc-86 bind to a highly symmetrical core sequence AT(A/T)A(T/A)T(A/T)AT (Gruber et al., 1997). In bilaterian animal models such as C. elegans, POU-IV is known to function as a terminal selector - a transcription factor that determines mature cell identity via direct regulation of effector genes (reviewed in (Leyva-Diaz et al., 2020). The cell type whose identity is defined by POU-IV across bilaterian lineages is the mechanosensory cell. In humans, mutations at one of the *pou-iv* loci – Brn-3c (Brn3.1 or POU4F3) – have been linked to autosomal dominant hearing loss (Vahava et al., 1998), and in Brn-3c knockout mice, auditory and vestibular hair cells fail to complete

differentiation (Erkman et al., 1996, Xiang et al., 1997b) and are lost by cell death (Xiang et al.,

155 1998). Likewise, in C. elegans, the pou-iv ortholog (unc-86) regulates differentiation of 156 mechanosensory touch cells (Chalfie and Sulston, 1981, Chalfie and Au, 1989, Finney and 157 Ruvkun, 1990, Duggan et al., 1998). In addition to its role in mechanoreceptor differentiation, 158 POU-IV defines the identity of olfactory chemosensory neurons in *Drosophila* (Clyne et al., 159 1999), as well as retinal ganglion cells (Brn-3b; (Erkman et al., 1996, Gan et al., 1996) and 160 subsets of sensory and CNS neurons in mice (Brn-3a; (Serrano-Saiz et al., 2018, McEvilly et al., 161 1996, Xiang et al., 1996). In Cnidaria, POU-IV is expressed not only in the developing 162 mechanoreceptor of Aurelia sp. 1 (Nakanishi et al., 2010) as described above, but also in the 163 statocysts of the freshwater hydrozoan jellyfish Craspedacusta sowerbii (Hroudova et al., 2012). 164 Also, POU-IV is required for postmitotic differentiation of cnidocytes, as well as elav::mOrange 165 neurons, in Nematostella vectensis (Tourniere et al., 2020). Consistent with cnidarian POU-IV 166 being a terminal selector, a genome-wide analysis of differential gene expression between POU-167 IV knockout mutant N. vectensis and their siblings indicates that POU-IV controls the expression 168 of effector genes that define mature neural identity, such as those involved in ion channel activity 169 (Tourniere et al., 2020). However, it remains unclear if cnidarian POU-IV directly regulates 170 effector gene expression, as expected for a terminal selector. Furthermore, although POU-IV 171 recognition element-like sequences have been previously identified in the N. vectensis genome 172 based on sequence similarity to bilaterian POU-IV-binding motifs (Sebe-Pedros et al., 2018), 173 cnidarian POU-IV recognition elements have not be experimentally defined, and consequently, 174 whether the conservation of POU-IV-binding sequence extends beyond Bilateria remains vague. 175 Sea anemones together with corals form the clade Anthozoa, which is sister to the 176 Medusozoa – a group characterized by typically having a pelagic medusa (jellyfish) stage -177 consisting of Staurozoa, Hydrozoa, Scyphozoa and Cubozoa (Collins et al., 2006, Zapata et al., 178 2015). Sea anemones have multicellular mechanosensory structures, known as the hair bundle 179 mechanoreceptors, in the ectoderm of the oral feeding tentacles (Mire-Thibodeaux and Watson, 180 1994, Mire and Watson, 1997, Watson et al., 1997). A hair bundle mechanoreceptor consists of a 181 central sensory cell surrounded by peripheral support cells (Figure 1 – Figure supplement 1). The 182 central sensory cell exhibits morphological hallmarks of concentric hair cells, with an apical 183 cilium surrounded by stereovilli, and basal neurites. Support cells contribute stereovilli or 184 microvilli that encircle the apical ciliary-stereovillar structure of the central hair cell. The cilium 185 and stereovilli of the central cell and stereovilli/microvilli of support cells are interconnected by

lateral linkages; in addition, extracellular linkages have been observed between the tips of stereovilli/microvilli of support cells, resembling the tip links of vertebrate mechanosensory hair cells (Watson et al., 1997). The apical sensory apparatus, or the hair bundle, of the mechanoreceptor thus consists of the cilium and stereovilli of the central hair cell and the peripheral stereovilli/microvilli of support cells (Mire and Watson, 1997). We note that in the literature, the support cells of hair bundle mechanoreceptors are sometimes referred to as hair cells (e.g. (Mire and Watson, 1997)). In this paper, in accordance with the morphological definition of cnidarian hair cells, a *hair cell* refers to the central sensory cell of the hair bundle mechanoreceptor, and a *support cell* refers to the cell that abuts the central sensory cell and contributes peripheral stereovilli/microvilli to the hair bundle.

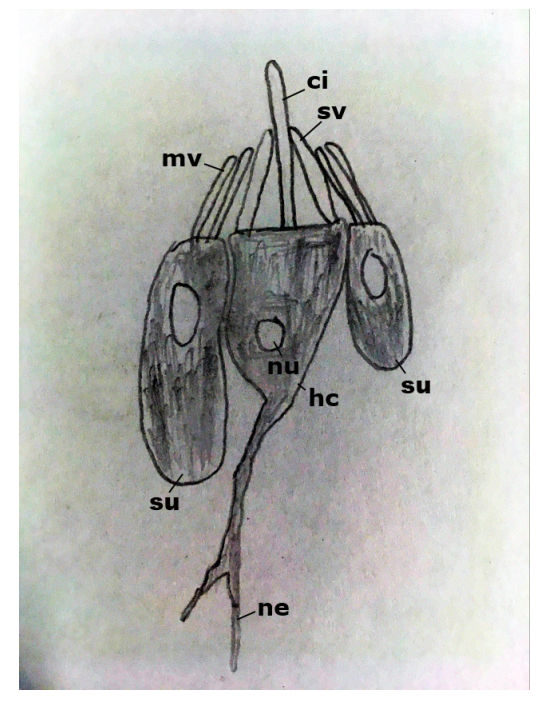


Figure 1 - Figure supplement 1: Diagram of the hair bundle mechanoreceptor of sea anemones.

A cilium (ci) extends from a central hair cell (hc). It is encircled by stereovilli (sv), also produced by the hair cell, as well as smaller-diameter microvilli (mv) contributed by surrounding support cells (su), forming a cone-shaped structure. Abbreviations: ne neurites; nu nucleus

In this report, we use the starlet sea anemone *N. vectensis* to investigate the role of POU-IV in the development of cnidarian hair cells. *N. vectensis* is a convenient model for studies of

mechanisms of cnidarian development because of the availability of the genome sequence (Putnam et al., 2007) and a wide range of powerful molecular genetic tools including CRISPR-Cas9 genome editing (Ikmi et al., 2014, Nakanishi and Martindale, 2018). During embryogenesis, N. vectensis gastrulates by invagination to form an embryo consisting of ectoderm and endoderm separated by the extracellular matrix known as the mesoglea (Kraus and Technau, 2006, Magie et al., 2007). The blastopore becomes the mouth/anus ("oral") opening of the animal (Fritzenwanker et al., 2007, Lee et al., 2007). The embryo develops into a free-swimming, ciliated planula larva, which transforms into a polyp with circum-oral tentacles that house mechanosensory hair cells in the ectoderm (Figure 1 - Figure supplement 2; (Nakanishi et al., 2012, Watson et al., 2009)). The polyp then grows and reaches sexual maturity. Previous studies have indicated that hair bundles of *N. vectensis* polyps are indeed sensitive to movement of surrounding water (Watson et al., 2009), and that stereovilli/microvilli of hair bundles express TRP (Transient Receptor Potential)-like cation channels (Mahoney et al., 2011) and a putative extracellular linkage component cadherin 23 (Watson et al., 2008). In the present work, we provide evidence that POU-IV regulates postmitotic differentiation of hair cells by directly activating effector genes that define mature cell identity.

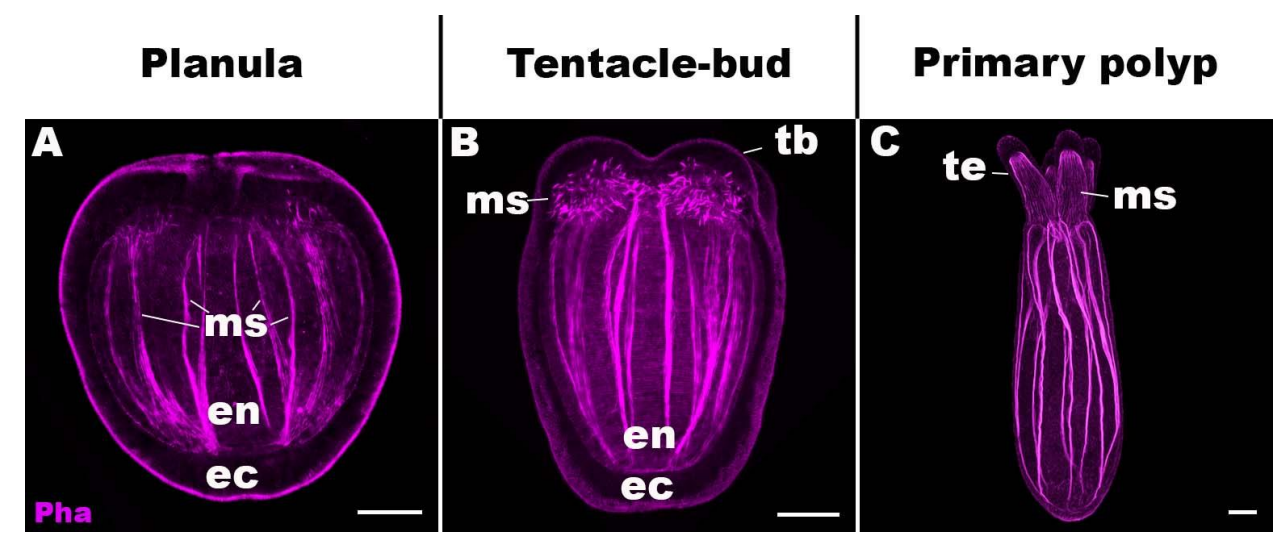


Figure 1 - Figure supplement 2: Life cycle transition in the sea anemone cnidarian

Nematostella vectensis

205

206

207

208

209

210

211

212

213

214

215

216

217

218

219

220

221222

223

224

225

226

Confocal sections of *Nematostella vectensis* at metamorphosis from a free-swimming planula (A; 3-5 days-post-fertilization (dpf)), through the tentacle-bud stage (B; 5-7 dpf), into a primary polyp (C; 7-10 dpf). Filamentous actin is labeled with phalloidin (Pha). All panels show side

227 views of the animal with the oral pole facing up. A: The planula consists of ectoderm (ec) and 228 endoderm (en) separated by an extracellular matrix, and develops muscle fibers (ms) in the 229 endoderm. B: At the tentacle-bud stage, four tentacle primordia known as the tentacle buds (tb) 230 emerge in the circumoral ectoderm. C: Four primary tentacles (te) and the body column then 231 elongate along the oral-aboral axis, forming a primary polyp. Scale bar: 50 µm 232 233 **Results:** 234 Sea anemone hair cell has an apical cilium surrounded by a circle of stereovilli and extends 235 basal neuronal processes. 236 We first examined the structure of hair cells in the oral tentacles of the sea anemone 237 Nematostella vectensis at the primary polyp stage by light and electron microscopy. We used 238 phalloidin to label F-actin enriched in stereovilli of hair cells, and the lipophilic dye DiI to label 239 the plasma membrane of hair cells. Hair cells are an epithelial cell type whose cell body is pear-240 shaped and occurs exclusively in the superficial stratum of pseudostratified ectoderm in oral 241 tentacles (Figure 1). The hair cell has an apical cilium surrounded by 8 large-diameter stereovilli 242 that extend actin filament-containing rootlets into the cytoplasm (Figure 1B-I). In primary polyps, 243 the apical cilium is 10-15 µm-long; stereovilli are 3-5 µm-long and 200-400 nm in diameter; 244 stereovillar rootlets are 2-3 µm-long. Electron-lucent vesicles ranging from 50-100 nm in 245 diameter are abundant in the cytoplasm of a hair cell (Figure 11). Stereovilli of a hair cell are 246 encircled by smaller-diameter microvilli (80-150 nm) contributed by adjacent support cells that 247 are enriched in electron-dense vacuoles in the apical cytoplasm (Figure 1E-I). This multicellular 248 apical sensory apparatus, consisting of the cilium and stereovilli of the hair cell surrounded by 249 stereovilli/microvilli of support cells, constitutes the hair bundle (Mire and Watson, 1997). A 250 subset of cnidocytes – nematocytes but not anthozoan-specific spirocytes – forms a 251 morphologically similar apical mechanosensory apparatus known as the ciliary cone (Fautin and 252 Mariscal, 1991); however, the ciliary cone of tentacular nematocytes in N. vectensis is less 253 pronounced than that of hair cells, and consists of a single cilium surrounded by short microvilli 254 (2-2.5 µm long) that lack actin rootlets (Figure 1 - Figure supplement 3). Basally, a hair cell 255 extends thin neuronal processes that likely form synapses with the tentacular nerve net and/or 256 longitudinal muscle fibers located at the base of the ectodermal epithelium alongside mesoglea 257 (Figure 1C, E, G).



261

262

263

264

265

266

267

268

269

270

271

272

273

274

275

276

277

278

279

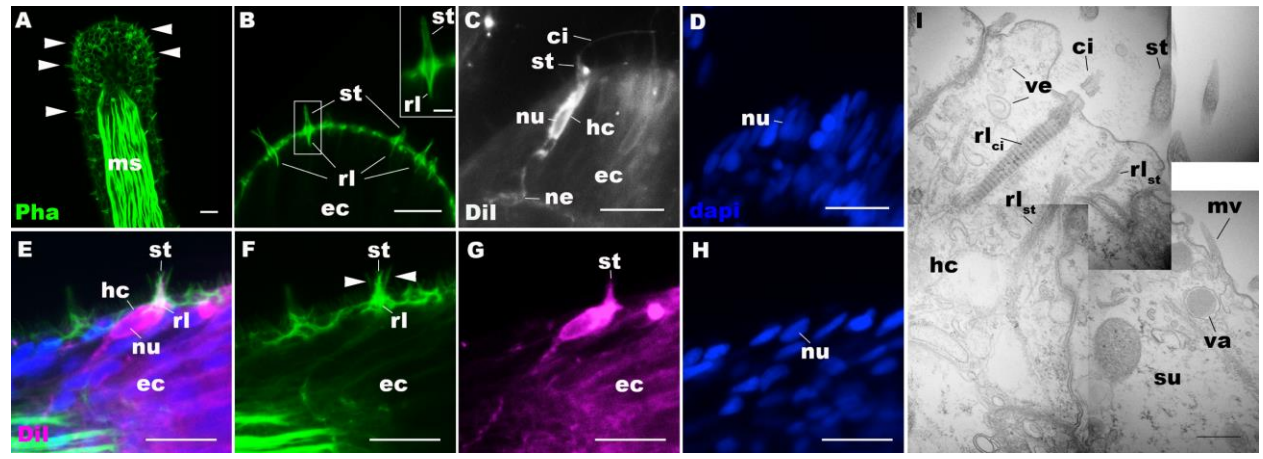


Figure 1: Morphology of sea anemone hair cells.

A-F: Confocal sections of oral tentacles of N. vectensis at the primary polyp stage. Filamentous actin is labeled with phalloidin (Pha), and nuclei are labeled with DAPI (dapi). DiI is used to label cell membrane of a subset of hair cells. In A, the distal end of the tentacle is to the top, and in B-I, the apical surface of the ectodermal epithelium is to the top. A: sections through the tentacle. Numerous hair bundles (arrowheads) are evident on the tentacle surface. B: sections through the hair bundles at the tentacle tip, showing stereovilli (st) and their prominent rootlets (rl) of central hair cells. C-D: sections through a DiI-labeled hair cell (hc) at the tentacle tip. Note that the hair cell has an apical cilium (ci) surrounded at its base by stereovilli (st), and basally extended thin neurites (ne). An empty space within the cell body shows the location of a nucleus (nu), as evidenced by DAPI staining (D). E-H: sections through a DiI-labeled hair cell (hc) located near the tip of a tentacle. Arrowheads in F point to microvilli of the mechanoreceptor hair bundle contributed by peripheral support cells, which are DiI-negative. I: Electron microscopic section of an apical region of the tentacular ectodermal epithelium of N. vectensis polyp, showing a hair cell (hc) and a support cell (su). The hair cell has stereovilli that extend dense filaments into the cytoplasm, forming 2-3 µm-long rootlets (rl_{st}), as well as numerous clear vesicles (ve), while the support cell has apical microvilli (mv) and electron-dense vacuoles (va). Abbreviations: ms muscle fibers; rl_{ci} ciliary rootlet; ec ectoderm. Scale bar: 10 μm (A-F); 2 μm (inset in B); 500 nm (G)

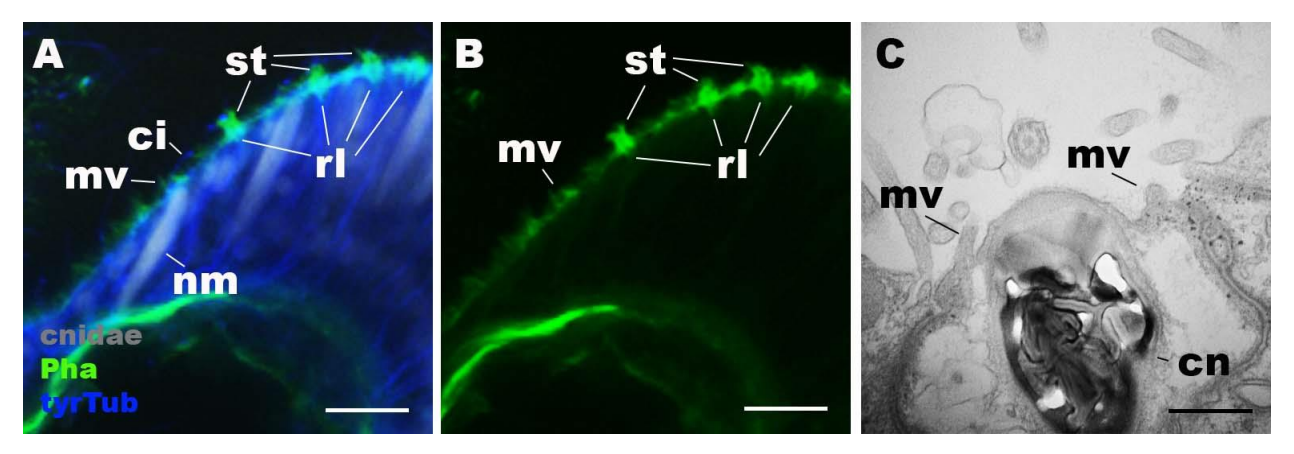


Figure 1 - Figure supplement 3: Morphology of nematocytes in the tentacles of *Nematostella vectensis* polyps.

A, B: Confocal sections of *Nematostella vectensis* primary polyp, labeled with an antibody against tyrosinated *∂*-tubulin ("tyrTub"). Filamentous actin is labeled with phalloidin (Pha), and mature enidocysts (enidae) are labeled with a high concentration of DAPI in the presence of EDTA (Szczepanek et al., 2002). The section shows the ectoderm at the tentacle tip, with the epithelial surface facing up. Note that nematocytes (nm) have an apical cilium (ci) surrounded by microvilli (mv) without rootlets. Stereovilli (st) and their prominent rootlets (rl) of hair cells are also shown. C: An electron micrograph of a section of *N. vectensis* primary polyp, showing an apical structure of a enida(en)-containing nematocyte in the tentacular ectoderm. Microvilli (mv) without rootlets occur on the apical cell surface. Scale bar: 10 μm (A, B); 500 nm (C)

Hair cells commence development at metamorphosis in the sea anemone.

We next sought to determine the timing of hair cell development by using phalloidin to label stereovilli – the morphological hallmark of hair cells in *N. vectensis*. We never found stereovilli in the circumoral ectoderm during planula development (Figure 1 - Figure supplement 4A, B). However, pronounced stereovilli became evident in the circumoral ectoderm at the tentacle-bud stage (Figure 1 - Figure supplement 4C, D). These observations suggest that the hair cell is a postembryonic cell type that does not initiate development until metamorphosis in *N. vectensis*.

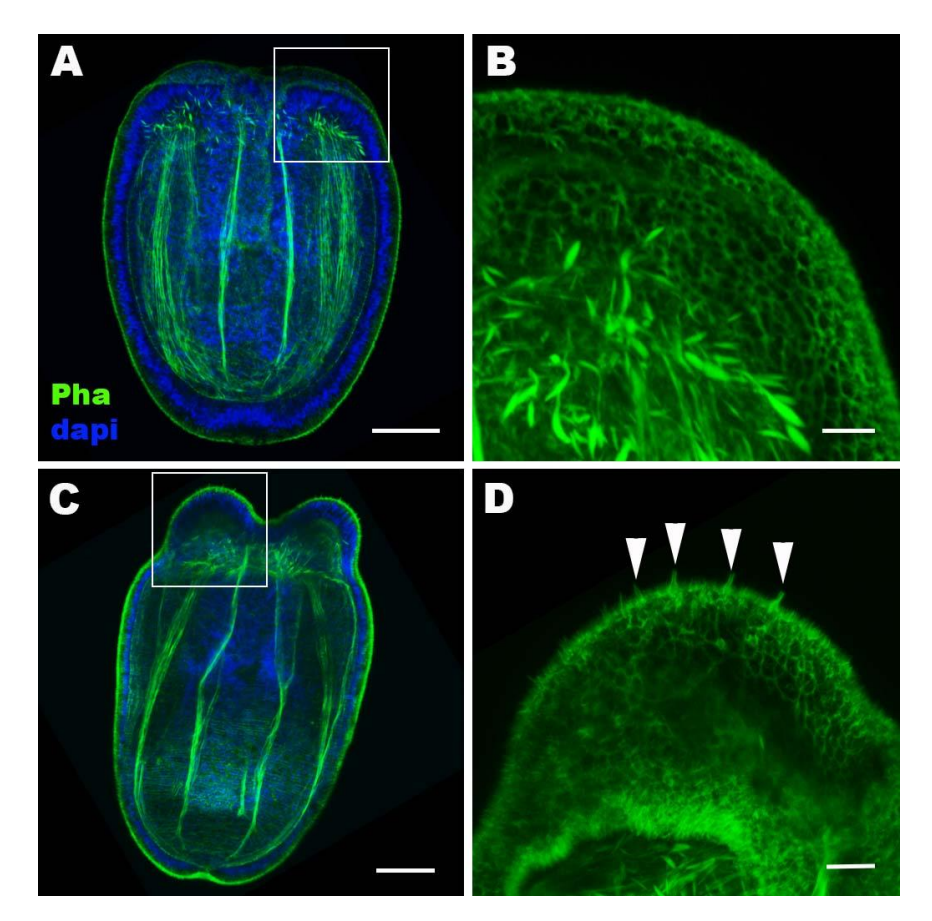


Figure 1 - Figure supplement 4: Hair cell development begins in the ectoderm of tentacle primordia at metamorphosis in sea anemones.

Confocal sections of *N. vectensis* at the late planula (A, B) and tentacle-bud (C, D) stages. Filamentous actin is labeled with phalloidin (Pha), and nuclei are labeled with DAPI (dapi). All panels show side views of animals with the blastopore/mouth facing up. A and C show longitudinal sections through the center, and B and D show surface ectoderm of tentacular primordia boxed in A and C, respectively. Note that 3-5 μ m-long stereovilli characteristic of hair cells become evident at the tentacle bud stage (arrowheads in D), indicative of hair cell differentiation. Scale bar: 50 μ m (A, C); 10 μ m (B, D)

Class IV POU transcription factor is postmitotically expressed in hair cells in the sea anemone.

The *N. vectensis* genome contains a single gene that encodes the class IV POU homeodomain transcription factor (Nv160868; (Tourniere et al., 2020, Nakanishi et al., 2010, Gold et al., 2014)), termed as *NvPOU4* by (Tourniere et al., 2020); in this paper, we will simplify the

nomenclature by referring to POU-IV/POU4/Brn3/unc-86 gene as pou-iv and its protein product as POU-IV. It has been previously shown that pou-iv mRNA is strongly expressed in circum-oral ectoderm during metamorphosis in N. vectensis (Tourniere et al., 2020), consistent with a role in tentacular morphogenesis. Although gene expression analysis using a transgenic reporter line has indicated that *pou-iv* is expressed in cnidocytes throughout the body including those in the tentacles (Tourniere et al., 2020), whether pou-iv is expressed in mechanosensory hair cells is not known. To address this, we first developed a rabbit polyclonal antibody against an N-terminal, non-DNA-binding region of the Nematostella vectensis POU-IV based on the amino acid sequence predicted from *pou-iv* cDNA (see Materials and Methods). As detailed in the next section, specificity of the antibody was confirmed by western blot analysis using *pou-iv* mutants and their wildtype siblings. In addition, immunostaining and in situ hybridization experiments showed that the pattern of anti-POU-IV immunoreactivity paralleled that of *pou-iv* mRNA expression (Figure 2 – Figure supplement 1), further supporting the specificity of the antibody. We therefore used immunostaining with the anti-POU-IV to analyze the expression pattern of POU-IV in developing oral tentacles in *N. vectensis* at metamorphosis. We found that POU-IV protein localized to nuclei of differentiating and differentiated hair cells, but not to those of support cells, in the ectoderm of developing tentacles (Figure 2A-L). In addition, we confirmed POU-IV expression in cnidocytes (Figure 2 - Figure supplement 2), consistent with the previous report (Tourniere et al., 2020). Nuclear labeling by the anti-POU-IV was abolished when the antibody was preadsorbed with the POU-IV antigen prior to immunostaining (Figure 2 - Figure supplement 3), evidencing that the antibody reacts with nuclear POU-IV. We then carried out EdU pulse labeling experiments to test whether any of the POU-IV-

We then carried out EdU pulse labeling experiments to test whether any of the POU-IV-expressing cells in the tentacular ectoderm were at S-phase and thus proliferative. As observed for *pou-iv* transcript-expressing cells during embryogenesis (Tourniere et al., 2020), we found that none of the POU-IV-expressing epithelial cells in the developing tentacles examined (n>220 cells across 3 tentacle-bud-stage animals and 8 primary polyps) incorporated EdU (e.g. Figure 2M-P), indicative of their postmitotic cell-cycle status. Taken together, the gene expression pattern suggests a role for POU-IV in postmitotic development of mechanosensory hair cells, as well as cnidocytes, in the tentacles of *N. vectensis* polyps.

317

318

319

320

321

322

323

324

325

326

327

328

329

330

331

332

333

334

335

336

337

338

339

340

341

342

343

344

345

346

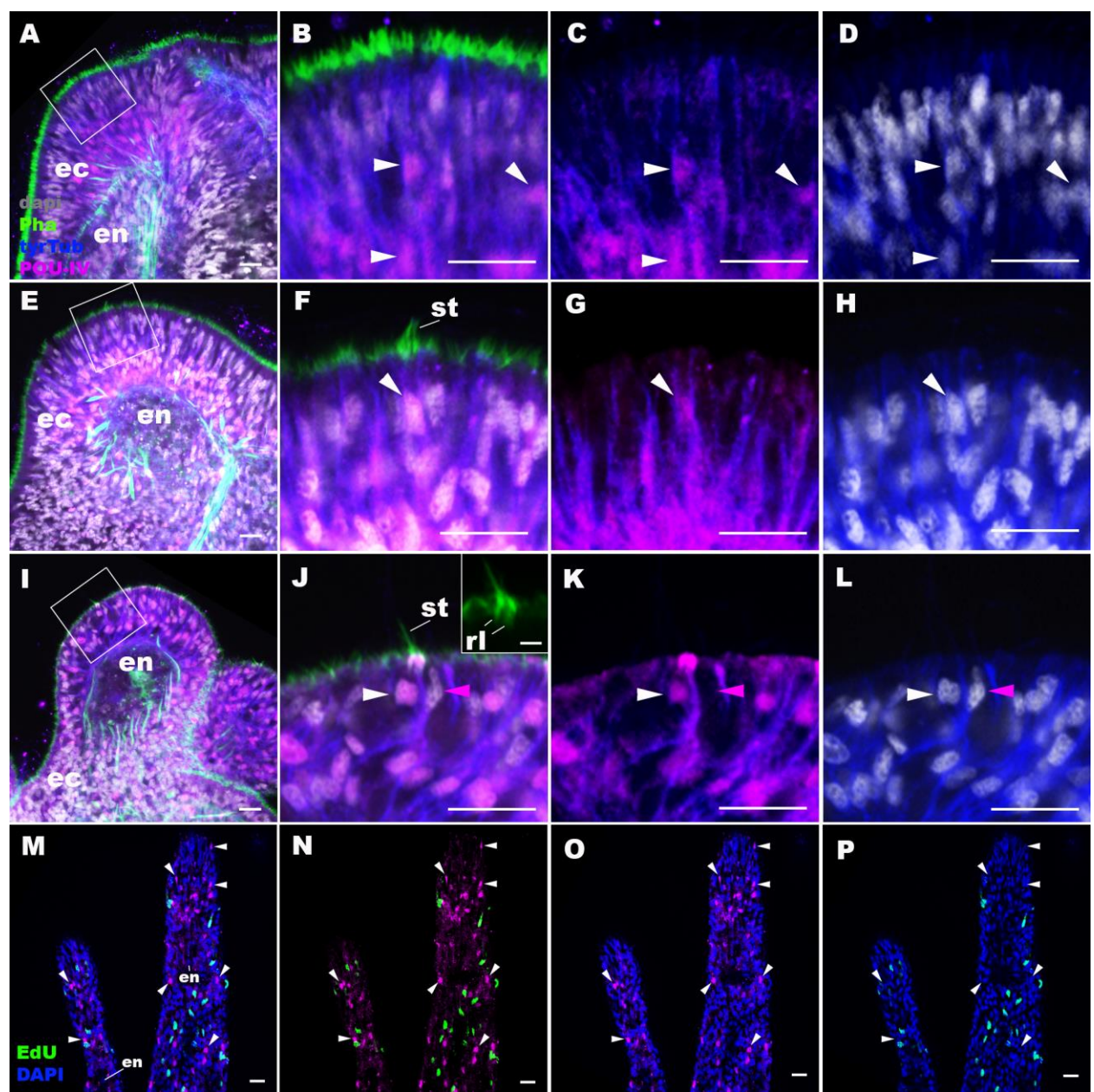


Figure 2: POU-IV is postmitotically expressed in hair cells of tentacular ectoderm at metamorphosis in the sea anemone.

Confocal sections of *N. vectensis* at metamorphosis, labeled with antibodies against POU-IV, and/or tyrosinated ∂-tubulin ("tyrTub"). Filamentous actin is labeled with phalloidin (Pha), and nuclei are labeled with DAPI (dapi). Proliferative cells are labeled by the thymidine analog EdU. A shows a section through the presumptive tentacle primordia with the blastopore/mouth facing up. E, I, M-P show sections through developing oral tentacles with the distal end of the tentacle facing up; M-P are tangential sections of tentacles at the level of the surface ectoderm and parts of the endoderm (en). B-D, F-H, and J-L are magnified views of the boxed regions in A, E and I,

respectively, with the apical epithelial surface facing up. A-D: late planula. E-H: tentacle-bud. I-P: primary polyp. At the late planula stage prior to hair cell differentiation, POU-IV-positive nuclei are primarily localized at the basal and middle layers of the ectoderm of presumptive tentacle primordia (arrowheads in B-D); few POU-IV-positive nuclei are detectable at the superficial stratum. At the tentacle-bud stage, hair cells with pronounced stereovilli (st) and POU-IV-positive nuclei begin to develop in the superficial stratum of the ectodermal epithelium in tentacle primordia (arrowheads in F-H). POU-IV-positive nuclei in the superficial layer specifically occur in hair cells (white arrowheads in J-L) and not in adjacent support cells (purple arrowheads in J-L). The inset in J shows a magnified view of stereovilli (st) of a POU-IV-positive hair cell; note the presence of stereovillar rootlets (rl). In addition to hair cells, cnidocytes express POU-IV in the tentacular ectoderm (Figure 2 - Figure supplement 2; (Tournier et al., 2020)). POU-IV-positive cells are EdU-negative (arrowheads in I-L), evidencing their postmitotic cell-cycle status. Abbreviations: ec ectoderm; en endoderm. Scale bar: 10 μm (A-P); 2 μm (inset in J)

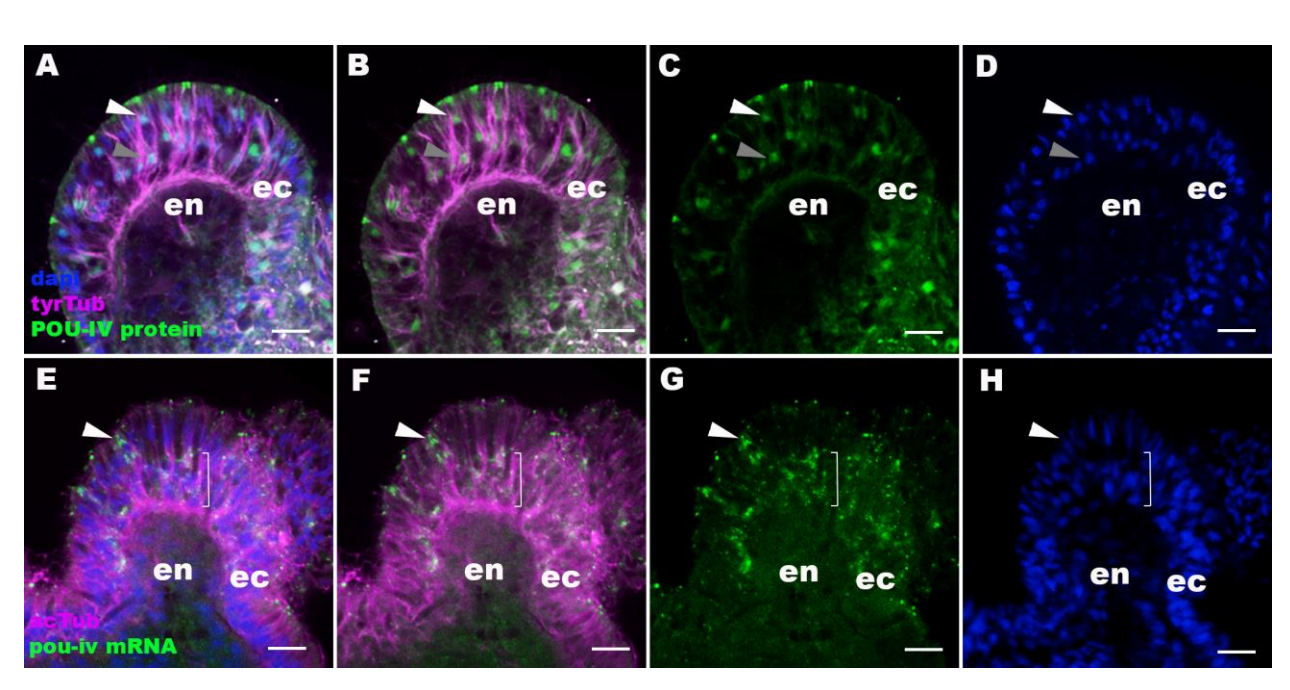


Figure 2 – Figure supplement 1: The pattern of immunoreactivity with an anti-POU-IV antibody recapitulates that of *pou-iv* mRNA expression.

Confocal sections of oral tentacles of *Nematostella vectensis* at the primary polyp stage, labeled with an anti-POU-IV antibody ("POU-IV protein"; A-D), or an antisense riboprobe against *pou-*

iv mRNA ("pou-iv mRNA"; E-H). Microtubules are labeled by antibodies against tyrosinated ∂-tubulin ("tyrTub"; A, B) or acetylated ∂-tubulin ("acTub"; E, F). Nuclei are labeled with DAPI (dapi). All panels show sections through oral tentacles with the distal end of the tentacle facing up. Anti-POU-IV immunoreactivity occurs in a subset of apical nuclei (white arrowhead in A-D) and the majority of basal nuclei (grey arrowhead in A-D) within the pseudostratified ectodermal epithelium (ec), suggesting nuclear localization of POU-IV proteins in these cells. Consistent with the pattern of Anti-POU-IV immunoreactivity, in situ hybridization signals of pou-iv mRNA occur in a subset of ectodermal epithelial cells whose cell bodies are located apically (white arrowhead in E-H), and in those ectodermal cells whose cell bodies are localized basally (bracketed in E-H). Anti-POU-IV immunoreactivity is absent in nuclei of tentacular endodermal cells (en in A-D), and in situ hybridization signals for pou-iv mRNA are not detectable in these cells (en in E-H), indicating the lack of pou-iv expression in tentacular endoderm. Scale bar: 10 μm

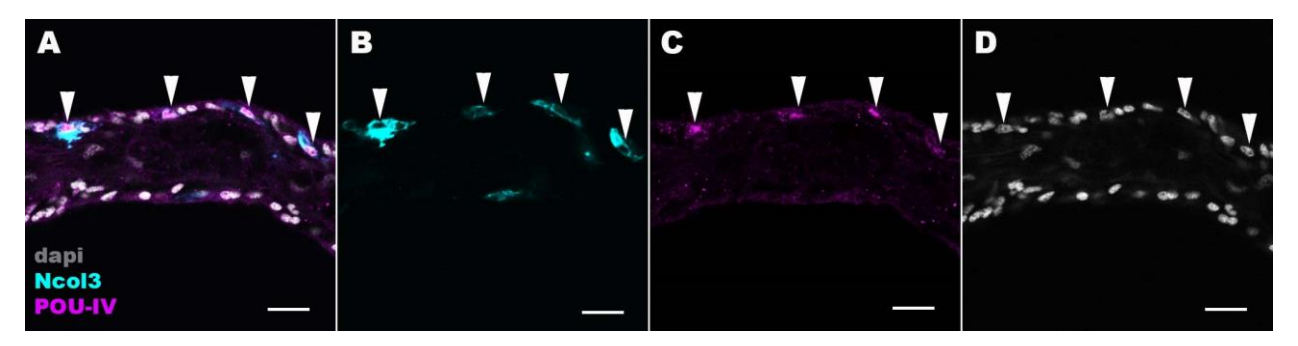


Figure 2 - Figure supplement 2: POU-IV localizes to the nuclei of cnidocytes in tentacular ectoderm of the sea anemone.

Confocal sections of an oral tentacle of *N. vectensis* at the primary polyp stage, labeled with antibodies against POU-IV and/or minicollagen 3 ("Ncol3"; (Zenkert et al., 2011)). Nuclei are labeled with DAPI (dapi). Arrowheads show POU-IV positive nuclei of Ncol3-positive cnidocytes that reside in the tentacular ectoderm. Scale bar: 10 µm

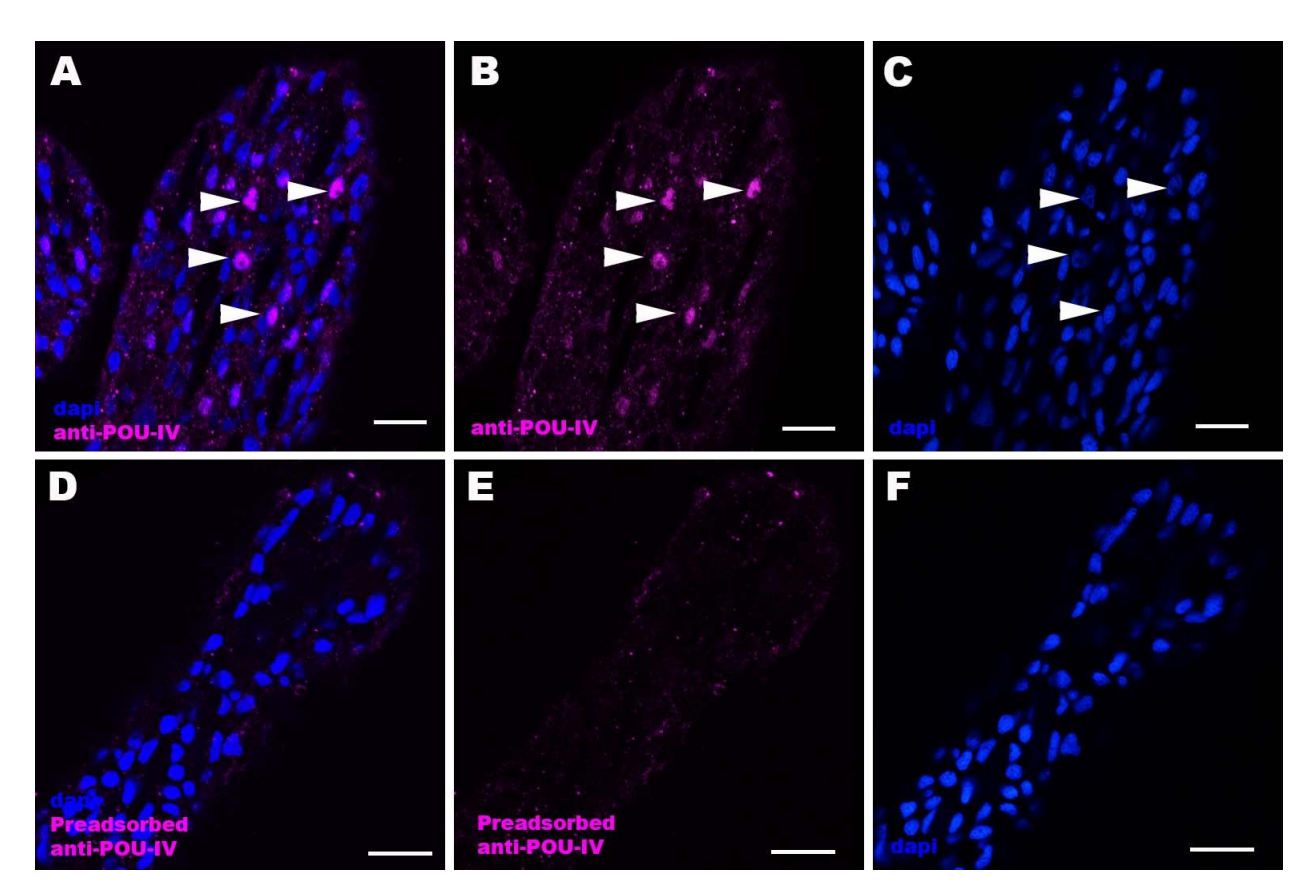


Figure 2 – Figure supplement 3: Immunostaining with a preadsorbed anti-POU-IV antibody.

Confocal sections of oral tentacles of *Nematostella vectensis* at the primary polyp stage, labeled with an anti-POU-IV antibody ("anti-POU-IV"; A-C) and an anti-POU-IV antibody preadsorbed with the POU-IV antigen (CQPTVSESQFDKPFETPSPINamide) used to generate the antibody ("Preadsorbed anti-POU-IV"; D-F). Nuclei are labeled with DAPI (dapi). In all panels, the distal end of the tentacle is to the top, and sections are at the level of surface ectoderm. Arrowheads indicate nuclear immunoreactivity that is abolished when the preadsorbed antibody is used, indicating that the anti-POU-IV reacts with nuclear POU-IV. Scale bar: 10 µm

Generation of POU-IV mutant sea anemones

To investigate the function of POU-IV in hair cell development in *N. vectensis*, we generated a *pou-iv* mutant line by CRISPR-Cas9-mediated mutagenesis. First, a cocktail containing *pou-iv*-specific single guide RNAs (sgRNAs) and the endonuclease Cas9 protein was injected into fertilized eggs to produce founder (F0) animals. Multiple sgRNAs were designed to cleave

flanking sites of the coding region of the pou-iv locus (Figure 3A; Figure 3 - Figure supplement 1). Large deletions were readily confirmed by genotyping PCR using genomic DNA extracted from single CRISPR-injected embryos (Figure 3 - Figure supplement 1). DNA sequencing of mutant bands confirmed that excision of both POU- and homeo-domains could be induced by this approach. F0 animals were raised and crossed with wildtype animals, in order to generate F1 heterozygous animals carrying a pou-iv knockout allele. Mutant allele carriers were identified by genotyping individual F1 polyps. One of the mutant alleles, which will be here referred to as pou-iv, had a 705bp deletion that removed most of the POU domain (i.e. all but the first four Nterminal residues) and all of the homeodomain at the *pou-iv* locus (Figure 3B; Figure 3 - Figure supplement 2). This mutant allele differs from the previously generated NvPOU4⁻ allele which harbors a frameshift mutation (31 bp deletion) at the start of the POU-domain-encoding sequence (Tourniere et al., 2020). F1 pou-iv +/- heterozygotes were subsequently crossed with each other to produce F2 offspring, a quarter of which, on average, were pou-iv -/- mutants. pou-iv -/mutants were identified by PCR-based genotyping methods (Figure 3B, C) using genomic DNA extracted from polyp tentacles (Ikmi et al., 2014) or from pieces of tissue isolated from early embryos (Nakanishi and Martindale, 2018, Silva and Nakanishi, 2019). Western blotting with the anti-POU-IV has confirmed that *pou-iv* -/- polyps express mutant POU-IV lacking DNA-binding domains (18.7kDa), but not wildtype POU-IV (35.2kDa) (Figure 3D), validating the specificity of the antibody.

415

416

417

418

419

420

421

422

423

424

425

426

427

428

429

430

431

432

433

434

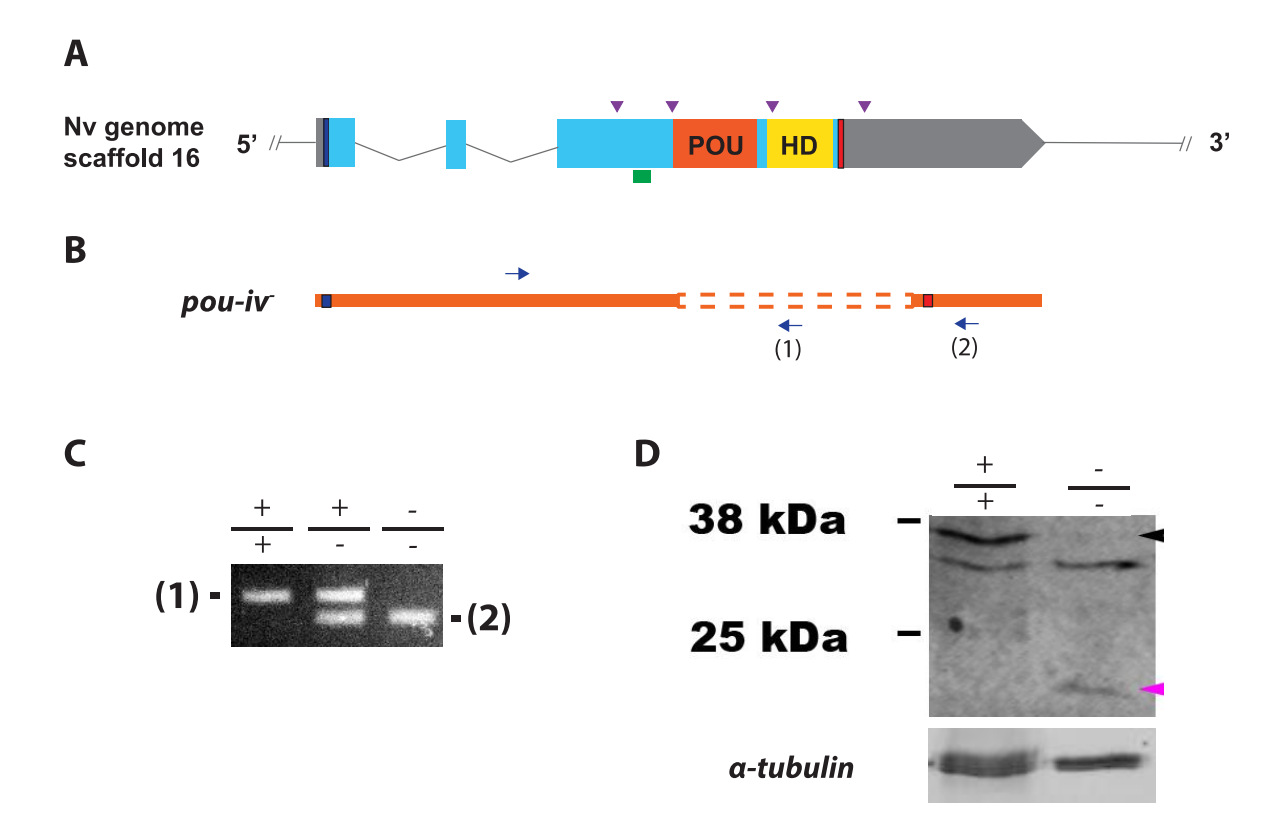


Figure 3: Generation of *pou-iv* null mutant sea anemones.

A, B: Diagrams of the *pou-iv* locus (A) and the disrupted mutant allele (*pou-iv*; B). Blue bars show predicted translation start sites; red bars show predicted translation termination sites. In A, filled boxes indicate exons, and the regions that encode the POU- and homeo-domains are highlighted in orange ("POU") and yellow ("HD"), respectively. Purple arrowheads show sgRNA target sites. The region that encodes peptides targeted by the antibody generated in this study is indicated by a green line. In B, deletion mutation is boxed in dotted orange lines, and blue arrows mark regions targeted in the PCR analysis shown in C; reverse primers are numbered (1)-(2). C: Genotyping PCR. Note that the wildtype allele-specific primer (1) generates a 689bp PCR product from the wildtype allele ('+') but cannot bind to the *pou-iv* allele due to deletion mutation. The primer (2) generates a 558 bp PCR product from the *pou-iv* allele, and a 1312 bp PCR product from the wildtype allele. D: Western blotting with an antibody against *N. vectensis* POU-IV. An antibody against acetylated α-tubulin ("α-tubulin"; ca. 52 kDa) was used as a loading control. The anti-POU-IV reacts with a protein of expected size for wildtype POU-IV (35.2kDa) in wildtype (+/+) polyp extracts, but not in *pou-iv* mutant (-/-) polyp extracts (black arrowhead). Also note that the antibody's reactivity with a protein of

expected size for mutant POU-IV lacking DNA-binding domains (18.7kDa) is detectable in mutant (-/-) extracts, but not in wildtype (+/+) extracts (purple arrowhead). The band just below the expected size of the wildtype POU-IV occur in both wildtype and mutant protein extracts, and therefore represents non-POU-IV protein(s) that are immunoreactive with the anti-POU-IV antibody.

Figure 3 – Source data 1: An original gel image used to generate Figure 3C and the original image with relevant lanes labelled.

Figure 3 – Source data 2: An original western blot image used to generate Figure 3D (top; anti-N. vectensis POU-IV) and the original image with relevant lanes labelled.

Figure 3 – Source data 3: An original western blot image used to generate Figure 3D (bottom; anti-acetylated α-tubulin) and the original image with relevant lanes labelled.



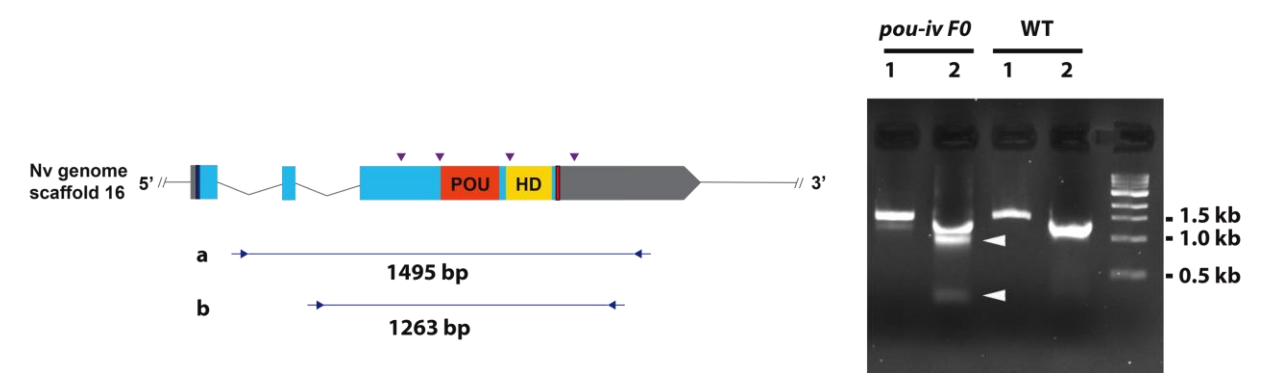


Figure 3 – Figure supplement 1: Generation of *pou-iv* F0 mosaic mutants by CRISPR-Cas9-mediated mutagenesis in *N. vectensis*.

A schematic view of the *pou-iv* locus (left), and genomic DNA PCR results of an uninjected wildtype embryo ("WT") and an F0 embryo injected with locus-specific sgRNAs and Cas9 ("*pou-iv* F0") (right). A blue bar shows the predicted translation start site, and a red bar shows the predicted translation termination site. The orange and yellow highlighted regions are POU-and Homeo- DNA-binding domains, respectively. Purple arrowheads show sgRNA target sites. Blue arrows mark regions targeted in the PCR analysis shown to the right. Note that genomic PCR of the WT embryo shows expected sizes of PCR fragments (1495 bp for primary PCR ("a"), and 1263 bp for secondary nested PCR ("b")), while F0 embryos show additional bands of smaller sizes (arrowheads), indicating that targeted deletions of different sizes have occurred

mosaically in each embryo. DNA sequencing of the <500 bp band (lower arrowhead) indicated that this mutant allele harbored 981 bp deletion encompassing the POU- and homeo-domain-encoding regions.

Figure 3 – Figure supplement 1 - Source data 1: An original gel image used to generate Figure 3 – Figure supplement 1 (right) and the original image with relevant lanes labelled.



Figure 3 – Figure supplement 2: Sequence alignment of wildtype and mutant *pou-iv* alleles.

A: Diagrams of the *pou-iv* locus and the disrupted mutant allele (*pou-iv*⁻). Blue bars show predicted translation start sites; red bars show predicted translation termination sites. In the schematic depicting the *pou-iv* locus, filled boxes indicate exons, and the regions that encode the POU- and homeo-domains are highlighted in orange ("POU") and yellow ("HD"), respectively. In the schematic of the *pou-iv* allele, deletion mutation is boxed in orange dotted lines. B: Alignment of nucleotide and translated amino acid sequences of wildtype ("+") and mutant ("*pou-iv*-") alleles boxed in A. POU- and homeo-domains are boxed in orange and yellow, respectively. Predicted translation termination sites are boxed in red, and 705 bp deletion mutation is boxed in dotted blue lines. Note that all but the first four residues of the POU domain and the entire homeodomain are deleted in the *pou-iv* allele.

POU-IV is necessary for touch-response behavior of tentacles in the sea anemone.

If POU-IV indeed plays a key role in postmitotic differentiation of mechanosensory hair cells, mechanosensitive behaviors of oral tentacles are expected to be perturbed in *pou-iv* null mutants. We tested this prediction by using F2 *pou-iv -/-* mutants and their heterozygous and wildtype siblings. In wildtype polyps, oral tentacles typically respond to touch stimuli by local contraction of longitudinal muscles. Strong and repeated touch stimuli of tentacles lead to excitation of longitudinal muscles in the body column, causing the tentacles to retract into the body column. In this study, a hair held in a tungsten needle holder was quickly depressed on the distal portion

of each tentacle, and the presence/absence of the touch-response behavior of tentacles was scored for each animal. 100% of the F2 *pou-iv* +/+ wildtype animals that were examined (n=44) contracted at least one tentacle in response to touch (Figure 4A, B; Figure 4 – video 1). In contrast, we observed that only 35% of the F2 *pou-iv* -/- knockout animals (n=40) showed any sign of tentacular retraction in response to touch; 65% of the knockout mutants exhibited no discernable tentacular response to tactile stimuli (Figure 4C, D; Figure 4 – video 2). The majority of F2 *pou-iv* +/- heterozygotes (87%, n=62) showed touch-induced, tentacular responses; 13% did not show touch responses, suggestive of dose-dependent effects of POU-IV expression on the mechanosensory behavior. The reduced tentacular response to touch in *pou-iv* -/- mutants is not due to the inability of tentacular muscles to contract, as *pou-iv* -/- mutants responded to crushed brine shrimp extract by contracting tentacles (100%, n=8 animals; Figure 4 - Figure supplement 1; Figure 4 - video 3, 4). Hence, *pou-iv* is specifically required for the touch-sensitive behavior of oral tentacles in *N. vectensis*, consistent with POU-IV having a role in regulating the development of the mechanosensory hair cells.

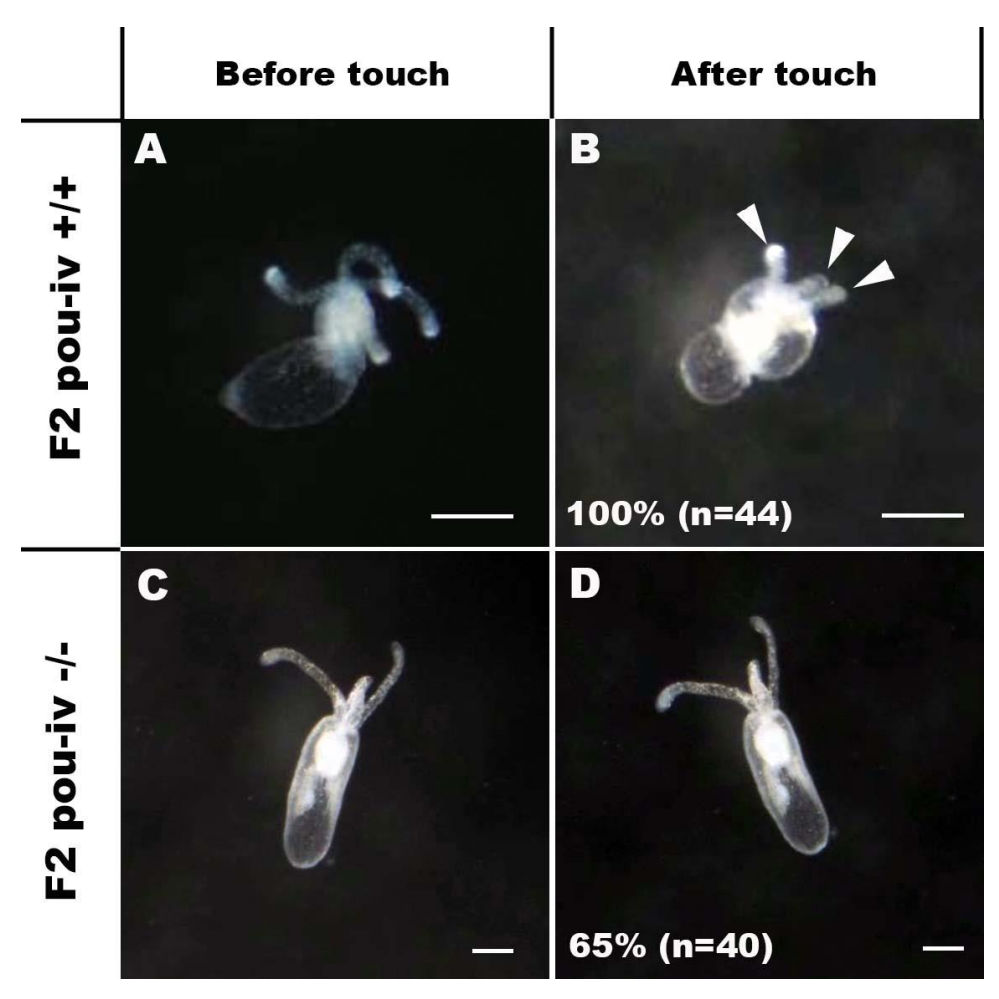


Figure 4: POU-IV is essential for touch-response behavior in the sea anemone.

A-D: Behavior of wildtype (F2 *pou-iv* +/+, A, B) and mutant (F2 *pou-iv* -/-, C, D) *N. vectensis* polyps in response to tactile stimuli to their oral tentacles. A hair held in a tungsten needle holder was used to touch the distal portion of each tentacle. Animals before (A, C) and after (B, D) tentacle touch are shown. Tactile stimuli to tentacles elicit tentacular retraction in the wildtype individual (100%, n=44; A, B). In contrast, the majority of *pou-iv* homozygous mutants were touch-insensitive (65%, n=40; B, D); only 35% of the animals showed any contractile response to touch stimuli. Arrowheads in B point to retracted tentacles. Scale bar: 1 mm

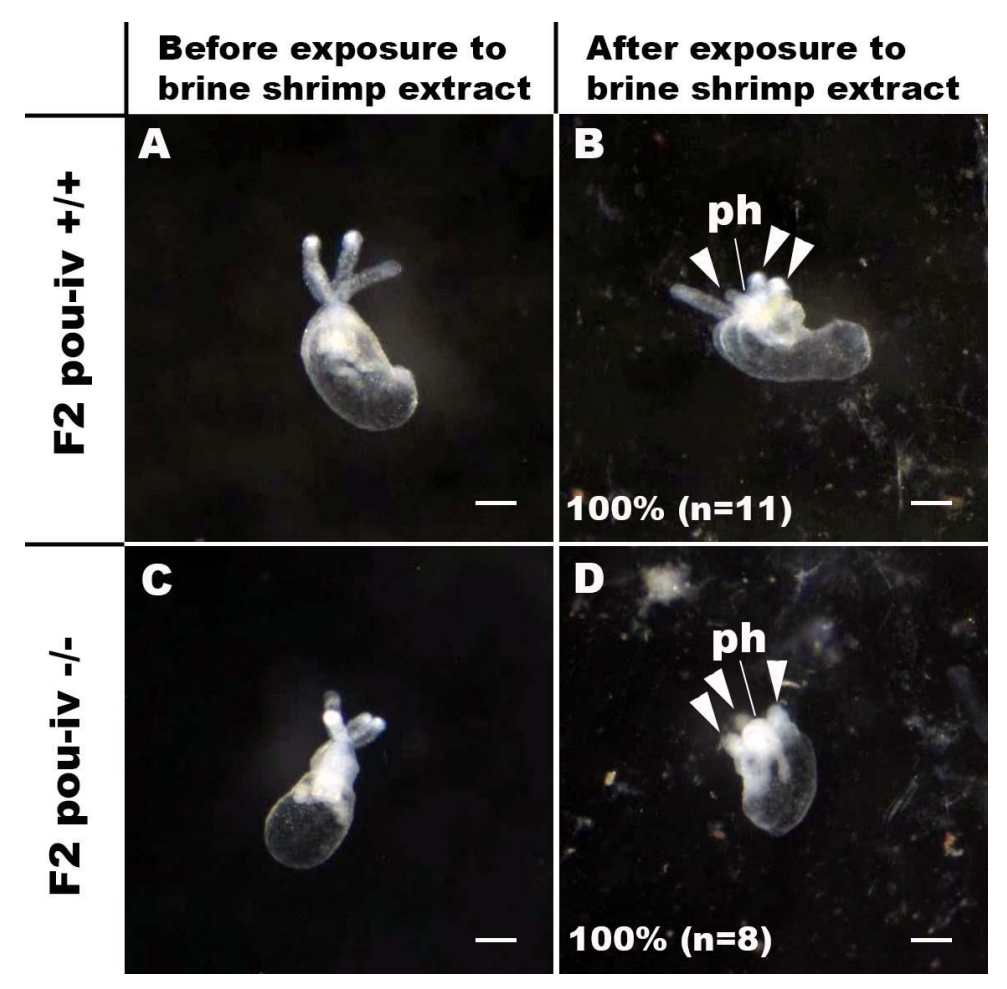


Figure 4 – Figure supplement 1: *pou-iv* mutants respond to brine shrimp extract by tentacular contraction and pharyngeal protrusion.

A-D: Behavior of wildtype (F2 *pou-iv* +/+, A, B) and mutant (F2 *pou-iv* -/-, C, D) *N. vectensis* polyps in response to exposure to *Artemia* extract. Both wildtype and mutant animals contracted tentacles (arrowheads in B and D), and protruded the pharynx (ph) within one minute of exposure to the extract (F2 *pou-iv* +/+, 100%, n=3; F2 *pou-iv* -/-, 100%, n=9). Scale bar: 1 mm

Figure 4 - Video 1: Touch-sensitive behavior of a wildtype (F2 *pou-iv* +/+) polyp.

Figure 4 - Video 2: Touch-sensitive behavior of a *pou-iv* mutant (F2 *pou-iv* -/-) polyp.

Figure 4 - Video 3: Behavior of a wildtype (F2 *pou-iv* +/+) polyp upon exposure to brine

shrimp extract.

Figure 4 - Video 4: Behavior of a *pou-iv* mutant (F2 *pou-iv* -/-) polyp upon exposure to

542 brine shrimp extract.

POU-IV is necessary for normal development of hair cells in the sea anemone.

To understand the structural basis of touch-insensitivity in *pou-iv* null mutants, we examined the morphology of tentacular cells in *pou-iv* null mutants and their heterozygous and wildtype siblings by light and confocal microscopy. At the primary polyp stage, F-actin labeling by phalloidin showed that the longitudinal muscles in the tentacle of F2 *pou-iv* -/- mutants developed normally (Figure 5A, D, G), consistent with the behavioral evidence demonstrating the ability of the mutant tentacles to contract in response to the brine shrimp extract. We have confirmed the previous finding that mature enidocytes with enidae fail to develop in *pou-iv* knockout mutants (Figure 5C, F, I; (Tourniere et al., 2020)). In addition, we found that mature hair cells with stereovillar rootlets were lacking in the tentacles of F2 *pou-iv* -/- polyps (n=6 animals), while mature hair cells formed normally in tentacles of *pou-iv* +/- (n=6 animals) and *pou-iv* +/+ (n=3 animals) siblings (Figure 5A-I). Ciliary cone-like structures lacking stereovillar rootlets occurred in *pou-iv* -/- mutants (Figure 5G-I), raising the possibility that hair cells might undergo partial differentiation in *pou-iv* -/- mutants.

Electron microscopic observations confirmed these findings. Stereovillar rootlets and cnidae were absent in the tentacles of F2 *pou-iv -/-* polyps (n=2 animals) but were present in the tentacles of their wildtype siblings (n=2 animals) (Figure 5J-L; Figure 5 - Figure supplement 1, 2). We also confirmed by electron microscopy the presence of a hair-cell-like cell that has an apical ciliary cone without stereovillar rootlets, surrounded by support cells with characteristic electron-dense vacuoles that contribute microvilli to the ciliary cone in *pou-iv -/-* mutants (Figure 5K, L); ciliary rootlets were observed in these hair-cell-like cells in *pou-iv -/-* mutants (Figure 5 – Figure supplement 3).

The lack of cnidae is consistent with the inability of *pou-iv* null mutants to capture prey as previously reported (Tourniere et al., 2020), but cannot explain the lack of tentacular contraction in response to touch. Stereovillar rootlets provide stereovilli with structural resilience against physical damage and are necessary for normal mechanosensitivity in vertebrate hair cells (Kitajiri et al., 2010). We therefore suggest that touch-insensitivity of oral tentacles in *pou-iv* null mutants results, at least in part, from the failure of hair cells to generate structurally robust apical mechanosensory apparatus (see Discussion).

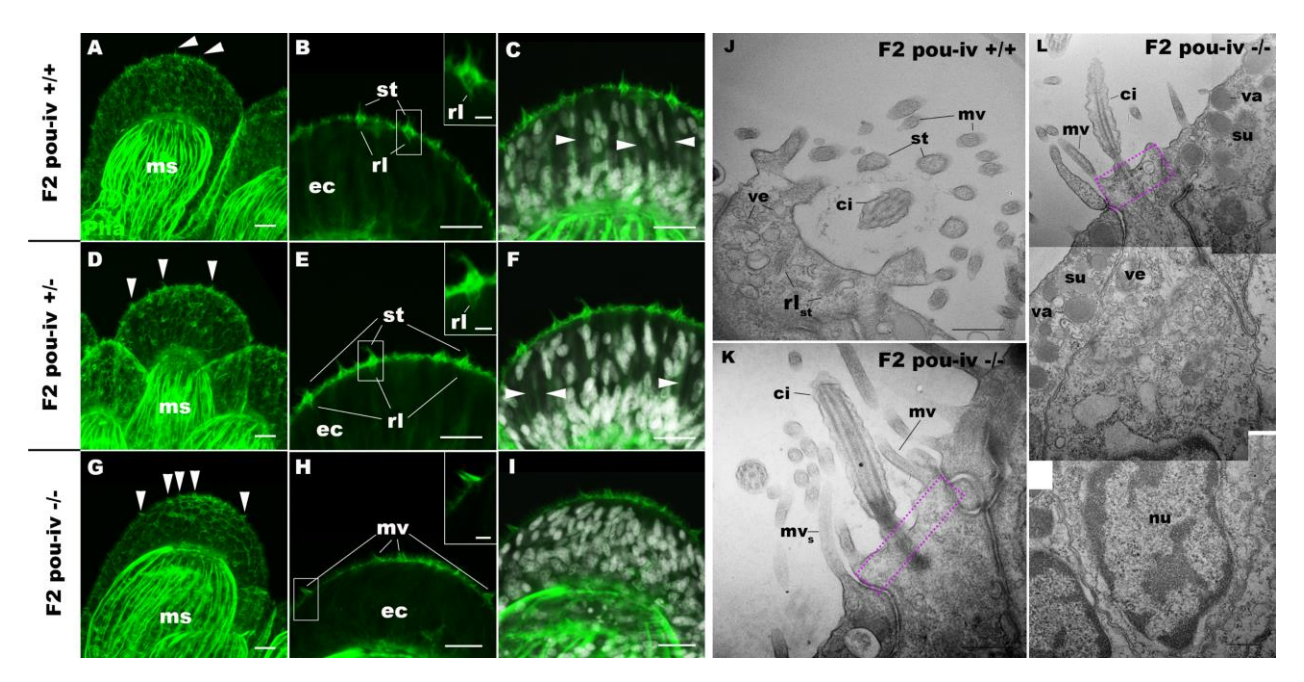


Figure 5: POU-IV is necessary for hair cell differentiation in the sea anemone.

576

577

578

579

580

581

582

583

584

585

586

587

588

589

590

591

592

593

594

A-I: Confocal sections of oral tentacles of wildtype (F2 pou-iv +/+, A-C), heterozygous (F2 pou-iv +/+, A-C) iv +/-, D-F) and homozygous pou-iv mutant (F2 pou-iv -/-, G-I) N. vectensis polyps. Filamentous actin is labeled with phalloidin (Pha), and nuclei are labeled with DAPI (dapi). In all panels, the distal end of the tentacle is to the top. A, D, G: sections through the tentacle. B, C, E, F, H, I: sections through hair bundles/ciliary cones at the tip of tentacles. Ciliary cones occur on the epithelial surface of the tentacle regardless of the genotype (arrowheads in A, D, G). However, stereovilli (st) with rootlets (rl) characteristic of mechanosensory hair cells are observed in wildtype (B) and heterozygous (E) siblings, but not in homozygous pou-iv mutants whose ciliary cones contain microvilli without prominent actin rootlets (my in H). Arrowheads in C and F indicate spaces occupied by cnidocysts in wildtype and heterozygous siblings, respectively, which are absent in *pou-iv* homozygous mutants (I; Figure 5 - Figure supplement 1). J-L: Electron microscopic sections of a hair cell of a F2 pou-iv +/+ polyp (J) and an epithelial cell with hair-cell-like morphologies in a F2 pou-iv -/- polyp (K, L). In all panels, apical cell surfaces face up. K and L are sections of the same cell at different levels. The hair cell-like epithelial cell of the mutant has a central apical cilium surrounded by a collar of rootlet-less microvilli (my in K, L), which are encircled by microvilli of the adjacent support cells (mv_s in L), forming a ciliary cone. It also has numerous clear vesicles (ve in L) in the cytoplasm, characteristic of hair cells (ve in J; Figure 1G). Support cells of mutants are morphologically indistinguishable from those of wildtype animals, having characteristic large electron-dense vacuoles (va in L) in addition to

apical microvilli (mv_s in L) that contribute to the ciliary cone/hair bundle. Consistent with light microscopy data (A-C, G-I), stereovillar rootlets (rl_{st}) are absent in the F2 *pou-iv* -/- polyp, but are present in hair cells of their wildtype siblings (J). In K and L, regions of apical cytoplasm where stereovillar rootlets would normally be observed are boxed with dotted purple lines. Abbreviations: ms muscle fibers; ec ectoderm; st stereovilli; ci cilium; rl_{st} stereovillar rootlets. Scale bar: 10 μm (A-I); 2 μm (insets in B, E, H); 500 nm (J-L)

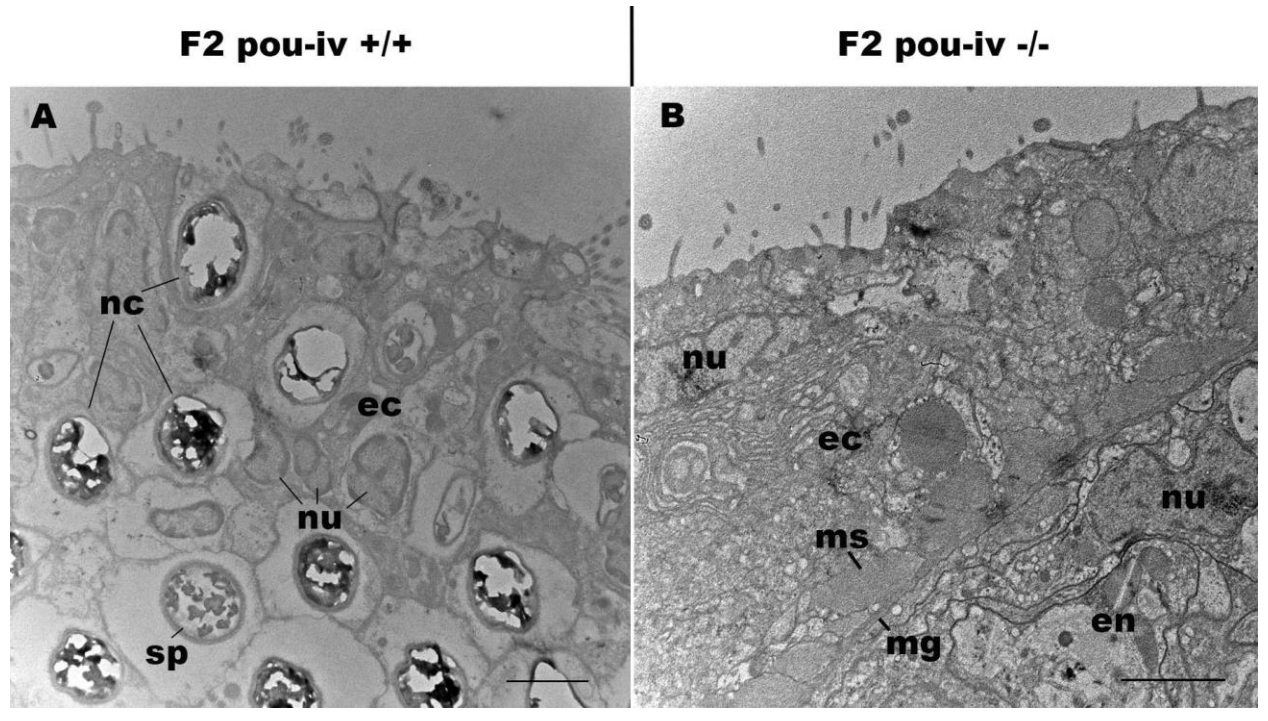


Figure 5 – Figure supplement 1: *pou-iv* mutants lack mature cnidocytes.

Electron microscopic sections of tentacular ectoderm of a F2 *pou-iv* +/+ polyp (A) and F2 *pou-iv* -/- polyp (B). Note the occurrence of numerous cnidae – nematocysts (nc) and spirocysts (sp) – in A that are absent in B. Abbreviations: nu nucleus; ec ectoderm; en endoderm; ms muscle fibers; mg mesoglea. Scale bar: 2 μm

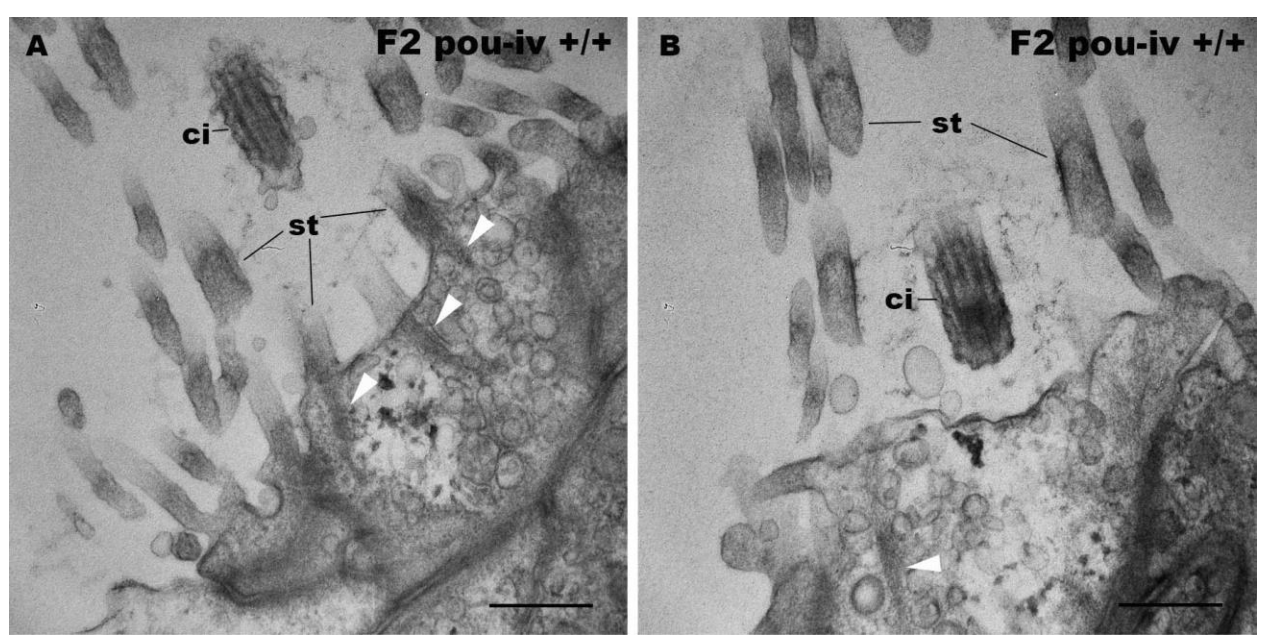


Figure 5 – Figure supplement 2: F2 *pou-iv* wildtype siblings develop hair cells with stereovillar rootlets.

Electron microscopic sections of hair cells of a F2 *pou-iv* +/+ polyp. In all panels, apical cell surfaces face up. Note the presence of stereovillar rootlets (arrowheads). Abbreviations: st stereovilli; ci cilium. Scale bar: 500 nm

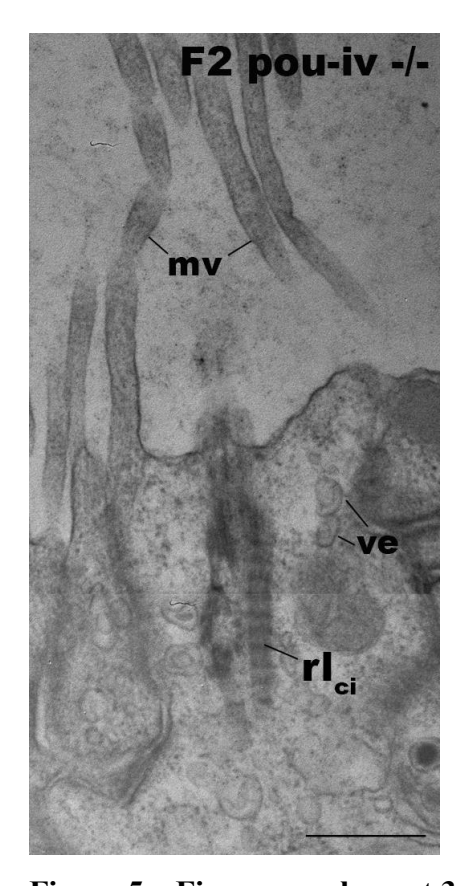


Figure 5 – Figure supplement 3: Hair-cell-like cells of *pou-iv* mutants have ciliary rootlets. Electron microscopic sections of a hair-cell-like cell of a F2 *pou-iv* -/- polyp, characterized by ciliary-cone-associated microvilli (mv). The apical cell surface faces up. Note the presence of a ciliary rootlet (rl_{ci}). Abbreviations: ve vesicles. Scale bar: 500 nm

POU-IV is necessary for maturation, but not initial differentiation or survival, of hair cells in the sea anemone.

The lack of functional hair cells in *pou-iv -/-* mutants is consistent with POU-IV having a necessary role in initial differentiation and/or maturation of hair cells. In order to more precisely define the functional role of POU-IV in hair cell development, we investigated the morphological and molecular characteristics of epithelial cells expressing the mutant form of POU-IV, which we refer to as POU-IV(-), in tentacular ectoderm of *pou-iv -/-* mutants. Because the epitope that the anti-POU-IV antibody reacts with is intact in the protein encoded by the *pou-iv* allele (Figure 3A, B, D), it was possible to use immunostaining with the anti-POU-IV to localize POU-IV(-) in *pou-iv -/-* mutants. A number of epithelial cells in the tentacular ectoderm were found to express POU-IV(-) (Figure 6A-C). In contrast to the primarily nuclear localization

of POU-IV in wildtype animals (cf. Figure 2), however, POU-IV(-) is distributed throughout the cytoplasm of POU-IV(-)-expressing cells in *pou-iv* -/- mutants (Figure 6A-F), presumably due to the lack of nuclear localization signal (located at the N-terminal end of the homeodomain (Sock et al., 1996)) in POU-IV(-) (Figure 3B). We found that the epithelial cells bearing apical ciliary cones in *pou-iv* -/- mutants expressed POU-IV(-) (Figure 6D-F) and therefore could represent partially differentiated hair cells that failed to undergo maturation. Alternatively, as ciliary cones characterize nematocytes in wildtype *N. vectensis*, it was possible that these ciliary cone-bearing epithelial cells in *pou-iv* -/- mutants were immature nematocytes without cnidae.

To clarify the identity of ciliary cone-bearing epithelial cells in *pou-iv -/-* mutants, we used an antibody against a pan-cnidocyte differentiation marker minicollagen 3 (Ncol3; (Babonis and Martindale, 2017, Zenkert et al., 2011)) to label immature cnidocytes. It was previously shown that Ncol3 was expressed in a subset of ectodermal epithelial cells of *pou-iv* knockout mutants despite the lack of mature cnidae, indicating that immature cnidocytes are present in *pou-iv* mutants and that *pou-iv* is not necessary for initial differentiation of cnidocytes (Tourniere et al., 2020). By using immunostaining with an anti-Ncol3, we confirmed that Ncol3-positive immature cnidocytes in *pou-iv -/-* mutants indeed expressed POU-IV(-) (Figure 6G-I). However, none of the Ncol3-positive immature cnidocytes in *pou-iv -/-* mutants had distinct apical ciliary cones (e.g. Figure 6J-L), suggesting that ciliary cone-bearing epithelial cells in *pou-iv -/-* mutants represent immature hair cells, and not immature nematocytes. Thus, hair cells appear to be present in their immature, yet morphologically differentiated, form in *pou-iv -/-* mutants. The presence of partially differentiated hair cells in *pou-iv -/-* mutants supports the hypothesis that POU-IV regulates maturation, but not initial differentiation, of hair cells in *N. vectensis*.

As discussed above, the absence of stereovillar rootlets in hair cells of *pou-iv -/-* mutants may underlie the observed touch-insensitivity of the mutants. It was also possible that these immature hair cells failed to extend basal neurites to form normal mechanosensory neural circuits. To examine this possibility, we visualized the morphology of immature hair cells in *pou-iv -/-* mutants by using a *pou-iv::kaede* transgenic reporter construct, in which the 3.2 kb genomic sequence upstream of the start codon of the *pou-iv* gene was placed in front of the Kaede fluorescent protein-encoding gene (Ando et al., 2002). We first confirmed that the *pou-iv::kaede* reporter construct indeed drove the expression of Kaede in POU-IV-positive cell types - hair cells and cnidocytes - in tentacular ectoderm of wildtype animals, recapitulating the

endogenous POU-IV expression pattern (Figure 6 - Figure supplement 1). Interestingly, we unexpectedly found that cnidocytes, in addition to hair cells, had basal neurite-like processes (Figure 6 - Figure supplement 1I-L), which has never been reported in cnidarian literature to our knowledge. We then injected *pou-iv::kaede* plasmids into *pou-iv* F2 zygotes, which were allowed to develop into primary polyps, and subsequently carried out immunostaining with antibodies against Kaede and Ncol3. Animals lacking mature cnidae based on Ncol3 staining were assumed to be *pou-iv -/-* mutants. In these presumptive mutants, Kaede-positive immature hair cells were readily identifiable based on morphology and position; their cell bodies were pear-shaped and located in the superficial stratum of the tentacular ectoderm, some of which contained apical microvilli that are organized into a ciliary cone-like microvillar structure (Figure 6M, N). These immature hair cells, however, developed morphologically normal basal neurites (Figure 6O), indicating that *pou-iv* is not necessary for neurite extension in hair cells. Neither is *pou-iv* required for the development of basal neurite-like processes in cnidocytes; basal processes were observed in Ncol3-positive immature cnidocytes (Figure 6 - Figure supplement 2). In mice, one of the *pou-iv* paralogs - *brn3c* – is thought to be required for survival of hair cells because the number of apoptotic cells increases in the inner ear sensory epithelia in Brn-3c null mutant mice (Xiang et al., 1998). We have therefore tested whether pou-iv regulates hair cell survival in N. vectensis, by carrying out the terminal deoxynucleotidyl transferase dUTP nick

663

664

665

666

667

668

669

670

671

672

673

674

675

676

677

678

679

680

681

682

683

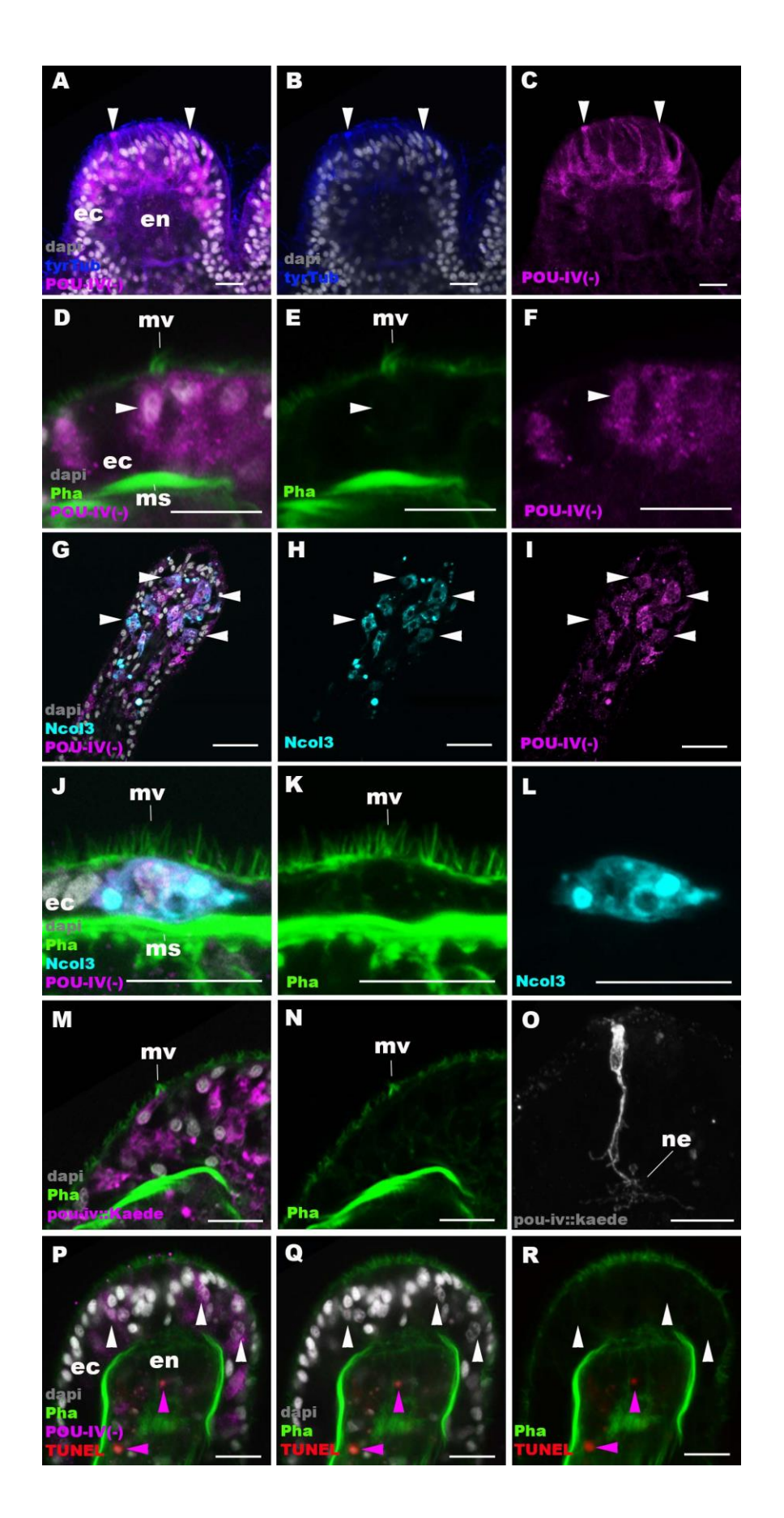
684

685

686

687

survival in *N. vectensis*, by carrying out the terminal deoxynucleotidyl transferase dUTP nick end-labeling (TUNEL) assay in *pou-iv -/-* mutants. We found that none of the POU-IV(-)-expressing epithelial cells examined in the tentacular ectoderm (n= 100 cells across 5 primary polyps) had TUNEL-positive, pyknotic nuclei indicative of apoptotic DNA fragmentation, although TUNEL-positive nuclear fragments were commonly observed in the endoderm (Figure 6P-R). Thus, in sea anemones, POU-IV does not appear to be directly involved in the survival of hair cells.



689 Figure 6: POU-IV is necessary for maturation of hair cells in the sea anemone. 690 Confocal sections of oral tentacles in F2 pou-iv -/- N. vectensis polyps, labeled with antibodies 691 against tyrosinated ∂-tubulin ("tyrTub"), minicollagen 3 ("Ncol3"; (Zenkert et al., 2011)) mutant 692 POU-IV ("POU-IV(-)"), and/or Kaede fluorescent protein ("pou-iv::kaede"). DNA fragmentation is labeled by TUNEL. Filamentous actin is labeled with phalloidin (Pha), and 693 694 nuclei are labeled with DAPI (dapi). In all panels, the apical surface of the tentacular ectodermal 695 epithelium is to the top. A-C: sections through developing oral tentacles with the distal end of the 696 tentacle facing up. Arrowheads point to a subset of POU-IV(-)-expressing epithelial cells, which 697 are abundant in the tentacular ectoderm (ec). Note the cytoplasmic distribution of the POU-IV(-) 698 likely resulting from the lack of nuclear localization signal. D-F: sections showing ciliary cone 699 microvilli (mv)-bearing cells. Ciliary cone-bearing epithelial cells express POU-IV(-) 700 (arrowheads). G-I: sections at the level of surface ectoderm of developing oral tentacles with the 701 distal end of the tentacle facing up. A subset of POU-IV(-)-expressing cells are Ncol3-positive 702 (arrowheads), representing immature cnidocytes. J-L: sections showing an immature cnidocyte 703 which expresses POU-IV(-) and Ncol-3. Note that the cell bears apical microvilli (mv) that do 704 not form a ciliary cone. M-O: sections showing immature hair cells in F2 pou-iv -/- N. vectensis 705 polyps injected with *pou-iv::kaede* construct. Note the presence of ciliary cone microvilli (mv) 706 and basal neurites (ne). P-R: sections through tentacles with the distal end facing up. White 707 arrowheads point to nuclei of POU-IV(-)-expressing ectodermal epithelial cells, which are 708 TUNEL-negative. TUNEL-positive, pyknotic nuclei are observed in the endoderm (purple 709 arrowheads). Abbreviations: ec ectoderm; en endoderm; ms muscle fiber. Scale bar: 10 µm 710

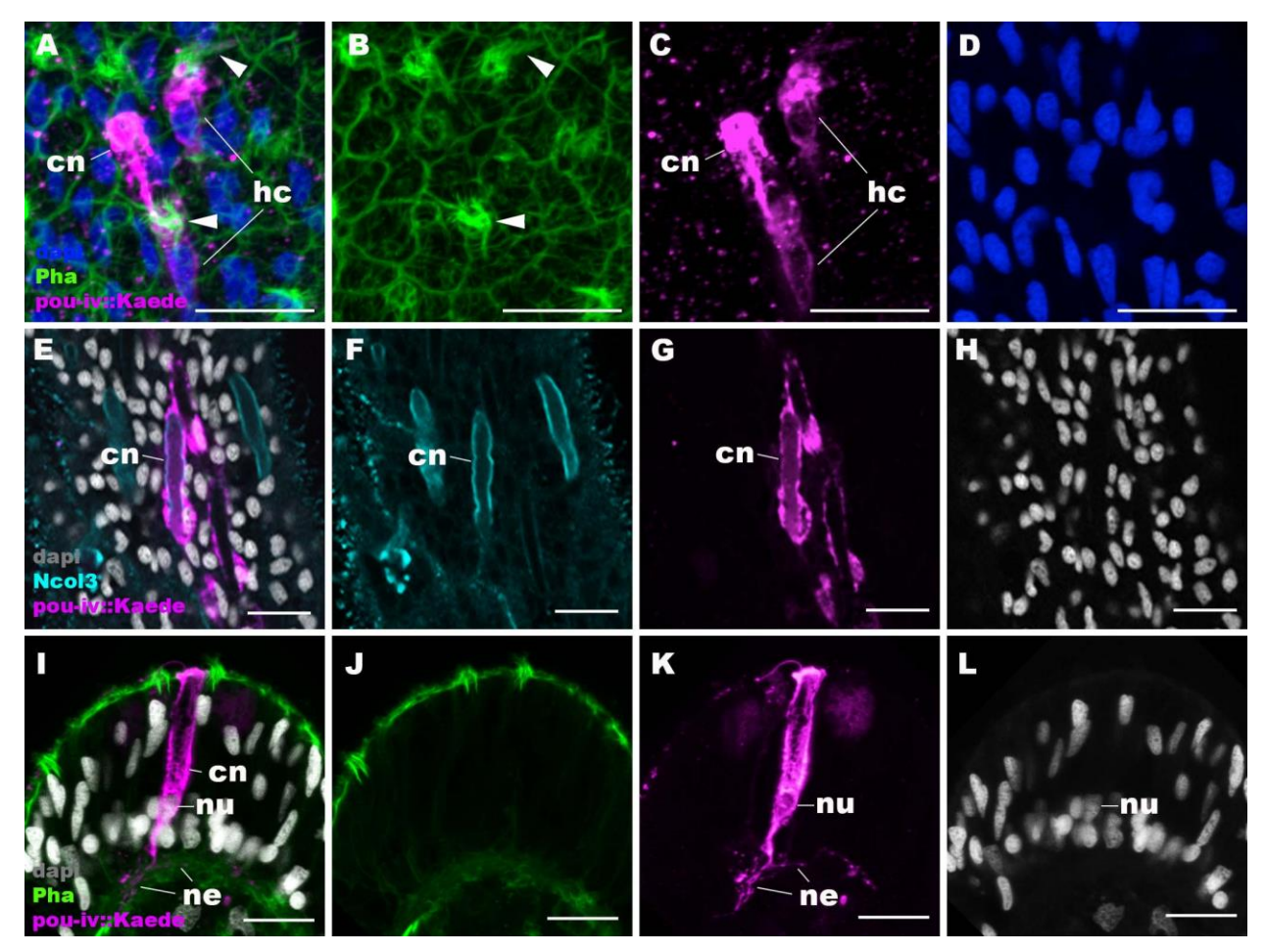


Figure 6 – Figure supplement 1: *pou-iv::Kaede* reporter construct drives transgene expression in hair cells and cnidocytes.

Confocal sections of oral tentacles of *N. vectensis* polyps injected with *pou-iv::kaede* construct, labeled with antibodies against Kaede ("pou-iv::kaede") and minicollagen 3 ("Ncol3"). Filamentous actin is labeled with phalloidin (Pha), and nuclei are labeled with DAPI (dapi). Panels A-H show tangential sections at the level of the surface ectoderm. Panels I-L show a side view of a cnidocyte (cn), with the apical cell surface facing up. *pou-iv::Kaede* expression occurs in hair cells (hc in A-D) and cnidocytes (cn in A-L). Arrowheads in A-C indicate stereovilli of hair cells. Cnidocytes have basally localized nuclei (nu) and extend basal neurite-like processes (ne). Scale bar: 10 µm

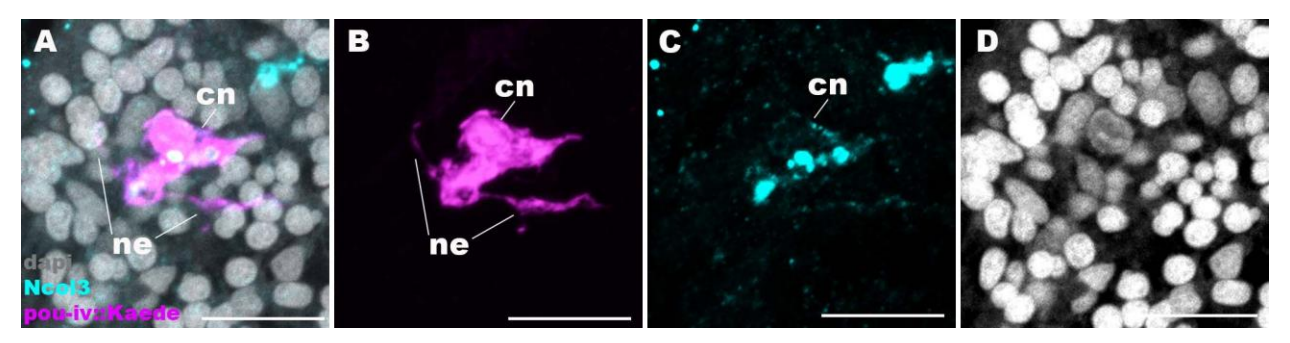


Figure 6 – Figure supplement 2: Cnidocytes in *pou-iv* null mutants develop basal processes.

Confocal sections of a cnidocyte (cn) in the body column of a F2 *pou-iv* +/+ polyp injected with *pou-iv::kaede* construct and labeled with antibodies against Kaede ("pou-iv::kaede") and minicollagen 3 ("Ncol3"). Nuclei are labeled with DAPI (dapi). Panels show tangential sections at the level of the basal ectoderm. Note that the cnidocyte extends neurite-like processes (ne).

729 Scale bar: 10 μm

POU-IV-binding motifs are conserved across Cnidaria and Bilateria.

The evidence presented above thus indicates that in *N. vectensis*, POU-IV is involved in the maturation of mechanosensory hair cells – in addition to that of cnidocytes (Tourniere et al., 2020). How, then, does POU-IV control the development of these two distinct mechanosensory cell types? One possibility is that the POU-IV transcription factor regulates the expression of a shared set of genes critical for differentiation of both cell types. Given that both hair cells and cnidocytes are mechanosensory, POU-IV might control the expression of the same set of mechanotransduction genes in these cell types. Another possibility is that POU-IV regulates the expression of distinct sets of genes in different neural cell types, actively driving the differentiation of the two mechanosensory cell types.

To begin to address this question, we identified genome-wide binding sites for POU-IV by chromatin immunoprecipitation sequencing (ChIP-seq) using the antibody against *N. vectensis* POU-IV. We used adult *N. vectensis* for this experiment, because 1) neurogenesis continues through adulthood (e.g. (Havrilak et al., 2021)), and 2) we needed over 1 gram of tissue samples, which was more difficult to obtain from other developmental stages including primary polyps. We sequenced anti-POU-IV immunoprecipitated DNA and input DNA, and mapped the reads to the *N. vectensis* genome (Putnam et al., 2007). We identified 12,972 genomic sites that were enriched in ChIP DNA (i.e. ChIP peaks) (Figure 7 – Source data 1). We

then performed a *de novo* motif search and motif enrichment analysis, and found three motifs rwrwaatmatgcattattaatatt (motif 1; E=5.2e-075), rmataaataatgcattatttatky (motif 2; E=1.2e-052) and tkcataaattatgmm (motif 3; E=4.8e-36) that were enriched towards the center of ChIP peaks (p=3.5e-368 and p=1.0e-138, respectively) (Figure 7A). When we compared these three motifs against the Jaspar database (Fornes et al., 2020), we discovered that they showed significant sequence similarity to *Homo sapiens* POU4F1, POU4F2 and POU4F3 binding motifs (Figure 7B; $p < 10^{-5}$, $p < 10^{-3}$ and $p < 10^{-3}$, respectively), indicative of deep conservation of POU-IV-binding motifs across Cnidaria and Bilateria. Indeed, the motifs we have identified contain the sequence AT(A/T)ATT(A/T)AT (shown in bold in motif sequences above), which is nearly identical to the core recognition sequence of bilaterian POU-IV, AT(A/T)A(T/A)T(A/T)AT (Gruber et al., 1997). In addition, the preference of GC residues 5' to the core recognition sequence is evident in motifs 1 and 2 (underlined in motif sequences above), and in bilaterian POU-IV binding sequences (Gruber et al., 1997), and therefore appears to be conserved. We tested the ability of POU-IV to bind to the core recognition motif-like sequences by electrophoretic mobility shift assays (EMSAs), and confirmed that they were indeed essential for DNA recognition by POU-IV (Figure 7C). We infer that in the last common ancestor of Cnidaria and Bilateria, POU-IV bound to the consensus DNA element GCAT(A/T)ATT(A/T)AT to regulate gene expression.

749

750

751

752

753

754

755

756

757

758

759

760

761

762

763

764

765

766

767

768 769

770

771

772

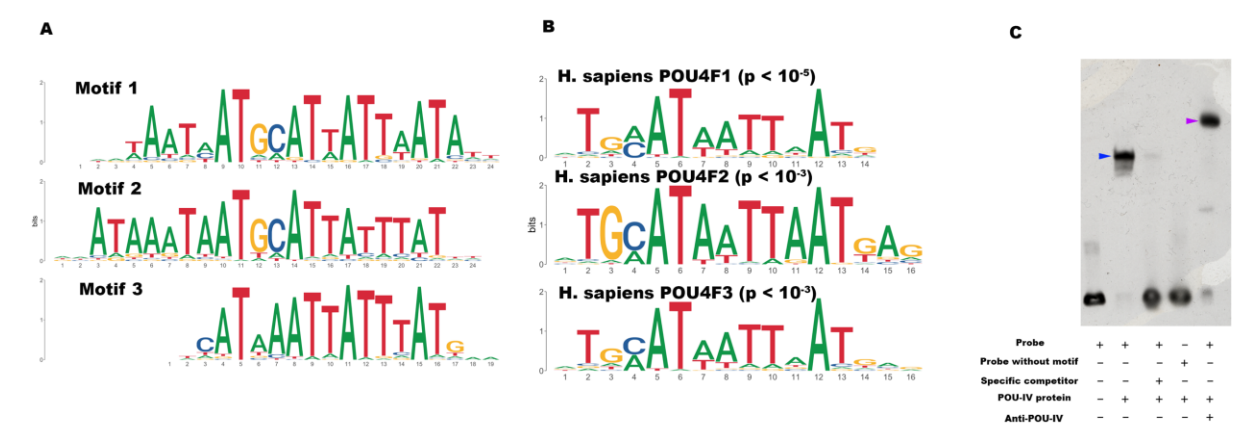


Figure 7: POU-IV-binding motifs are conserved across Cnidaria and Bilateria.

A: Motifs enriched in *Nematostella vectensis* POU-IV ChIP-seq peaks. B: *Homo sapiens* POU motifs resulting from sequence alignment and comparison against the Jaspar database. The p-value reported corresponds to the highest p value for any of the three *Nematostella vectensis*

773 POU4 motifs found. C: Electrophoretic mobility shift assay (EMSA) using purified N. vectensis 774 POU-IV protein and a 50 bp DNA probe containing the conserved core motif CATTATTAAT. 775 Note that retardation of probe migration occurs in the presence of POU-IV protein (blue 776 arrowhead; lane 2), indicative of formation of the protein-DNA complex. Retardation is inhibited 777 in the presence of an unlabeled competitor probe ("Specific competitor"; lane 3). Removal of the 778 motif sequence in the probe ("Probe without motif") abolishes retardation of probe migration by 779 POU-IV (lane 4), demonstrating that the motif is necessary for formation of the protein-DNA 780 complex. The mobility of the probe is further decreased in the presence of the anti-POU-IV 781 antibody (purple arrowhead; lane 5), confirming that the protein bound to the probe is POU-IV. 782 783 Figure 7 – Source data 1: List of 12,972 genome-wide binding sites for POU-IV. 784 Figure 7 – Source data 2: An original gel image used to generate Figure 7C and the original 785 image with relevant lanes labelled. 786 787 Downstream target genes of POU-IV are enriched with effector genes likely involved in 788 neural function in the sea anemone. 789 We next sought to identify downstream target genes of POU-IV, based on the criteria that a 790 target gene has at least one POU-IV ChIP peak within the gene locus which includes the 791 promoter region – 350 bp upstream and 100 bp downstream of the transcription start site – and 792 the gene body. Using this criterion, we found a total of 4188 candidate POU-IV downstream 793 target genes (Supplementary File 1). We then examined which of these candidate POU-IV target 794 genes were activated/repressed by POU-IV, using publicly available transcriptome data from 795 NvPOU4 mutant polyps and their siblings (Tourniere et al., 2020). Re-analysis of the 796 transcriptome data identified 577 genes that were downregulated in NvPOU4 mutants relative to 797 their siblings (Supplementary File 2), and 657 genes that were upregulated in the mutants 798 (Supplementary File 3) (adjusted p-value <0.01). Consistent with the previous report (Tourniere 799 et al., 2020), Gene Ontology terms overrepresented in genes downregulated in NvPOU4 mutants 800 included those related to nervous system function such as "synaptic transmission" and "detection 801 of stimulus" (Supplementary File 4). GO terms overrepresented in genes upregulated in mutants 802 included "endoplasmic reticulum", as identified by Tourniere et al., 2020), as 803 well as a number of additional ones, such as "proteolysis" and "activation of signaling protein

805 downregulated in NvPOU4 mutants relative to their siblings, 293 were POU-IV target genes 806 (Supplementary File 6), while out of the 657 genes upregulated in NvPOU4 mutants 807 (Supplementary File 7), 178 were POU-IV target genes; we assume that the former represent 808 genes that are directly activated by POU-IV, while the latter represent those directly repressed by 809 POU-IV. Among the POU-IV-repressed genes is the *pou-iv* gene itself, indicating that POU-IV 810 negatively regulates its own expression. Gene Ontology analysis found that 84 GO terms were 811 overrepresented in the 293 genes directly activated by POU-IV, which include terms related to 812 nervous system function such as "synaptic transmission" (p-adjusted<0.05) (Supplementary File 813 8). No GO terms were significantly overrepresented in the 178 genes directly repressed by POU-814 IV (p-adjusted<0.05). 815 816 POU-IV regulates the expression of the hair-cell-specific effector gene polycystin 1 in the 817 sea anemone. 818 To shed light on the mechanism by which POU-IV regulates hair cell maturation, we assessed 819 which genes were directly activated by POU-IV in hair cells. Among the 577 genes significantly 820 downregulated in NvPOU4 mutants relative to their siblings is a transmembrane receptor-821 encoding polycystin-like gene (JGI ID: 135278). By using in situ hybridization, we found that 822 this gene was specifically expressed in tentacular epithelial cells whose cell bodies were located 823 in the superficial stratum of the pseudostratified epithelium, resembling the hair cell (Figure 8A-824 F). We discovered by RTPCR that this gene and another *polycystin-like* gene (JGI ID: 218539) 825 upstream – which was also one of the 577 genes significantly downregulated in NvPOU4 826 mutants relative to their siblings – together constitute a single *polycystin-like* gene. The transcript 827 of the polycystin-like is 11,279 bases long, and encodes a protein that is 3457 amino acids long 828 (Figure 8 - Figure supplement 1; GenBank accession number, OK338071). ChIP-seq data show 829 that there are two POU-IV-binding motifs around the transcription start site of this locus (Figure 830 8G), suggesting that the *polycystin-like* gene is directly regulated by POU-IV. 831 We predicted the structure of the *polycystin-like* based on sequence similarity to known 832 polycysin 1 proteins. Transmembrane-spanning regions were predicted by using Phyre2 (Kelley 833 et al., 2015) and based on the alignment with human and Fugu PKD1 sequences (GenBank 834 accession numbers AAC37576 and AAB86683, respectively). Non-transmembrane-spanning

activity involved in unfolded protein response" (Supplementary File 5). Out of the 577 genes

regions were predicted by using NCBI conserved domain search with default Blast search parameters. The N. vectensis polycystin 1-like protein was predicted to have a Polycystin 1 (PKD1)-like domain structure, containing the extracellular PKD domain and REJ (receptor for egg jelly) module that are uniquely shared by Polycystin 1 proteins (Moy et al., 1996, Bycroft et al., 1999), the extracellular WSC (cell wall integrity and stress component) carbohydrate-binding domain, the intracellular PLAT (polycystin-1, lipoxygenase and alpha toxin) domain (Bateman and Sandford, 1999), the extracellular TOP (tetragonal opening for polycystins) domain (Grieben et al., 2017), and 11 transmembrane domains (Sandford et al., 1997) (Figure 8 - Figure supplement 1). However, unlike vertebrate Polycystin 1, Leucine rich repeat, C-type lectin, and LDL-like domains that reside in the N-terminal extracellular tail and a coiled-coil domain at the C-terminal intracellular tail were not identifiable. The last six transmembrane domains of Polycystin 1 are thought to be homologous to transient receptor potential (TRP) cation channels including Polycystin 2 (PKD2) (Mochizuki et al., 1996); in addition, the TOP domain is shared across Polycystin 1 and 2 (Grieben et al., 2017). We therefore generated an amino acid sequence alignment of the TOP domain and transmembrane domains of Polycystin 1 and Polycystin 2 proteins, and used it to carry out maximum likelihood phylogeny estimation. The results robustly placed the newly discovered Nematostella vectensis polycystin-1-like within the Polycystin 1 group (Figure 8 - Figure supplement 2). We therefore designate this gene as Nematostella vectensis polycystin 1. To better resolve the cell type in which *polycystin 1* is expressed, we generated a reporter construct using 3704bp sequence encompassing the two POU-IV-binding motifs and upstream promoter region of the gene (scaffold 353:49,338-53,412). We injected this construct into

835

836

837

838

839

840

841

842

843

844

845

846

847

848

849

850

851

852

853

854

855

856

857

858

859

860

861

862

863

promoter region of the gene (scaffold 353:49,338-53,412). We injected this construct into wildtype zygotes and confirmed reporter gene expression specifically in hair cells at the primary polyp stage (Figure 8H-K). In addition, we have validated by *in situ* hybridization that *polycystin1* expression is lost in *pou-iv -/-* mutants (n=5) but not in their siblings (n=3) (Figure 8L-S). Taken together, these results suggest that *polycystin1* is directly activated by POU-IV in hair cells. To our knowledge, *polycystin1* represents the first molecular marker specific to cnidarian hair cells.

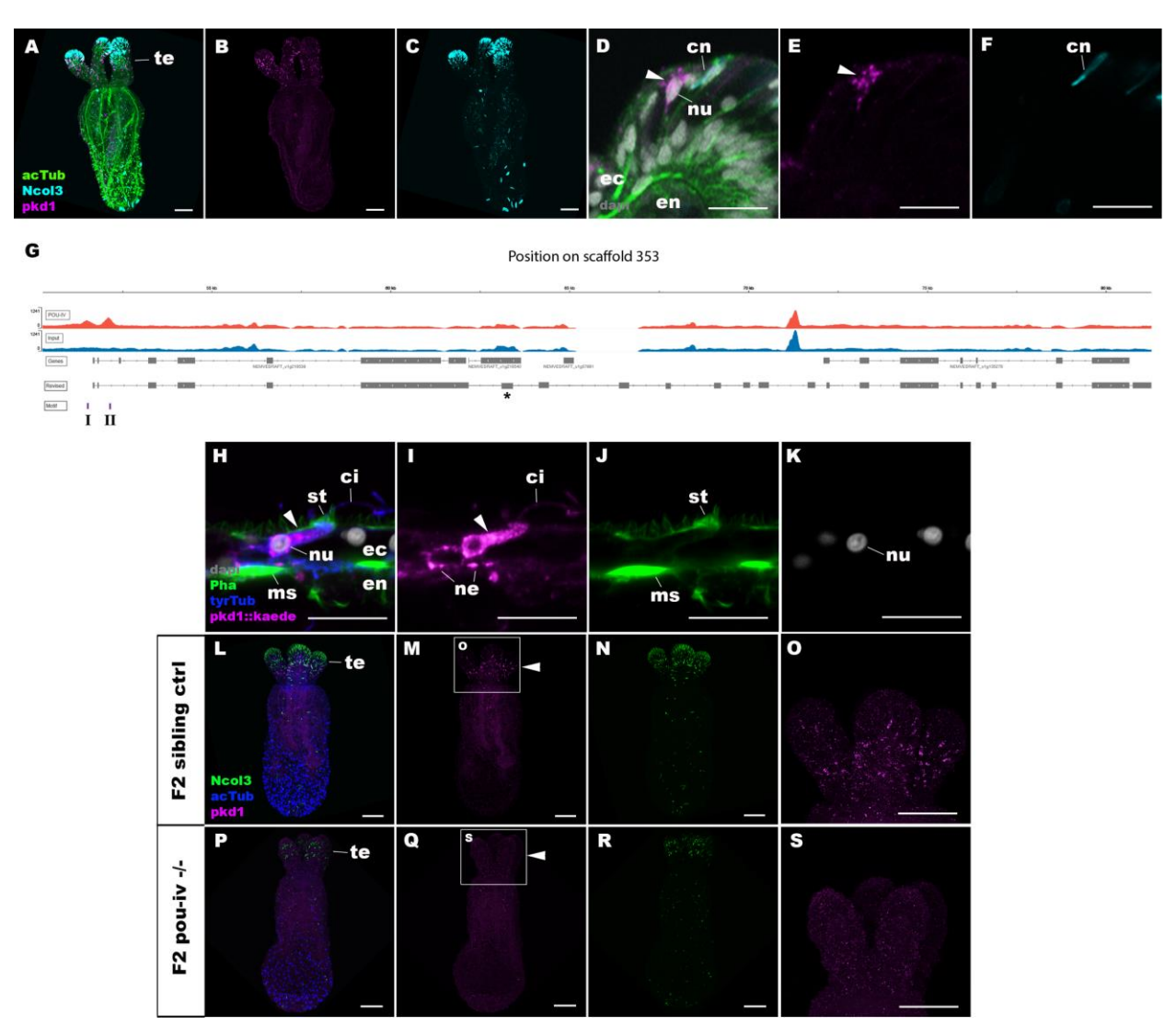


Figure 8: POU-IV activates the expression of *polycystin 1* specifically in hair cells.

A-F: Confocal sections of primary polyps labeled with an antisense riboprobe against *polycystin1* transcript ("pkd1") and antibodies against acetylated ∂-tubulin ("acTub") and minicollagen 3 ("Ncol3"; (Zenkert et al., 2011)). Nuclei are labeled with DAPI ("dapi"). A-C are side views of the animal with the oral opening facing up. Expression of *polycystin1* occurs exclusively in the ectoderm of the oral tentacles (te). D-F are side views of a *polycystin1*-expressing epithelial cell (arrowhead) in the tentacular ectoderm (ec) with its apical surface facing up. Note that the cell body is localized apically and lacks minicollagen 3 expression. G: A schematic of the *polycystin1* locus, showing the distribution of POU-IV ChIP DNA ("POU-IV") and input DNA from adult polyps. JGI gene models ("Genes") and the revised gene model based on RTPCR ("Revised") and the locations of the consensus POU-IV-binding motif - AT(A/T)ATT(A/T)AT - are numbered as I and II. X-axis shows the position along the genomic scaffold, and Y-axis

877 shows the number of reads. * shows an exon whose sequence is missing in the publicly available 878 N. vectensis genome (v.1.0; (Putnam et al., 2007)). H-K: Confocal sections of an oral tentacle of 879 a primary polyp injected with *polycystin1::Kaede* construct, labeled with an antibody against 880 Kaede ("pkd1::kaede"). Filamentous actin is labeled with phalloidin (Pha). The apical surface of 881 the tentacular ectodermal epithelium is to the top. Note that the Kaede-positive cell (arrowhead) 882 has an apical cilium (ci) and stereovilli (st), a central nucleus (nu), and basal neurites (ne), 883 exhibiting morphological hallmarks of a hair cell. No other cell types were found to be Kaede-884 positive. L-S: Confocal sections of a homozygous pou-iv mutant ("F2 pou-iv -/-", P-S) and its sibling control (F2 pou-iv +/+ or pou-iv +/-, "F2 sibling ctrl", L-O) at the primary polyp stage, 885 886 labeled with an antisense riboprobe against *polycystin1* transcript ("pkd1") and antibodies 887 against acetylated ∂-tubulin ("acTub") and minicollagen 3 ("Ncol3"; (Zenkert et al., 2011)). 888 Panels show side views of the animal with the oral opening facing up. Animals lacking mature 889 cnidocysts based on Ncol3 staining were assumed to be pou-iv -/- mutants; animals with mature 890 cnidocysts were assumed to be pou-iv +/+ or pou-iv +/-. O and S are magnified views of 891 tentacles boxed in M and Q, respectively. Note that *polycystin1* expression in tentacular 892 ectoderm (arrowhead in M; O) is absent in the POU-IV null mutant (arrowhead in Q; S), 893 demonstrating that POU-IV is necessary for *polycystin1* expression. Abbreviations: en 894 endoderm; cn cnidocyst; nu nucleus; ms muscle fiber. Scale bar: 50 µm (A-C, L-S); 10 µm (D-F, 895 H-K)

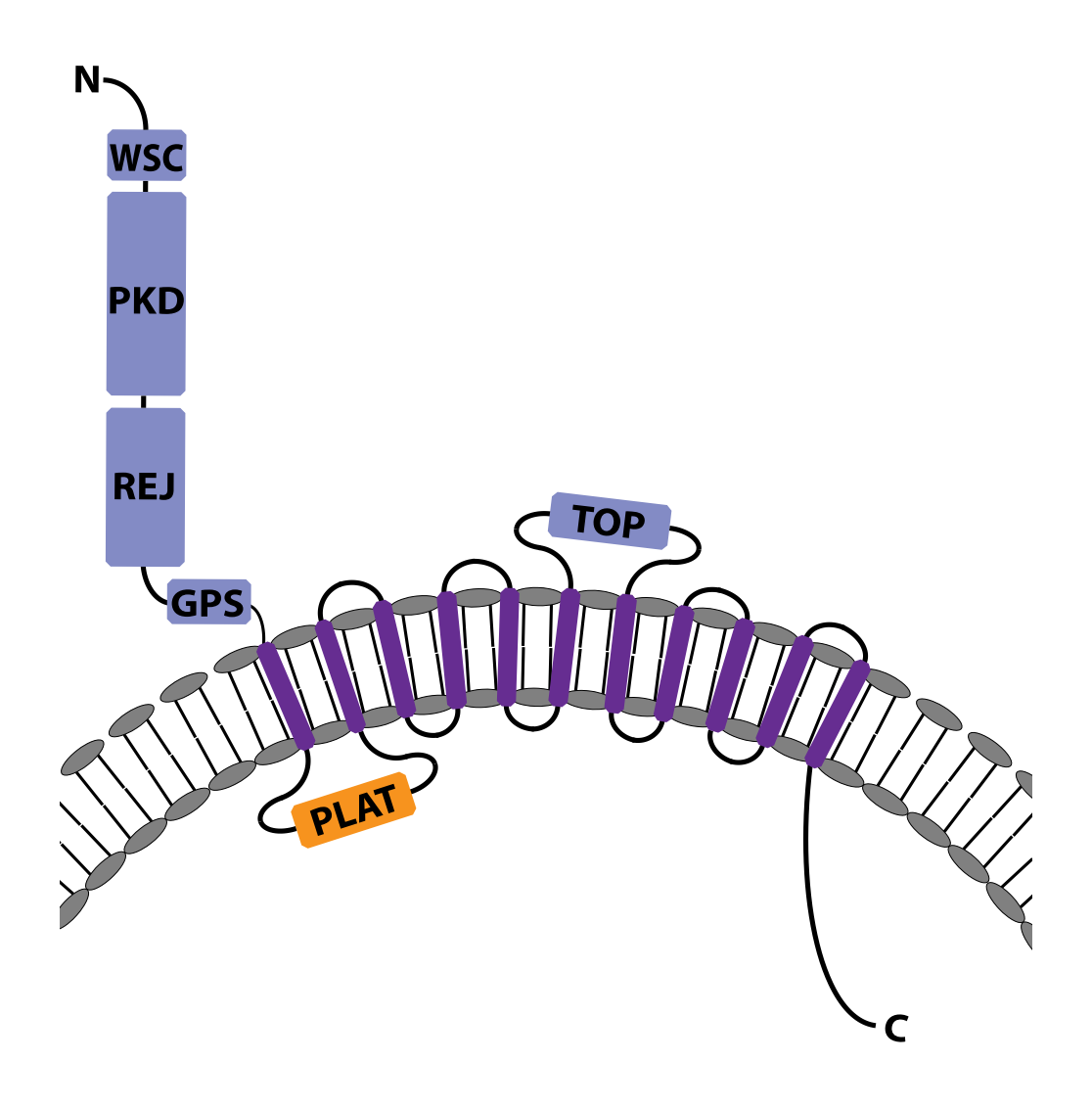


Figure 8 – Figure supplement 1: The predicted protein structure of the *Nematostella* vectensis polycystin 1-like.

The predicted protein structure of *Nematostella vectensis polycystin 1-like*. Extracellular domains are shown in blue, the intracellular domains in orange, and the transmembrane domains in purple. Transmembrane-spanning regions were predicted by using Phyre2 (Kelley et al., 2015) and based on alignment with human and *Fugu* PKD1 sequences. Non-transmembrane-spanning regions were predicted by using NCBI conserved domain search with default Blast search parameters. The PKD domain and the REJ module are specific to Polycystin 1 (PKD1) proteins. Abbreviations: WSC, cell wall integrity and stress response component; REJ, receptor for egg jelly; GPCR, G-protein coupled receptor; TM, transmembrane domain; PLAT, polycystin-1, lipoxygenase and alpha toxin; TOP, tetragonal opening for polycystins

Figure 8 – Figure supplement 1 – Source Data 1: Partial cDNA sequence of Nematostella vectensis polycystin 1-like, in which the start codon and stop codon are highlighted in green and red, respectively.

Figure 8 – Figure supplement 1 – Source Data 2: Tanslated amino acid sequence of Nematostella vectensis polycystin 1-like, in which conserved domains are highlighted in light blue for transmembrane-spanning regions and in purple for other domains.

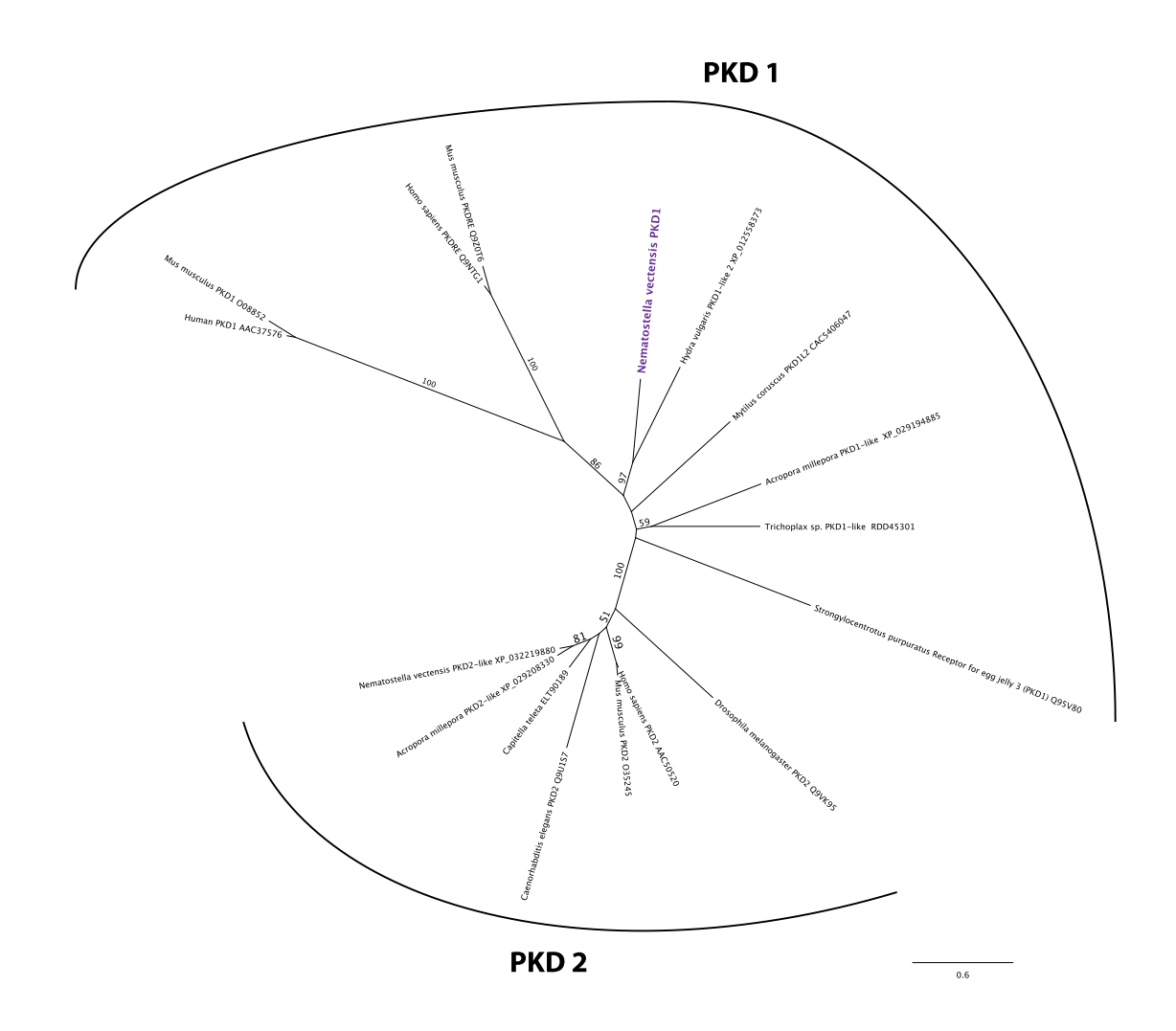


Figure 8 – Figure supplement 2: *Nematostella vectensis polycystin 1-like* belongs to the Polycystin 1/PKD1 group.

Unrooted maximum likelihood phylogeny of Polycystin protein families based on the alignment of Polycystin 1 (PKD1) and Polycystin 2 (PKD2) protein sequences that span the conserved TOP

921 and transmembrane domains over 323 amino acid sites. NCBI accession numbers are shown with 922 the name of each sequence. Bootstrap support values are shown at each node except when lower 923 than 50%. The unit of the branch length is the number of substitutions per site. Note the strong 924 support for the placement of Nematostella vectensis polycystin 1-like (Nematostella vectensis 925 PKD1, highlighted in purple) within the PKD1 group, and for that of N. vectensis PKD2-like 926 within the PKD2 group. The JGI ID for *N. vectensis* PKD2 (polycystin 2)-like is 160849. 927 928 Figure 8 – Figure supplement 2 – Source Data 1: Alignment of polycystin 1 and polycystin 2 929 amino acid sequences used to construct phylogeny shown in Figure 8 – Figure supplement 930 2. 931 932 POU-IV controls the maturation of hair cells and cnidocytes via distinct gene regulatory 933 mechanisms. 934 Next, we have utilized publicly available single-cell transcriptome data from N. vectensis 935 wildtype adults (Sebe-Pedros et al., 2018) to uncover additional candidate genes that are directly 936 activated by POU-IV in hair cells. Both polycystin-like gene models (JGI IDs: 135278 and 937 218539) that are part of the newly discovered *polycystin 1* are uniquely represented in one of 938 Sebe-Pedros et al.'s transcriptomically defined adult cell types ("c79") referred to as the 939 metacells (Sebe-Pedros et al., 2018). We have therefore deduced that the adult metacell c79 940 represents the hair cell, which enabled identification of additional POU-IV target genes activated 941 in hair cells. Out of the 293 genes directly activated by POU-IV, we found a total of 32 genes 942 that were represented in the adult metacell c79 (the presumptive hair cell) (Supplementary File 9). 943 They include potassium channel-like (NVE ID: 12832; no JGI ID), GABA receptor-like (JGI 944 gene ID: 98897), and polycystin 2 (JGI gene ID: 160849; Figure 8 - Figure supplement 2), in 945 addition to polycystin 1 identified above. 3 of the 32 genes – coagulation factor/neuropilin-like 946 (JGI gene ID: 202575), CD59 glycoprotein-like (NVE ID: 735; no JGI ID), and polycystin 1 – 947 are not found in any other metacell. No transcription factor-encoding genes were found to be 948 activated by POU-IV in hair cells. Gene Ontology analysis found that 5 GO terms were 949 overrepresented in POU-IV activated genes in hair cells (p-adjusted<0.05), including "potassium" 950 ion transmembrane transport" and "sensory perception of sound" (Supplementary File 10). In 951 contrast, out of the 178 genes that are repressed by POU-IV, only two genes – pou-iv itself and

peptidylglycine alpha-amidating monooxygenase-like (JGI gene ID: 172604) – are represented in the adult metacell c79 (Supplementary File 9). These results are consistent with the hypothesis that POU-IV controls the maturation of hair cells by activating a cell-type-specific combination of effector genes that confer hair cell identity.

952

953

954

955

956

957

958

959

960

961

962

963

964

965

966

967

968

969

970

971

972

973

974

975

976

977

978

979

980

981

982

We have taken a similar approach to examine how POU-IV regulates the maturation of cnidocytes. Sebe-Pedro et al. categorized cnidocytes into eight transcriptomically distinct metacells (c1-c8), out of which c8 expresses pou-iv (Sebe-Pedros et al., 2018). Of the 293 genes activated by POU-IV, we found 3 genes in c8, which consisted of two transmembrane propyl 4hydroxylase-like genes (JGI gene IDs: 239358 and 118978) and a serine transporter-like gene (JGI gene ID: 238501) (Supplementary File 11). serine transporter-like and one of the hydroxylase-like genes (JGI gene IDs: 239358) are represented specifically in chidocyte metacells and not in others (Sebe-Pedros et al., 2018). As in hair cells, transcription factorencoding genes were not found to be activated by POU-IV in cnidocytes. Of the 178 genes that are repressed by POU-IV, 13 genes were found in the cnidocyte metacell c8, which included genes encoding zinc finger and Sox transcription factors (Supplementary File 11) and showed significant enrichment of the GO term "transcription from RNA polymerase II promoter" (padjusted<0.05; Supplementary File 12). Importantly, we found no overlap in genes activated by POU-IV between hair cells and cnidocytes, which indicates that POU-IV controls the maturation of hair cells and enidocytes by regulating the expression of distinct sets of genes. In addition, POU-IV may have a more significant role as a leaky repressor – to fine-tune gene expression levels – in chidocytes than in hair cells, as the proportion of POU-IV-repressed genes relative to the total number of POU-IV targets represented in a given metacell was substantially higher in the cnidocyte (13/16; 81.25%) than in the hair cell (3/35; 8.6%). This pattern of gene regulation by POU-IV appears to be specific to cnidocytes. The proportion of POU-IV-repressed genes relative to the total number of POU-IV targets represented in non-cnidocyte, POU-IV-positive adult metacells – namely, c63, c64, c65, c66, c75, c76, and c102, in addition to c79 – was low, ranging from 2.2% to 13%, while that in POU-IV-positive, adult cnidocyte metacells - c100 that expresses spirocyte-specific minicollagen (JGI gene ID: 81941) and c101 that expresses nematocyte-specific minicollagen I (JGI gene ID: 211803) (Sebe-Pedros et al., 2018) – was 83.9% in c100 and 82.1% in c101 (Supplementary File 13), similar to the cnidocyte metacell c8. Taken together, these data suggest that POU-IV directs the maturation of cnidocytes not only by

activating a unique combination of effector genes, but also by negatively controlling the expression levels of a larger number of genes, including those encoding transcriptional regulators, in a leaky manner. Thus, the gene regulatory mechanisms by which POU-IV orchestrates the differentiation of hair cells and cnidocytes appear to be remarkably distinct.

Discussion:

In this paper, we identified the class IV POU homeodomain transcription factor (POU-IV) as an essential developmental regulator of cnidarian mechanosensory hair cells. This is the first discovery of a gene regulatory factor necessary for the development of classical mechanosensory neurons – that transmit mechanosensory information to other cells to elicit coordinated behavior – from a non-bilaterian, early-evolving animal group. Using the starlet sea anemone Nematostella vectensis, we have shown that POU-IV is postmitotically expressed in hair cells in the ectodermal epithelium of feeding tentacles during development. In addition, we have found that null mutation of pou-iv renders the animal unable to respond to tactile stimulation to its tentacles, and results in the loss of stereovillar rootlets, but not of neurites, in hair cells. Furthermore, we have presented evidence that POU-IV binds to deeply conserved DNA sequence motifs, and directly activates the expression of a unique combination of effector genes, but not transcription factor-encoding genes, specifically in hair cells. Among the POU-IV target effector genes we discovered the first chidarian hair cell-specific molecular marker, polycystin1, which encodes a transmembrane receptor of the TRP channel superfamily. The results suggest that POU-IV plays a necessary role in regulating the maturation of mechanosensory hair cells in the sea anemone by directly activating the expression of cell-type-specific effector genes. Our findings strongly support POU-IV being the terminal selector of hair cell identity in the sea anemone.

Several lines of evidence indicate that POU-IV is specifically involved in the maturation, and not progenitor proliferation, initial differentiation, or survival, of hair cells in the tentacular ectoderm in *N. vectensis*. First, POU-IV is postmitotically expressed in hair cells in tentacular ectoderm, and thus is unlikely to have roles in proliferation or generation of their progenitor cells. Second, in POU-IV null mutants, we have found ciliary-cone-bearing epithelial cells that resemble hair cells in morphology and position within the epithelium; these cells are characterized by having an apical cilium surrounded by a circle of microvilli, a pear-shaped cell

body located in the superficial stratum of the pseudostratified epithelium, and basal neurites. None of the ciliary-cone-bearing epithelial cells express the pan-cnidocyte marker minicollagen 3, suggesting that the ciliary-cone-bearing cells in POU-IV null mutants do not represent partially differentiated nematocytes. The existence of differentiated hair cells in POU-IV null mutants implies that POU-IV is not involved in the initial differentiation of hair cells. However, the hair-cell-like cells of POU-IV null mutants failed to form a mature apical mechanosensory apparatus with stereovillar rootlets, indicating that POU-IV is essential for maturation of hair cells. Lastly, we have found no evidence that the epithelial cells expressing the non-functional form of POU-IV protein in POU-IV null mutants undergo programmed cell death in the tentacular ectoderm. Thus, POU-IV does not seem to be required for the survival of hair cells in the tentacles. Taken together, these data support the hypothesis that POU-IV regulates the maturation, but not progenitor proliferation, initial differentiation, or survival, of mechanosensory hair cells in the sea anemone.

The loss of stereovillar rootlets in hair cells in *pou-iv* mutants suggests that the POU-IV transcription factor regulates the expression of genes that are involved in stereovillar development. Given that stereovillar rootlets consist of actin filaments, actin-binding proteins may be regarded as potential regulators of stereovillar rootlet formation in hair cells. Among the identified POU-IV target genes expressed in hair cells is *polycystin 1*, which encodes a large transmembrane receptor with multiple extracellular and intracellular domains and TRP-channel-like transmembrane domains. Interestingly, its mouse homolog (PC-1) colocalizes with F-actin in inner ear hair cell stereovilli and is necessary for maintenance of stereovillar structure and normal hearing (Steigelman et al., 2011). In addition, PC-1 has been shown to regulate actin cytoskeleton reorganization in canine kidney epithelial cells (Boca et al., 2007). If the function of Polycystin 1 in modulating the organization of actin cytoskeleton is broadly conserved, *N. vectensis* Polycystin 1 might control the structural integrity of stereovilli in hair cells through its interaction with F-actin. POU-IV may therefore direct stereovillar development in cnidarian hair cells by activating *polycystin 1*. Functional analysis of *N. vectensis polycystin 1* to evaluate its role in stereovillar development is warranted.

We have proposed that the lack of tentacular response to tactile stimuli in *pou-iv* mutants is due to the loss of structural rigidity in the apical mechanosensory apparatus – stereovilli, in particular – of hair cells, resulting from the failure of hair cells to form stereovillar rootlets. We

note, however, that it could additionally be because of the functional defects in mechanotransduction channels. POU-IV is known to directly activate the expression of the mechanotransduction channel-encoding gene, *mec-4*, that is necessary for touch-cell function in *C. elegans* (Duggan et al., 1998). The Polycystin 1 protein discussed above contains transmembrane domains that are homologous to the transient receptor potential (TRP) calcium channel. If this channel is involved in mechanotransduction, the loss of *polycystin 1* expression in *pou-iv* mutants would directly lead to loss of mechanotransduction channel function. This hypothesis may be evaluated by specifically examining the role of the channel-encoding region of *N. vectensis polycystin 1* in mechanotransduction.

Alternatively, the loss of *polycystin 1* expression may indirectly perturb channel function. In epithelial cells of vertebrate kidneys, Polycystin 1 interacts with the calcium ion channel Polycystin 2 to form a complex that functions as a fluid flow sensor with Polycystin 1 acting as a mechanosensitive cell surface receptor and Polycystin 2 as an ion-permeant pore (reviewed in (Delmas, 2004)). The *Nematostella vectensis* genome encodes *polycystin 2* (Figure 8 - Figure supplement 2), which is co-expressed with *polycystin 1* in the adult metacell c79 (i.e. the hair cell) (Supplementary File 9; (Sebe-Pedros et al., 2018)). If these two proteins form a mechanically gated ion channel complex in hair cells as in vertebrate kidney epithelial cells, the loss of expression of *polycystin 1* would perturb the ability of the complex to sense mechanical stimuli, resulting in defects in channel function. To explore this hypothesis, the important next step will be to assess whether Polycystin 1 and 2 form a complex in *N. vectensis*.

We note that, although our findings are consistent with the hypothesis that cnidarian hair cells function as mechanosensors, we do not rule out the possibility that cnidarian hair cells might be multimodal sensory cells; they might have additional functions as chemoreceptors and/or photoreceptors. Indeed, hair cells of the sea anemone *Haliplanella luciae* have been reported to respond to N-acetylated sugars by elongating their stereovilli (Mirethibodeaux and Watson, 1994, Watson and Roberts, 1995), indicative of chemosensory function. The metacell c79 (the presumptive hair cell) of adult *N. vectensis* expresses several G-protein-coupled receptor (GPCR)-encoding genes (Supplementary File 14; (Sebe-Pedros et al., 2018), some of which might encode chemosensory receptors; none were found to encode opsins. Functional analyses of these GPCRs may shed light on the molecular basis of sensory multimodality in cnidarian hair cells.

Our results indicate that the role for POU-IV in mechanoreceptor development is broadly conserved across Cnidaria and Bilateria. As mentioned above, one of the vertebrate pou-iv paralogs (Brn3c) is necessary for maturation and survival of inner ear hair cells in mice (Xiang et al., 1998, Xiang et al., 1997a, Erkman et al., 1996). Likewise, in C. elegans, differentiation of mechanosensory touch cells requires a *pou-iv* ortholog *unc-86* (Chalfie and Sulston, 1981, Chalfie and Au, 1989, Finney and Ruvkun, 1990, Duggan et al., 1998, Chalfie et al., 1981). In Cnidaria, pou-iv is expressed in mechanosensory organs in scyphozoan and hydrozoan jellyfish (Nakanishi et al., 2010, Hroudova et al., 2012), and is necessary for differentiation of the lineage-specific mechanosensory-effector cell, the cnidocyte, in N. vectensis (Tournier et al., 2020). In this report, we have demonstrated that *pou-iv* has an essential role in the maturation of the classical mechanosensory neuron of Cnidaria – the hair cell – using *N. vectensis*. These comparative data show that POU-IV-dependent regulation of mechanosensory cell differentiation is pervasive across Cnidaria and Bilateria, and likely predates their divergence. How early the role of POU-IV in mechanoreceptor differentiation emerged in animal evolution remains unresolved, and requires comparative data from placozoans and sponges, which are wanting.

We note, however, that POU-IV has a broad role in the differentiation of multiple neural cell types across Cnidaria and Bilateria. In *N. vectensis*, POU-IV expression is not restricted to mechanosensory hair cells and cnidocytes, but also found in RFamidergic neurons and *NvElav1*-positive endodermal neurons (Tournier et al., 2020). Likewise in Bilateria, POU-IV regulates the differentiation of a variety of neural cell types beyond mechanosensory cells, including chemosensory neurons in insects (Clyne et al., 1999) and photosensory neurons in vertebrates (retinal ganglion cells; e.g. Erkman et al., 1996, Gan et al., 1996)). Therefore, it seems plausible that POU-IV was ancestrally involved in the differentiation of multiple neural cell types in addition to mechanosensory cells.

Interestingly, POU-IV is required for normal development of stereovilli in hair cells in both sea anemones (this study) and mice (Xiang et al., 1998), raising the possibility that POU-IV controlled the formation of the apical sensory apparatus of mechanosensory cells in the last common ancestor of Cnidaria and Bilateria, potentially via regulation of *polycyctin 1*. Alternatively, the essential role for POU-IV in stereovillar formation in mechanosensory cells could have evolved independently in Cnidaria and vertebrates. Comparative studies of the

mechanism of stereovillar formation across sea anemones and vertebrates, along with mechanistic studies of POU-IV gene function in phylogenetically informative taxa, such as medusozoan chidarians and acoel bilaterians, are needed to evaluate these alternative hypotheses.

Regulatory factors acting upstream of POU-IV in cnidarian hair cell development remain unknown. In Bilateria, members of the Atonal basic-loop-helix-loop-helix (bHLH) transcription factor family appear to have a conserved role in positive regulation of POU-IV expression (reviewed in (Leyva-Diaz et al., 2020)). For instance, vertebrate *atonal* genes act upstream of *pou-iv* genes to drive the differentiation of inner ear hair cells (Ikeda et al., 2015, Masuda et al., 2011, Yu et al., 2021) and retinal ganglion cells (Liu et al., 2001). Similarly, *C. elegans atonal* ortholog *lin-32* controls the expression of the *pou-iv* ortholog *unc-86* in touch sensory neurons (Baumeister et al., 1996). Although cnidarians lack unambiguous *atonal* orthologs, they have divergent bHLH genes that belong to the Atonal superfamily, which consists of Atonal and related bHLH gene families including Neurogenin, and NeuroD (Gyoja et al., 2012, Simionato et al., 2007). Whether these *atonal-like* bHLH factors function upstream of POU-IV in the context of cnidarian hair cell development needs to be assessed, as it may provide insights into the evolution of gene regulatory mechanisms underpinning mechanoreceptor development across Cnidaria and Bilateria.

In light of new comparative data reported herein emerges a model of mechanosensory cell differentiation in the last common ancestor of Cnidaria and Bilateria. We assume that the embryo of the Cnidaria-Bilateria ancestor had neurogenic ectoderm (Nakanishi et al., 2012). During late embryogenesis or postembryonic development of this ancestor, mechanosensory cell progenitors differentiated into postmitotic sensory cells in the ectoderm, extending apical cilia and basal neurites. These postmitotic sensory cells expressed the terminal selector POU-IV, which translocated to the cell nuclei, and bound to the DNA recognition motif GCAT(A/T)ATT(A/T)AT (i.e. the consensus motif across Bilateria and Cnidaria) associated with target genes in these cells. This activated the expression of effector genes, possibly including *polycystin 1*, whose protein products generated mechanoreceptor-specific structures necessary for mechanosensory function, such as the apical mechanosensory apparatus consisting of a cilium surrounded by a ring of stereovilli. The mature identity of the mechanosensory cell was thereby established.

Following the divergence of Cnidaria and Bilateria, POU-IV may have been recruited for the evolution of the lineage-specific mechanosensory effector – the cnidocyte – in Cnidaria, as pou-iv is essential for chidocyte development in N. vectensis (Tourniere et al., 2020). How POU-IV would have come to direct enidocyte development remains unclear. Given that both hair cells and cnidocytes are mechanosensory cell types, it seems reasonable to expect that an ancestral POU-IV gene regulatory network that defined mechanosensory cell identity was repurposed for the emergence of cnidocytes, and should be shared across these two cell types. However, we found no evidence in support of this hypothesis; instead, our results suggest that POU-IV controls distinct sets of genes in each cell type. One possible evolutionary scenario to account for this observation is that POU-IV initially activated the same battery of effector genes in the ancestral cnidocytes and hair cells, but POU-IV target genes diverged substantially during cnidarian evolution so that they no longer overlap between the two cell types. Another possibility is that POU-IV regulated a unique set of genes in the ancestral chidocytes when POU-IV became part of the cnidocyte gene regulatory network. This possibility seems conceivable if POU-IV expression was activated in epigenetically distinct cell lineages, so that between the cnidocyte lineage and the hair cell lineage 1) POU-IV cooperated with different co-factors, and/or 2) the accessibility of POU-IV target genes differed, which would result in differential expression of POU-IV target genes. Evidence from bilaterian models such as C. elegans and mice indicates that POU-IV cooperates with a range of different co-factors to define distinct neural identities (reviewed in (Leyva-Diaz et al., 2020), suggesting an important role for POU-IV cofactors in the diversification of neural cell types. Whether evolution of POU-IV cofactors played a role in the evolution of cnidocytes remains to be tested. Investigation into the mechanism by which POU-IV activates distinct sets of genes across enidocytes and hair cells will be the critical next step for shedding light on how POU-IV may have contributed to the evolution of the novel mechanosensory cell type of Cnidaria.

1162

1163

1137

1138

1139

1140

1141

1142

1143

1144

1145

1146

1147

1148

1149

1150

1151

1152

1153

1154

1155

1156

1157

1158

1159

1160

1161

Materials and Methods:

Key Resources Table	Kev	Resources	Table
----------------------------	-----	-----------	--------------

Reagent type (species) or resource	Designation	Source or reference	Identifiers	Additional information
Strain, strain background (Nematostella vectensis)	F1 <i>pou-iv</i> +/-	This paper	Nv F1 <i>pou-iv</i> +/-, this paper	Nakanishi lab, University of Arkansas
Antibody	POU- IV/Brn-3; rabbit; polyclonal	This paper	RRID:AB_2895 562	(1:200) dilution used; Nakanishi lab, University of Arkansas

1168

Animal culture

- Nematostella vectensis were cultured as previously described (Fritzenwanker and Technau, 2002,
- Hand and Uhlinger, 1992).

RNA extraction, cDNA synthesis and gene cloning

- Total RNA was extracted from a mixture of planulae and primary polyps using TRIzol (Thermo
- 1170 Fisher Scientific). cDNAs were synthesized using the SMARTer RACE cDNA Amplification
- 1171 Kit (Cat. No. 634858; Takara, Mountain View, CA, USA). *In silico* predicted *pou-iv* gene
- sequence was retrieved from the Joint Genome Institute genome database (*Nematostella*
- vectensis v1.0, protein ID 160868; http://genome.jgi-psf.org/Nemve1/Nemve1.home.html). 5'
- and 3' RACE PCR experiments were conducted, following manufacturer's recommendations, in
- order to confirm gene prediction. Gene specific primer sequences used for RACE PCR are: 3'
- 1176 RACE Forward 5'-CGATGTCGGGTCCGCGCTTGCACATTTG-3'; 5' RACE Forward 5'-
- 1177 GCCGCGCGATAGACGTGCGTTTACG-3'. RACE PCR fragments were cloned into a
- pCR4-TOPO TA vector using the TOPO TA Cloning kit (Cat. No. K457501; ThermoFisher
- 1179 Scientific), and sequenced at Genewiz, New Jersey.
- The *polycystin 1* cDNA sequence (GenBank accession number: OK338071) was obtained
- by subcloning small overlapping gene fragments (1.5-4kb). Gene fragments were generated by
- 1182 RTPCR using RACE-ready cDNAs as templates. Gene specific primer sequences used to
- amplify *polycystin 1* cDNA are listed in Supplementary File 15. The PCR products were then

- cloned into a pCR4-TOPO TA vector using the TOPO TA Cloning kit (Cat. No. K457501;
- 1185 ThermoFisher Scientific), and sequenced at Eurofins Genomics, Kentucky.
- 1186 Generation of an antibody against N. vectensis POU-IV
- An antibody against a synthetic peptide CQPTVSESQFDKPFETPSPINamide corresponding in
- amino acid sequence to N-terminal QPTVSESQFDKPFETPSPIN of N. vectensis POU-IV
- (Figure 4A) was generated in rabbit (YenZym Antibodies, LLC). TBLASTN search of the
- antigen sequence against the *N. vectensis* genome
- 1191 (http://metazoa.ensembl.org/Nematostella_vectensis/Info/Index) yielded a single hit at the *pou-iv*
- locus (<u>NEMVEscaffold_16:1069268-1069327</u>); there were no significant matches to other loci.
- Following immunization, the resultant antiserum was affinity purified with the
- 1194 CQPTVSESQFDKPFETPSPINamide peptide.
- 1195 CRISPR-Cas9-mediated mutagenesis
- 1196 20 nt-long sgRNA target sites were manually identified in the *N. vectensis pou-iv* genomic locus.
- To minimize off-target effects, target sites that had 17 bp-or-higher sequence identity elsewhere
- in the genome (*Nematostella vectensis v1.0*;
- http://genome.jgi.doe.gov/Nemve1/Nemve1.home.html) were excluded. Selected target
- sequences were as follows.
- 1201 5'- CTACGATGCGCACGATATTT-3' (Cr1)
- 1202 5'- ACGAGAGCTGGAATGGTTCG-3' (Cr2)
- 1203 5'- TAAACGCACGTCTATCGGCG-3' (Cr3)
- 1204 5'- AATAATGGACATCTACGCCG-3' (Cr4)
- The sgRNA species were synthesized *in vitro* (Synthego), and mixed at equal
- 1206 concentrations. The sgRNA mix and Cas9 endonuclease (PNA Bio, PC15111, Thousand Oaks,
- 1207 CA, USA) were co-injected into fertilized eggs at concentrations of 500 ng/µl and 1000 ng/µl,
- 1208 respectively.
- 1209 Genotyping of embryos and polyps
- Genomic DNA from single embryos or from tentacles of single polyps was extracted by using a
- published protocol (Ikmi et al., 2014), and the targeted genomic locus was amplified by nested
- 1212 PCR. Primer sequences used for nested genomic PCR are: "1" Forward 5'-
- 1213 CGAATTCCTCTGCAATAATCACTGATCG-3', "1" Reverse 5'-
- 1214 CTCGTTGGCAGGTGCGGAAAGAG-3', "2" Forward 5'-

- 1215 CGTTCGACTTCATTTCCGCTCGTC-3', "2" Reverse 5'-
- 1216 CGGAAGTTAACGTCGTTAATGCGAAGG-3'. To determine the sequence of mutant alleles,
- PCR products from genomic DNA extracted from F1 mutant polyps were gel-purified, cloned
- and sequenced by using a standard procedure. Using the sequence information of the *pou-iv*-
- mutant allele, genotyping primers for F2 animals were designed as follows (Figure 4B).
- 1220 Forward 5'- CGTTCGACTTCATTTCCGCTCGTC-3'
- Reverse (1), 5'- GCCGCGCCGATAGACGTGCGTTTACG-3' (pou-iv+ -specific; expected size
- of PCR product, 689 bp)
- Reverse (2), 5'- CGGAAGTTAACGTCGTTAATGCGAAGG-3' (expected size of PCR
- 1224 product: *pou-iv+*, 1312 bp; *pou-iv-*, 558 bp)
- 1225 Behavioral analysis
- 1226 Animals were selected for behavior analyses if they were 10-16dpf, unfed, had reached the
- primary polyp stage, and had two or more tentacles present. Animals were only tested if their
- tentacles protruded from their bodies at time of testing initiation. All behavior experiments were
- performed with the experimenter blind to the animal's genotype until after testing was completed.
- 1230 Animals were allowed to rest for at least two hours between tests. Behavioral analyses were
- performed under a Zeiss Stemi 508 microscope with Nikon DSL-4 camera attachment.
- To examine response to touch, a hair attached to a microdissection needle holder (Roboz
- Surgical Instrument Co., Gaithersburg, MD, USA) was pressed briefly on the distal end of each
- tentacle. The stimulus was applied once more to remaining unretracted tentacles, to ensure that a
- tentacle was not missed during the first stimulus. The number of primary polyps that retracted
- one or more tentacles upon touch was counted. If any other part of the body was touched
- accidentally during tentacle stimulation, data for that animal was discarded and the trial was
- repeated two hours or more after the previous test.
- 1239 Chemosensory response of primary polyps to *Artemia* chemical cues was analyzed as
- follows. Artemia shrimp extract was made from 1 day old Artemia brine shrimp, ground with a
- micropestle (USA Scientific) in 1/3 artificial sea water (Instant Ocean), at a concentration of
- approximately 1 shrimp per 1 microliter. 2 microliters of shrimp extract was applied with an
- Eppendorf pipette to the head and tentacle area of each sea anemone. The animal was observed
- for 1 minute to examine the occurrence of tentacular reraction.
- 1245 **CM-Dil labeling**

1246 The lipophilic tracer CM-DiI (Molecular Probes, C7000) was used to label the cell membrane of 1247 a subset of mature hair cells of the polyp tentacles. Primary polyps were incubated in 1/3 1248 seawater with 10 µM CM-DiI for 1 hour at room temperature. The labelled polyps were rinsed in 1249 fresh 1/3 seawater, and were anesthetized in 2.43% MgCl₂ for 20 minutes. They were then fixed 1250 in 4% formaldehyde for 1 hour at room temperature. Specimens were washed in PBSTr (1xPBS 1251 + 0.5% Triton-X100) for 1 hour to permeabilize the tissue, before labeling filamentous actin and 1252 nuclei with AlexaFluor 488-conjugated phalloidin (1:25, Molecular Probes A12379) and the 1253 fluorescent dye 4',6-diamidino-2-phenylindole (DAPI; 1:1,000, Molecular Probes), respectively. 1254 EdU pulse labeling 1255 Primary polyps were incubated in 1/3 seawater containing 200 µM of the thymidine analogue, 1256 EdU (Click-iT EdU AlexaFluor 488 cell proliferation kit, C10337, Molecular Probes), for 20 1257 minutes to label S-phase nuclei. Following washes in fresh 1/3 seawater, the polyps were 1258 immediately fixed as described previously (Martindale et al., 2004, Nakanishi et al., 2012), and 1259 immunohistochemistry was then carried out as described below. Following the 1260 immunohistochemistry procedure, fluorescent labelling of incorporated EdU was conducted 1261 according to the manufacture's recommendations prior to DAPI labelling. 1262 Western blotting 1263 3–4-week-old polyps were lysed in AT buffer (20 mM Hepes pH7.6, 16.8 mM Na₄P₂O₇, 10 mM 1264 NaF, 1 mM Na₃VO₄,0.5 mM DTT, 0.5 mM EDTA, 0.5 mM EGTA, 20% glycerol, 1% Triton X-1265 100, and protease inhibitor cocktail (Sigma)) on ice with a plastic pestle in a microcentrifuge 1266 tube until there were no large fragments. The mixture was then sonicated with a Branson Digital 1267 Sonifier 3 times with the setting of 0.5 s on 1 s off for 10 s at an amplitude of 10%. NaCl was 1268 added to the lysate to a final concentration of 150 mM. The samples were centrifuged at 21,000 g 1269 for 20 min at 4 °C. The supernatant was transferred to a new centrifuge tube and the pellet was 1270 discarded. Protein concentration of the supernatant was determined by Bradford Reagent (Sigma). 1271 The proteins were then separated on a 12% SDS-PAGE (40 µg protein/lane), transferred to a 1272 PVDF membrane (Amersham Hybond; 0.2 um). After blocking with the Odyssey Blocking 1273 Buffer (TBS) for 30 min at room temperature, the membrane was incubated with an anti-POU-1274 IV polyclonal antibody (rabbit, 1:1000) at 4 °C overnight. The membranes were then washed 1275 extensively with TBST and incubated with 1:10,000 IRDye 800CW donkey anti-rabbit IgG at

1276 room temperature for 1 h. After washing, protein bands were visualized on a LI-COR (9120) 1277 Imaging System. Anti-tubulin (T6793 Sigma) was used as a loading control. 1278 Chromatin immunoprecipitation and Sequencing (ChIP-seq) 1279 Adult animals (~1.2 g wet weight) were harvested and washed with PBS twice. The animals 1280 were treated with 2 % formaldehyde in PBS for 12 min at room temperature, and the cross-1281 linking reagent was quenched with 0.125 M glycine for 5 min at room temperature. After 1282 washing with PBS twice, the crosslinked samples were resuspended in 10 ml buffer1 (50 mM 1283 Hepes, pH 7.5, 140 mM NaCl, 1 mM EDTA, 10% glycerol, 0.5% NP-40, 0.25% Triton X-100, 1 1284 mM DTT, and protease inhibitors (Sigma)) and lysed with 10 slow strokes of a tight-fitting 1285 pestle (type B) in a 15 ml *Dounce* homogenizer. The lysate was centrifuged at 500 g for 5 min at 1286 4 °C, and the resulting pellet was resuspended in 10 ml Buffer1 and homogenized as described above. The homogenization processes were repeated 1-2 more times. In the last homogenization, 1287 1288 the lysate was centrifuged at 2000 g for 10 min at 4 °C, and the pellet (nuclei) was resuspended 1289 in 4 ml SDS lysis buffer (50 mM Tris-HCl, pH 8.0, 10 mM EDTA,1% SDS, and protease 1290 inhibitors). The chromatin was sheared to 200-500 bp fragments by sonicating the samples 12 times (1" on and 1" off for 1 min) at an amplitude of 50% with a Branson Digital Sonifier. The 1291 1292 sonicated samples were centrifuged at 21,000 g for 10 min at 4 °C and then diluted 10X with 1293 CHIP dilution buffer (17.7 mM Tris-HCl, pH 8.0, 167 mM NaCl, 1.2 mM EDTA, 1.1% Triton 1294 X-100, 0.01% SDS, and protease inhibitors). After the lysate was cleared with Protein A and G 1295 magnetic beads (Cell Signaling), 50 µl of the cleared sample was set aside as input DNA, and 5 1296 ml of lysate was incubated with 10 µg anti-Brn3 Rabbit polyclonal antibody, which was 1297 conjugated to 30 µl of protein A+G magnetic beads. After incubation at 4 °C overnight, the 1298 beads were washed 3 times with 1 ml of Low salt buffer (20 mM Tris-HCl, pH 8.0, 150 mM 1299 NaCl, 2 mM EDTA, 1% Triton X-100, 0.1% SDS), 3 times with 1 ml of High salt buffer (20mM 1300 Tris-HCl, pH 8.0, 500 mM NaCl, 2 mM EDTA, 1% Triton X-100, 0.01% SDS), 3 times with 1 1301 ml of LiCl wash buffer (10 mM Tris-HCl, pH 8.0, 0.25 M LiCl, 0.5% NP-40, 0.5% sodium 1302 dexycholate, and 1 mM EDTA), and 3 times with 1 ml of TE buffer (10 mM Tris-HCl, pH 8.0, 1303 and 1 mM EDTA). The chromatin was eluted in SDS Elution buffer (50 mM Tris-HCl, pH8.0, 1304 1% SDS, and 1mM EDTA), followed by reverse cross-linking at 65 °C overnight. After being 1305 treated with RNase A (1 mg/ml) at 37 °C for 1 h and then with protease K (0.2 mg/ml) at 45 °C

for 1 h, the DNA fragments were purified with QIAquick Spin columns (QIAGEN) and the

- 1307 purified DNA samples were quantified by Qubit4 (ThermoFisher). 20 ng of the 1308 immunoprecipitated DNA or input DNA was used to generate a library with the NEBNext Ultra 1309 II DNA Library kit following the manufacturer's protocol. Libraries were initially quantified by 1310 Qubit4 and the size profiles were determined by TapeStation (Agilent) and then quantified by 1311 qPCR (NEBNext Library Quant Kit) for high-throughput sequencing. Four biological replicates 1312 of libraries of immunoprecipitated DNA and the input DNA were pooled in equimolar ratio and 1313 the pooled libraries were sequenced on a DNBseq Sequencing platform (BGI, China) for PE 100 1314 1315 Expression and purification of POU-IV protein 1316 cDNA encoding POU-IV was inserted into a modified PET28a plasmid in which POU-IV was 1317 expressed under a 2X Flag tag and a tobacco etch virus (TEV) protease cleavage site by PCR using forward primer 5'-1318 1319 GATGACAAGGGAGGTGGATCCATGAACCGGGACGGATTGCTTAAC-3' and reverse 1320 primer 5'-GGTGGTGGTGCTCGAGTCAATGTACGGAGAACTTCATTCTC-3'. The 1321 construct was transformed into BL21 (DE3) cells (C2530, NEB). After the transformed cells 1322 were grown in LB medium to 0.6 at OD600, the expression of the protein was induced by 1mM 1323 of Isopropyl β-D-1-thiogalactopyranoside (IPTG) at 30 °C for 5 h. The cells were lysed by 1324 sonication in Lysis buffer (20 mM Tris pH7.5, 150 mM NaCl, 1% TritonX-100, 10% glycerol, 1 1325 mM EDTA and protease inhibitor (P8340, Sigma)). The lysate was cleared by centrifugation at 1326 30,000 g for 30 min at 4 °C, and the supernatant was incubated with anti- Flag M2 Affinity Gel 1327 (A2220, Sigma) overnight at 4 °C. After washing with Wash Buffer (20 mM Tris pH7.5, 150 1328 mM NaCl, 0.5% TritonX-100, and 1 mM EDTA), the bound proteins were eluted with Elution 1329 buffer [50 mM Tris pH 7.5, 30 mM NaCl, and 0.25 mg/ml 3X Flag peptide (F4799, Sigma)]. The 1330 buffer for the eluted protein was changed to 20 mM Tris pH7.5, and 100 mM NaCl using an 1331 Amicon Ultra Centricon with 10 kDa cut-off. The purified protein was stored at -80 °C for 1332 further use.
- 1333 Electrophoretic mobility shift assay (EMSA)
- 1334 The biotin-labeled DNA oligonucleotides with or without motif were purchased from Integrated
- DNA Technologies. For the experiment shown in Figure 8C, the probe sequence with motif was
- 1336 5'- AAACAAAGATTCTAAGCATC*CATTATTAAT*ATACATCCCTAGAAAAAATC-3'
- 1337 (motif in bold and italics; scaffold 353:52091-52140,

1338	https://mycocosm.jgi.doe.gov/Nemve1/Nemve1.home.html), and that without motif was 5'-			
1339	ATCGAAAACAAAGATTCTAAGCATCATACATCCCTAGAAAAAATCTCCGC-3'.			
1340	The two complementary strands were annealed together by mixing equivalent molar amounts of			
1341	each oligonucleotide, heating at 95 °C for 5 min, and slow cooling on bench to room temperature			
1342	Gel mobility shift assay was carried out using Gelshift Chemiluminescent EMSA kit (#37341,			
1343	Active Motif) with modifications. Briefly, 0.25 µg POU-IV protein, 20 fmol biotin-labeled			
1344	probes with or without motif were incubated in Binding Buffer (10 mM Tris pH7.4, 50 mM KCl,			
1345	$2~\text{mM}$ MgCL $_2,~1~\text{mM}$ EDTA, $1~\text{mM}$ DTT, 5% glycerol, $4~\mu\text{g/ml}$ BSA, and $0.125\text{ug/}\mu\text{l}$ salmon			
1346	sperm DNA) in a total volume of 20 µl at RT for 30 min. For the competition, unlabeled probe			
1347	was added to the reaction mixture at 300-fold molar excess of the biotin labeled probe. For			
1348	supershift assay, 2 µg POU-IV antibody was incubated with POU-IV protein for 1 h at room			
1349	temperature before the biotin-labeled probe was added. The DNA-protein complexes were			
1350	separated with a 5% nondenaturing polyacrylamide gel in 0.5X TBE buffer at 100 V for 1 h. The			
1351	probes were then transferred to a positively charged Nylon Membrane (Nytran SPC, Cytiva) in			
1352	0.5X TBE buffer at 380 mA for 30 min at 4 C°. After cross-linking the transferred probes to the			
1353	membrane by CL-1000 Ultraviolet Crosslinker (UVP) at 120 mJ/cm ² for 1 min, the membrane			
1354	was incubated with HRP-conjugated streptavidin, and the chemiluminescence of the biotin-			
1355	labeled probes were detected with ECL HRP substrate in X-ray film.			
1356	Immunofluorescence, in situ hybridization, and TUNEL			
1357	Animal fixation and immunohistochemistry were performed as previously described (Martindale			
1358	et al., 2004, Nakanishi et al., 2012). For immunohistochemistry, we used primary antibodies			
1359	against POU-IV (rabbit, 1:200), minicollagen 3 (guinea pig, 1:200; (Zenkert et al., 2011)), Kaede			
1360	(rabbit; 1:500; Medical & Biological Laboratories, PM012M), and tyrosinated ∂-tubulin (mouse,			
1361	1:500, Sigma T9028), and secondary antibodies conjugated to AlexaFluor 568 (1:200, Molecular			
1362	Probes A-11031 (anti-mouse) or A-11036 (anti-rabbit)) or AlexaFluor 647 (1:200, Molecular			
1363	Probes A-21236 (anti-mouse) or A-21245 (anti-rabbit)). Nuclei were labeled using the			
1364	fluorescent dye DAPI (1:1,000, Molecular Probes D1306), and filamentous actin was labeled			
1365	using AlexaFluor 488-conjugated phalloidin (1:25, Molecular Probes A12379). For in situ			
1366	hybridization, antisense digoxigenin-labeled riboprobes against Nematostella vectensis pou-iv			
1367	and polycystin 1 were synthesized from 5' and 3' RACE products, respectively (MEGAscript			
1368	transcription kit: Ambion), and were used at a final concentration of 1 ng/ul. TUNEL assay was			

- 1369 carried out after immunostaining, by using In Situ Cell Death Detection Kit (TMR red cat no. 1370 1684795, Roche, Indianapolis, IN, USA) according to manufacturer's recommendation. 1371 Specimens were mounted in ProlongGold antifade reagent (Molecular Probes, P36930). 1372 Fluorescent images were recorded using a Leica SP5 Confocal Microscope or a Zeiss LSM900. 1373 Images were viewed using ImageJ. 1374 **Transmission Electron Microscopy** 1375 1-4 week old primary polyps were anesthetized in 2.43% MgCl₂ for 20 minutes, and then fixed in 2.5% glutaraldehyde and 0.1 M cacodylate buffer at 4°C overnight. Fixed polyps were washed 1376 1377 four times in 0.1 M cacodylate buffer for 10 min, and post-fixed for one hour in 0.1 M 1378 cacodylate buffer and 1% OsO₄. Specimens were rinsed with five 5 min washes of 0.1 M 1379 cacodylate buffer, followed by dehydration in a graded ethanol series consisting of 15 min 1380 washes in 30%, 50%, 70%, 80%, and 95% ethanol, followed by two 15 min washes in 100% 1381 ethanol. Dehydrated polyps were placed in a 1:1 solution of ethanol/Spurr's resin and left in a 1382 desiccator for 1 hr. The ethanol/resin mixture was replaced with a 100% resin solution, and 1383 polyps were left in a desiccator overnight. Samples were then transferred to flat-embedding 1384 molds filled with 100% Spurr's resin and placed in an oven at 70°C for 14 hours. 1385 Blocks containing embedded polyps were trimmed with a razor blade and cut into ultra-1386 thin sections using a diamond knife on a Sorval Porter-Blum ultramicrotome. Sections were 1387 transferred to carbon/formvar coated copper grids, which were then stained with 2% uranyl 1388 acetate and lead citrate and viewed on a JEOL JEM-1011 transmission electron microscope at 1389 100 kV. 1390 Generation of *kaede* transgenic animals 1391 The pou-iv::kaede and pkd1::kaede transgenic animals were produced by I-SceI-mediated 1392 transgenesis as described previously (Renfer et al., 2010) with modifications. To generate pou-
- iv::kaede plasmid, 3199 bp genomic sequence upstream of the start codon of the Nematostella
- 1394 *vectensis pou-iv* (scaffold 16: 1065408-1068606;
- https://mycocosm.jgi.doe.gov/Nemve1/Nemve1.home.html) was cloned in front of the open
- reading frame of the Kaede gene (Ando et al., 2002) by FastCloning (Li et al., 2011). To
- generate pkd1::kaede plasmid, 3704 bp genomic sequence upstream of the 5th base in exon 3 of
- the Nematostella vectensis polycystin 1 (scaffold 353: 49524-53227;
- https://mycocosm.jgi.doe.gov/Nemve1/Nemve1.home.html) was cloned in front of the open

- 1400 reading frame of the Kaede gene. The plasmid was digested with I-SceI for 15-30 minutes at 37 1401 ^oC and injected into zygotes at 50 ng/ ul. The injected animals were raised to primary polyps, and 1402 Kaede was visualized by using an anti-Kaede antibody. 1403 Phylogenetic analysis 1404 Sequence alignment and phylogenetic analyses were performed on the Geneious Prime platform 1405 (v.2019.2.), polycystin 1 and polycystin 2 sequences were retrieved from GenBank at the NCBI 1406 website (http://blast.ncbi.nlm.nih.gov/Blast.cgi), either directly or via the protein BLAST search 1407 using the N. vectensis sequences as queries. Peptide sequences were aligned with MUSCLE 1408 (v3.7) [57] configured for highest accuracy (MUSCLE with default settings). After alignment, 1409 ambiguous regions (i.e. containing gaps and/or poorly aligned) were manually removed. The 1410 final alignment spanned the conserved TOP and transmembrane domains over 323 amino acid 1411 sites (Figure 8 – Figure supplement 2 – Source Data 1). Phylogenetic trees were reconstructed 1412 using the maximum likelihood method implemented in the PhyML program [58]. The WAG 1413 substitution model [59] was selected assuming an estimated proportion of invariant sites and 4 1414 gamma-distributed rate categories to account for rate heterogeneity across sites. The gamma 1415 shape parameter was estimated directly from the data. Reliability for internal branches of 1416 maximum likelihood trees was assessed using the bootstrapping method (100 bootstrap 1417 replicates). 1418 RNA-seq data analysis 1419 The accession number from the RNA-seq data used in this study is E-MTAB-8658. The raw 1420 fastq files were filtered for low quality reads using Trimmomatic v0.39 1421 (SLIDINGWINDOW:4:15, MINLEN:60, HEADCROP:10) (Bolger et al., 2014). Filtered reads 1422 were aligned to the *Nemastostella vectensis* genome (ENA accession: GCA 000209225) using 1423 STAR v 2.7.5a (sjdbOverhang: 99)(Dobin et al., 2013). The alignment files were processed 1424 using Samtools v1.9 (Danecek et al., 2021) and reads on genes were counted using HTSeq 1425 v0.12.4 (-t gene) (Anders et al., 2015). Genome annotation reported by Fredman, et al. (Fredman 1426 et al., 2013) was used. The differential expression analysis and normalization were performed in
- 1428 ChIP-seq data analysis

1429 ChIP-seq data are available at the BioProject database (accession number: PRJNA767103). The

R, using the DESeq2 (Love et al., 2014) and Apeglm (Zhu et al., 2019) packages.

raw data was trimmed using Trimmomatic v0.39 (Bolger et al., 2014). Reads were aligned to the

- Nemastostella vectensis genome (ENA accession: GCA 000209225) using STAR v 2.7.5a 1431 1432 (Dobin et al., 2013) and alignment files were processed using Samtools v1.9 (Danecek et al., 1433 2021). Peak calling was performed in the aligned readings with MACS2 (Zhang et al., 2008). 1434 The quality of the peaks in the replicates (n=3) was checked using phantompeakqualtools (Landt 1435 et al., 2012). To improve sensitivity and specificity of peak calling, and identify consensus 1436 regions of the multiple replicates, we used Multiple Sample Peak Calling (MSPC: -r tec -w 1e-4 1437 -s 1e-8) (Jalili et al., 2015). A de novo motif search and motif enrichment was performed using 1438 RSAT local-word-analysis (Thomas-Chollier et al., 2012). The motif comparison tool TomTom 1439 (Gupta et al., 2007) was used to search enriched motifs against the Jaspar database (Fornes et al., 1440 2020). 1441 The scripts for RNA-Seq and ChIP-seq analysis are available here: 1442 [https://github.com/pyrosilesl97/POU-IV analysis]. 1443 1444 **Acknowledgements:** 1445 We thank Suat Özbek for providing us with the antibodies against minicollagens, and Sakura 1446 Rieck for helping with the behavioral analysis of *pou-iv* mutants. We are also grateful to Betty 1447 Martin and Mourad Benamara at the Arkansas Nano & Bio Materials Characterization Facility 1448 for their assistance with confocal microscopy and transmission electron microscopy. Finally, we 1449 would like to thank reviewers for comments on the earlier version of the manuscript, which 1450 greatly improved the manuscript. 1451 **Competing interests:** 1452 No competing interests declared. 1453 1454 **Funding:** 1455 This work was supported by Arkansas Bioscience Institute, University of Arkansas, and National 1456 Science Foundation Grant No.1931154. 1457
- 1458 References:

ANDERS, S., PYL, P. T. & HUBER, W. 2015. HTSeq-a Python framework to work with highthroughput sequencing data. *Bioinformatics*, 31, 166-169.

- ANDO, R., HAMA, H., YAMAMOTO-HINO, M., MIZUNO, H. & MIYAWAKI, A. 2002. An optical marker based on the UV-induced green-to-red photoconversion of a fluorescent protein. *Proceedings of the National Academy of Sciences of the United States of America*, 99, 12651-12656.
- ARKETT, S. A., MACKIE, G. O. & MEECH, R. W. 1988. Hair cell mechanoreception in the jellyfish Aglantha digitale. *Journal of Experimental Biology*, 135, 329-342.
- BABONIS, L. S. & MARTINDALE, M. Q. 2017. PaxA, but not PaxC, is required for cnidocyte development in the sea anemone Nematostella vectensis. *Evodevo*, 8.
- BATEMAN, A. & SANDFORD, R. 1999. The PLAT domain: a new piece in the PKD1 puzzle.

 Current Biology, 9, R588-R590.
- BAUMEISTER, R., LIU, Y. X. & RUVKUN, G. 1996. Lineage-specific regulators couple cell lineage asymmetry to the transcription of the Caenorhabditis elegans POU gene unc-86 during neurogenesis. *Genes & Development*, 10, 1395-1410.
- BEISEL, K. W., HE, D., HALLWORTH, R. & FRITZSCH, B. 2008. 3.05 Genetics of
 Mechanoreceptor Evolution and Development. *In:* MASLAND, R. H., ALBRIGHT, T.
 D., ALBRIGHT, T. D., MASLAND, R. H., DALLOS, P., OERTEL, D., FIRESTEIN, S.,
 BEAUCHAMP, G. K., CATHERINE BUSHNELL, M., BASBAUM, A. I., KAAS, J. H.
 & GARDNER, E. P. (eds.) *The Senses: A Comprehensive Reference*. New York:
 Academic Press.
- BEZARES-CALDERON, L. A., BERGER, J. & JEKELY, G. 2020. Diversity of cilia-based
 mechanosensory systems and their functions in marine animal behaviour. *Philosophical Transactions of the Royal Society B-Biological Sciences*, 375.

1485

1486

1487

1488

1489

1490

1491

1492

1493

1494

1495

- BOCA, M., D'AMATO, L., DISTEFANO, G., POLISHCHUK, R. S., GERMINO, G. G. & BOLETTA, A. 2007. Polycystin-1 induces cell migration by regulating phosphatidylinositol 3-kinase-dependent cytoskeletal Rearrangements and GSK3 beta-dependent cell-cell mechanical adhesions. *Molecular Biology of the Cell*, 18, 4050-4061.
- BOEKHOFF-FALK, G. 2005. Hearing in Drosophila: Development of Johnston's organ and emerging parallels to vertebrate ear development. *Developmental Dynamics*, 232, 550-558.
- BOLGER, A. M., LOHSE, M. & USADEL, B. 2014. Trimmomatic: a flexible trimmer for Illumina sequence data. *Bioinformatics*, 30, 2114-2120.
- BRINKMANN, M., OLIVER, D. & THURM, U. 1996. Mechanoelectric transduction in nematocytes of a hydropolyp (Corynidae). *Journal of Comparative Physiology A Sensory Neural and Behavioral Physiology*, 178, 125-138.
- BUDELMANN, B. U. 1989. Hydrodynamic receptor systems in invertebrates. *The mechanosensory lateral line*. New York: Springer-Verlag.
- BYCROFT, M., BATEMAN, A., CLARKE, J., HAMILL, S. J., SANDFORD, R., THOMAS, R.
 L. & CHOTHIA, C. 1999. The structure of a PKD domain from polycystin-1:
 Implications for polycystic kidney disease. *Embo Journal*, 18, 297-305.
- 1500 CHALFIE, M. & AU, M. 1989. Genetic control of differentiation of the Caenorhabditis elegans touch receptor neurons. *Science*, 243, 1027-33.
- 1502 CHALFIE, M., HORVITZ, H. R. & SULSTON, J. E. 1981. Mutations that lead to reiterations in the cell lineages of C. elegans. *Cell*, 24, 59-69.
- 1504 CHALFIE, M. & SULSTON, J. 1981. Developmental genetics of the mechanosensory neurons of Caenorhabditis elegans. *Dev Biol*, 82, 358-70.

- 1506 CLYNE, P. J., CERTEL, S. J., DE BRUYNE, M., ZASLAVSKY, L., JOHNSON, W. A. & CARLSON, J. R. 1999. The odor specificities of a subset of olfactory receptor neurons are governed by Acj6, a POU-domain transcription factor. *Neuron*, 22, 339-47.
- 1509 COFFIN, A., KELLEY, M., MANLEY, G. A. & POPPER, A. N. 2004. Evolution of sensory 1510 hair cells. *Springer Handbook of Auditory Research*, 22, 55-94.
- 1511 COLLINS, A. G., SCHUCHERT, P., MARQUES, A. C., JANKOWSKI, T., MEDINA, M. & SCHIERWATER, B. 2006. Medusozoan phylogeny and character evolution clarified by new large and small subunit rDNA data and an assessment of the utility of phylogenetic mixture models. *Syst Biol*, 55, 97-115.
- DANECEK, P., BONFIELD, J. K., LIDDLE, J., MARSHALL, J., OHAN, V., POLLARD, M.
 O., WHITWHAM, A., KEANE, T., MCCARTHY, S. A., DAVIES, R. M. & LI, H. 2021.
 Twelve years of SAMtools and BCFtools. *Gigascience*, 10.
- DELMAS, P. 2004. Polycystins: From mechanosensation to gene regulation. *Cell*, 118, 145-148.
- DOBIN, A., DAVIS, C. A., SCHLESINGER, F., DRENKOW, J., ZALESKI, C., JHA, S.,
 BATUT, P., CHAISSON, M. & GINGERAS, T. R. 2013. STAR: ultrafast universal
 RNA-seq aligner. *Bioinformatics*, 29, 15-21.
- DUGGAN, A., MA, C. & CHALFIE, M. 1998. Regulation of touch receptor differentiation by the Caenorhabditis elegans mec-3 and unc-86 genes. *Development*, 125, 4107-19.
- ERKMAN, L., MCEVILLY, R. J., LUO, L., RYAN, A. K., HOOSHMAND, F., O'CONNELL, S. M., KEITHLEY, E. M., RAPAPORT, D. H., RYAN, A. F. & ROSENFELD, M. G. 1996. Role of transcription factors Brn-3.1 and Brn-3.2 in auditory and visual system development. *Nature*, 381, 603-6.
- ERWIN, D. H., LAFLAMME, M., TWEEDT, S. M., SPERLING, E. A., PISANI, D. & PETERSON, K. J. 2011. The Cambrian Conundrum: Early Divergence and Later Ecological Success in the Early History of Animals. *Science*, 334, 1091-1097.
- 1531 FAIN, G. L. 2003. *Sensory Transduction*, Sunderland, Massachusetts U.S.A., Sinauer Associates, 1532 Inc.
- FAUTIN, D. G. & MARISCAL, R. N. 1991. Cnidaria: Anthozoa. *In:* HARRISON, F. W. (ed.) *Microscopic anatomy of invertebrates.* New York: Wiley-Liss.
- FINNEY, M. & RUVKUN, G. 1990. The unc-86 gene product couples cell lineage and cell identity in C. elegans. *Cell*, 63, 895-905.
- FORNES, O., CASTRO-MONDRAGON, J. A., KHAN, A., VAN DER LEE, R., ZHANG, X., RICHMOND, P. A., MODI, B. P., CORREARD, S., GHEORGHE, M., BARANASIC, D., SANTANA-GARCIA, W., TAN, G., CHENEBY, J., BALLESTER, B., PARCY, F., SANDELIN, A., LENHARD, B., WASSERMAN, W. W. & MATHELIER, A. 2020. JASPAR 2020: update of the open-access database of transcription factor binding profiles. *Nucleic Acids Research*, 48, D87-D92.
- FREDMAN, D., SCHWAIGER, M., RENTZSCH, F. & TECHNAU, U. 2013. Nematostella vectensis transcriptome and gene models v2.0. *figshare*.
- FRITZENWANKER, J. H., GENIKHOVICH, G., KRAUS, Y. & TECHNAU, U. 2007. Early development and axis specification in the sea anemone Nematostella vectensis.

 Developmental Biology, 310, 264-279.
- FRITZENWANKER, J. H. & TECHNAU, U. 2002. Induction of gametogenesis in the basal cnidarian Nematostella vectensis(Anthozoa). *Dev Genes Evol*, 212, 99-103.

- GAN, L., XIANG, M., ZHOU, L., WAGNER, D. S., KLEIN, W. H. & NATHANS, J. 1996.
 POU domain factor Brn-3b is required for the development of a large set of retinal ganglion cells. *Proc Natl Acad Sci U S A*, 93, 3920-5.
- GOLD, D. A., GATES, R. D. & JACOBS, D. K. 2014. The Early Expansion and Evolutionary Dynamics of POU Class Genes. *Molecular Biology and Evolution*, 31, 3136-3147.
- GRIEBEN, M., PIKE, A. C. W., SHINTRE, C. A., VENTURI, E., EL-AJOUZ, S., TESSITORE,
 A., SHRESTHA, L., MUKHOPADHYAY, S., MAHAJAN, P., CHALK, R., BURGESS BROWN, N. A., SITSAPESAN, R., HUISKONEN, J. T. & CARPENTER, E. P. 2017.
 Structure of the polycystic kidney disease TRP channel Polycystin-2 (PC2). Nature
 Structural & Molecular Biology, 24, 114-+.
- GRUBER, C. A., RHEE, J. M., GLEIBERMAN, A. & TURNER, E. E. 1997. POU domain factors of the Brn-3 class recognize functional DNA elements which are distinctive, symmetrical, and highly conserved in evolution. *Molecular and Cellular Biology*, 17, 2391-2400.
- GUPTA, S., STAMATOYANNOPOULOS, J. A., BAILEY, T. L. & NOBLE, W. S. 2007. Quantifying similarity between motifs. *Genome Biology*, 8.

1567

1568

1569

1570

1571

15721573

1574

1575

1576

15771578

1579

1580

- GYOJA, F., KAWASHIMA, T. & SATOH, N. 2012. A genomewide survey of bHLH transcription factors in the coral Acropora digitifera identifies three novel orthologous families, pearl, amber, and peridot. *Development Genes and Evolution*, 222, 63-76.
- HAND, C. & UHLINGER, K. R. 1992. The Culture, Sexual and Asexual Reproduction, and Growth of the Sea-Anemone Nematostella-Vectensis. *Biological Bulletin*, 182, 169-176.
- HAVRILAK, J. A., AL-SHAER, L., BABAN, N., AKINCI, N. & LAYDEN, M. J. 2021. Characterization of the dynamics and variability of neuronal subtype responses during growth, degrowth, and regeneration of Nematostella vectensis. *Bmc Biology*, 19.
- HEJNOL, A., OBST, M., STAMATAKIS, A., OTT, M., ROUSE, G. W., EDGECOMBE, G. D., MARTINEZ, P., BAGUNA, J., BAILLY, X., JONDELIUS, U., WIENS, M., MULLER, W. E. G., SEAVER, E., WHEELER, W. C., MARTINDALE, M. Q., GIRIBET, G. & DUNN, C. W. 2009. Assessing the root of bilaterian animals with scalable phylogenomic methods. *Proceedings of the Royal Society B-Biological Sciences*, 276, 4261-4270.
- HERR, W. & CLEARY, M. A. 1995. The Pou Domain Versatility in Transcriptional Regulation by a Flexible 2-in-One DNA-Binding Domain. *Genes & Development*, 9, 1679-1693.
- HOLLAND, L. Z. 2005. Non-neural ectoderm is really neural: Evolution of developmental patterning mechanisms in the non-neural ectoderm of chordates and the problem of sensory cell homologies. *Journal of Experimental Zoology Part B Molecular and Developmental Evolution*, 304B, 304-323.
- HOLTMAN, M. & THURM, U. 2001. Variations of concentric hair cells in a cnidarian sensory epithelium (Coryne tubulosa). *Journal of Comparative Neurology*, 432, 550-563.
- HORRIDGE, G. A. 1969. Statocysts of medusae and evolution of stereocilia. *Tissue & Cell*, 1, 341-353.
- HROUDOVA, M., VOJTA, P., STRNAD, H., KREJCIK, Z., RIDL, J., PACES, J., VLCEK, C.
 & PACES, V. 2012. Diversity, Phylogeny and Expression Patterns of Pou and Six
 Homeodomain Transcription Factors in Hydrozoan Jellyfish Craspedacusta sowerbyi.
 PLoS ONE, 7, e36420, 1-11.
- HUNDGEN, M. & BIELA, C. 1982. Fine structure of touch-plates in the scyphomedusan Aurelia aurita. Journal of ultrastructure research, 80, 178-184.

- 1596 IKEDA, R., PAK, K., CHAVEZ, E. & RYAN, A. F. 2015. Transcription Factors with Conserved 1597 Binding Sites Near ATOH1 on the POU4F3 Gene Enhance the Induction of Cochlear 1598 Hair Cells. *Molecular Neurobiology*, 51, 672-684.
- 1599 IKMI, A., MCKINNEY, S. A., DELVENTHAL, K. M. & GIBSON, M. C. 2014. TALEN and CRISPR/Cas9-mediated genome editing in the early-branching metazoan Nematostella vectensis. *Nature Communications*, 5.
- JALILI, V., MATTEUCCI, M., MASSEROLI, M. & MORELLI, M. J. 2015. Using combined evidence from replicates to evaluate ChIP-seq peaks. *Bioinformatics*, 31, 2761-2769.
- JARMAN, A. P. 2002. Studies of mechanosensation using the fly. *Human Molecular Genetics*, 11, 1215-1218.
- JØRGENSEN, J. M. Evolution of Octavolateralis Sensory Cells. 1989 New York, NY. Springer New York, 115-145.
- KELLEY, L. A., MEZULIS, S., YATES, C. M., WASS, M. N. & STERNBERG, M. J. E. 2015.
 The Phyre2 web portal for protein modeling, prediction and analysis. *Nature Protocols*, 10, 845-858.
- KITAJIRI, S., SAKAMOTO, T., BELYANTSEVA, I. A., GOODYEAR, R. J., STEPANYAN,
 R., FUJIWARA, I., BIRD, J. E., RIAZUDDIN, S., RIAZUDDIN, S., AHMED, Z. M.,
 HINSHAW, J. E., SELLERS, J., BARTLES, J. R., HAMMER, J. A., RICHARDSON, G.
 P., GRIFFITH, A. J., FROLENKOV, G. I. & FRIEDMAN, T. B. 2010. Actin-Bundling
 Protein TRIOBP Forms Resilient Rootlets of Hair Cell Stereocilia Essential for Hearing.
 Cell, 141, 786-798.
- KRAUS, Y. & TECHNAU, U. 2006. Gastrulation in the sea anemone Nematostella vectensis occurs by invagination and immigration: an ultrastructural study. *Dev Genes Evol*, 216, 119-32.
- 1620 LANDT, S. G., MARINOV, G. K., KUNDAJE, A., KHERADPOUR, P., PAULI, F., 1621 BATZOGLOU, S., BERNSTEIN, B. E., BICKEL, P., BROWN, J. B., CAYTING, P., 1622 CHEN, Y. W., DESALVO, G., EPSTEIN, C., FISHER-AYLOR, K. I., EUSKIRCHEN, 1623 G., GERSTEIN, M., GERTZ, J., HARTEMINK, A. J., HOFFMAN, M. M., IYER, V. R., 1624 JUNG, Y. L., KARMAKAR, S., KELLIS, M., KHARCHENKO, P. V., LI, Q. H., LIU, 1625 T., LIU, X. S., MA, L. J., MILOSAVLJEVIC, A., MYERS, R. M., PARK, P. J., PAZIN, 1626 M. J., PERRY, M. D., RAHA, D., REDDY, T. E., ROZOWSKY, J., SHORESH, N., 1627 SIDOW, A., SLATTERY, M., STAMATOYANNOPOULOS, J. A., TOLSTORUKOV, 1628 M. Y., WHITE, K. P., XI, S., FARNHAM, P. J., LIEB, J. D., WOLD, B. J. & SNYDER, 1629 M. 2012. ChIP-seq guidelines and practices of the ENCODE and modENCODE 1630 consortia. Genome Research, 22, 1813-1831.
- LEE, P. N., KUMBUREGAMA, S., MARLOW, H. Q., MARTINDALE, M. Q. & WIKRAMANAYAKE, A. H. 2007. Asymmetric developmental potential along the animal-vegetal axis in the anthozoan cnidarian, Nematostella vectensis, is mediated by Dishevelled. *Developmental Biology*, 310, 169-186.
- 1635 LESH-LAURIE, G. E. & SUCHY, P. E. 1991. Cnidaria: Scyphozoa and Cubozoa. *In:* 1636 HARRISON, F. W. (ed.) *Microscopic anatomy of invertebrates*. New York: Wiley-Liss.
- LEYVA-DIAZ, E., MASOUDI, N., SERRANO-SAIZ, E., GLENWINKEL, L. & HOBERT, O. 2020. Brn3/POU-IV-type POU homeobox genes-Paradigmatic regulators of neuronal identity across phylogeny. *Wiley Interdisciplinary Reviews-Developmental Biology*, 9.

- LI, C. K., WEN, A. Y., SHEN, B. C., LU, J., HUANG, Y. & CHANG, Y. C. 2011. FastCloning: a highly simplified, purification-free, sequence- and ligation-independent PCR cloning method. *Bmc Biotechnology*, 11.
- LIU, W., MO, Z. Q. & XIANG, M. Q. 2001. The Ath5 proneural genes function upstream of Brn3 POU domain transcription factor genes to promote retinal ganglion cell development. *Proceedings of the National Academy of Sciences of the United States of* America, 98, 1649-1654.
- LOPEZ-ESCARDO, D., GRAU-BOVE, X., GUILLAUMET-ADKINS, A., GUT, M.,
 SIERACKI, M. E. & RUIZ-TRILLO, I. 2019. Reconstruction of protein domain
 evolution using single-cell amplified genomes of uncultured choanoflagellates sheds light
 on the origin of animals. *Philosophical Transactions of the Royal Society B-Biological* Sciences, 374.
- LOVE, M. I., HUBER, W. & ANDERS, S. 2014. Moderated estimation of fold change and dispersion for RNA-seq data with DESeq2. *Genome Biology*, 15.
- LYONS, K. M. 1973. Collar Cells in Planula and Adult Tentacle Ectoderm of Solitary Coral
 Balanophyllia-Regia (Anthozoa Eupsammiidae). Zeitschrift Fur Zellforschung Und
 Mikroskopische Anatomie, 145, 57-74.
- MAGIE, C. R., DALY, M. & MARTINDALE, M. Q. 2007. Gastrulation in the cnidarian Nematostella vectensis occurs via invagination not ingression. *Developmental Biology*, 305, 483-497.
- MAHONEY, J. L., GRAUGNARD, E. M., MIRE, P. & WATSON, G. M. 2011. Evidence for involvement of TRPA1 in the detection of vibrations by hair bundle mechanoreceptors in sea anemones. *Journal of Comparative Physiology A Sensory Neural and Behavioral Physiology*, 197, 729-742.

1665

1666

1667

- MANLEY, G. A. & LADHER, R. 2008. 3.01 Phylogeny and Evolution of Ciliated Mechanoreceptor Cells. *In:* MASLAND, R. H., ALBRIGHT, T. D., ALBRIGHT, T. D., MASLAND, R. H., DALLOS, P., OERTEL, D., FIRESTEIN, S., BEAUCHAMP, G. K., CATHERINE BUSHNELL, M., BASBAUM, A. I., KAAS, J. H. & GARDNER, E. P. (eds.) *The Senses: A Comprehensive Reference*. New York: Academic Press.
- MARTINDALE, M. Q., PANG, K. & FINNERTY, J. R. 2004. Investigating the origins of triploblasty: 'mesodermal' gene expression in a diploblastic animal, the sea anemone Nematostella vectensis (phylum, Cnidaria; class, Anthozoa). *Development*, 131, 2463-74.
- MASUDA, M., DULON, D., PAK, K., MULLEN, L. M., LI, Y., ERKMAN, L. & RYAN, A. F.
 2011. Regulation of Pou4f3 Gene Expression in Hair Cells by 5 'DNA in Mice.
 Neuroscience, 197, 48-64.
- MCEVILLY, R. J., ERKMAN, L., LUO, L., SAWCHENKO, P. E., RYAN, A. F. & ROSENFELD, M. G. 1996. Requirement for Brn-3.0 In differentiation and survival of sensory and motor neurons. *Nature*, 384, 574-577.
- MEDINA, M., COLLINS, A. G., SILBERMAN, J. D. & SOGIN, M. L. 2001. Evaluating hypotheses of basal animal phylogeny using complete sequences of large and small subunit rRNA. *Proceedings of the National Academy of Sciences of the United States of America*, 98, 9707-9712.
- MIRE, P. & WATSON, G. M. 1997. Mechanotransduction of hair bundles arising from multicellular complexes in anemones. *Hearing Research*, 113, 224-234.

- MIRE-THIBODEAUX, P. & WATSON, G. M. 1994. Morphodynamic hair bundles arising from sensory cell/supporting cell complexes frequency-tune nematocyst discharges in sea anemones. *Journal of Experimental Zoology*, 268, 282-292.
- MIRETHIBODEAUX, P. & WATSON, G. M. 1994. Morphodynamic Hair Bundles Arising from Sensory Cell/Supporting Cell Complexes Frequency-Tune Nematocyst Discharge in Sea-Anemones. *Journal of Experimental Zoology*, 268, 282-292.
- MOCHIZUKI, T., WU, G. Q., HAYASHI, T., XENOPHONTOS, S. L., VELDHUISEN, B., SARIS, J. J., REYNOLDS, D. M., CAI, Y. Q., GABOW, P. A., PIERIDES, A., KIMBERLING, W. J., BREUNING, M. H., DELTAS, C. C., PETERS, D. J. M. & SOMLO, S. 1996. PKD2, a gene for polycystic kidney disease that encodes an integral membrane protein. *Science*, 272, 1339-1342.
- MOY, G. W., MENDOZA, L. M., SCHULZ, J. R., SWANSON, W. J., GLABE, C. G. &
 VACQUIER, V. D. 1996. The sea urchin sperm receptor for egg jelly is a modular
 protein with extensive homology to the human polycystic kidney disease protein, PKD1.
 Journal of Cell Biology, 133, 809-817.
- NAKANISHI, N. & MARTINDALE, M. Q. 2018. CRISPR knockouts reveal an endogenous role for ancient neuropeptides in regulating developmental timing in a sea anemone. *eLife*, 7, e39742.
- NAKANISHI, N., RENFER, E., TECHNAU, U. & RENTZSCH, F. 2012. Nervous systems of the sea anemone Nematostella vectensis are generated by ectoderm and shaped by distinct mechanisms. *Development*, 139, 347-357.
- NAKANISHI, N., YUAN, D., HARTENSTEIN, V. & JACOBS, D. K. 2010. Evolutionary origin of rhopalia: insights from cellular-level analyses of Otx and POU expression patterns in the developing rhopalial nervous system. *Evolution & Development*, 12, 404-1708 415.
- OLIVER, D. & THURM, U. 1996. Mechanoreception by concentric hair cells of hydropolyps.
 In: ELSNER, N. & SCHNITZLER, H. U. (eds.) Gottingen Neurobiology Report.
 Stuttgart: Georg Thieme.
- PUTNAM, N. H., SRIVASTAVA, M., HELLSTEN, U., DIRKS, B., CHAPMAN, J.,
 SALAMOV, A., TERRY, A., SHAPIRO, H., LINDQUIST, E., KAPITONOV, V. V.,
 JURKA, J., GENIKHOVICH, G., GRIGORIEV, I. V., LUCAS, S. M., STEELE, R. E.,
 FINNERTY, J. R., TECHNAU, U., MARTINDALE, M. Q. & ROKHSAR, D. S. 2007.
 Sea anemone genome reveals ancestral eumetazoan gene repertoire and genomic organization. *Science*, 317, 86-94.
- RENFER, E., AMON-HASSENZAHL, A., STEINMETZ, P. R. H. & TECHNAU, U. 2010. A muscle-specific transgenic reporter line of the sea anemone, Nematostella vectensis. *Proceedings of the National Academy of Sciences of the United States of America*, 107, 104-108.
- RICHARDS, G. S. & RENTZSCH, F. 2014. Transgenic analysis of a SoxB gene reveals neural progenitor cells in the chidarian Nematostella vectensis. *Development*, 141, 4681-4689.
- 1724 RICHARDS, G. S. & RENTZSCH, F. 2015. Regulation of Nematostella neural progenitors by SoxB, Notch and bHLH genes. *Development*, 142, 3332-3342.
- SANDFORD, R., SGOTTO, B., APARICIO, S., BRENNER, S., VAUDIN, M., WILSON, R. K., CHISSOE, S., PEPIN, K., BATEMAN, A., CHOTHIA, C., HUGHES, J. & HARRIS, P. 1997. Comparative analysis of the polycystic kidney disease 1 (PKD1) gene reveals an

- integral membrane glycoprotein with multiple evolutionary conserved domains. *Human Molecular Genetics*, 6, 1483-1489.
- 1731 SCHLOSSER, G. 2020. 2.17 Evolution of Hair Cells1. *In:* FRITZSCH, B. (ed.) *The Senses: A Comprehensive Reference (Second Edition)*. Oxford: Elsevier.
- SEBE-PEDROS, A., SAUDEMONT, B., CHOMSKY, E., PLESSIER, F., MAILHE, M. P., RENNO, J., LOE-MIE, Y., LIFSHITZ, A., MUKAMEL, Z., SCHMUTZ, S., NOVAULT, S., STEINMETZ, P. R. H., SPITZ, F., TANAY, A. & MARLOW, H. 2018. Cnidarian Cell Type Diversity and Regulation Revealed by Whole-Organism Single-Cell RNA-Seq. Cell, 173, 1520-+.
- SERRANO-SAIZ, E., LEYVA-DIAZ, E., DE LA CRUZ, E. & HOBERT, O. 2018. BRN3-type POU Homeobox Genes Maintain the Identity of Mature Postmitotic Neurons in Nematodes and Mice. *Curr Biol*, 28, 2813-2823 e2.
- 1741 SILVA, M. A. P. & NAKANISHI, N. 2019. Genotyping of Sea Anemone during Early 1742 Development. *Jove-Journal of Visualized Experiments*.
- SIMIONATO, E., LEDENT, V., RICHARDS, G., THOMAS-CHOLLIER, M., KERNER, P., COORNAERT, D., DEGNAN, B. M. & VERVOORT, M. 2007. Origin and diversification of the basic helix-loop-helix gene family in metazoans: insights from comparative genomics. *Bmc Evolutionary Biology*, 7.
- 1747 SINGLA, C. L. 1975. Statocysts of Hydromedusae. Cell and Tissue Research, 158, 391-407.
- SINGLA, C. L. 1983. Fine-Structure of the Sensory Receptors of Aglantha-Digitale (Hydromedusae, Trachylina). *Cell and Tissue Research*, 231, 415-425.
- SOCK, E., ENDERICH, J., ROSENFELD, M. G. & WEGNER, M. 1996. Identification of the nuclear localization signal of the POU domain protein Tst-1/Oct6. *Journal of Biological Chemistry*, 271, 17512-17518.
- SOLE, M., LENOIR, M., FONTUNO, J. M., DURFORT, M., VAN DER SCHAAR, M. & ANDRE, M. 2016. Evidence of Cnidarians sensitivity to sound after exposure to low frequency noise underwater sources. *Scientific Reports*, 6.
- STEIGELMAN, K. A., LELLI, A., WU, X. D., GAO, J. G., LIN, S., PIONTEK, K.,
 WODARCZYK, C., BOLETTA, A., KIM, H., QIAN, F., GERMINO, G., GELEOC, G.
 S. G., HOLT, J. R. & ZUO, J. 2011. Polycystin-1 Is Required for Stereocilia Structure
 But Not for Mechanotransduction in Inner Ear Hair Cells. *Journal of Neuroscience*, 31,
 12241-12250.
 - TARDENT, P. & SCHMID, V. 1972. Ultrastructure of Mechanoreceptors of Polyp Coryne-Pintneri (Hydrozoa, Athecata). *Experimental Cell Research*, 72, 265-&.
- THOMAS, M. & EDWARDS, N. 1991. Cnidaria: Hydrozoa. *In:* FW, H. (ed.) *Microscopic* anatomy of invertebrates. New York: Wiley-Liss.

- TOURNIERE, O., DOLAN, D., RICHARDS, G. S., SUNAGAR, K., COLUMBUS-SHENKAR,
 Y. Y., MORAN, Y. & RENTZSCH, F. 2020. NvPOU4/Brain3 Functions as a Terminal
 Selector Gene in the Nervous System of the Cnidarian Nematostella vectensis. *Cell Rep*,
 30, 4473-4489 e5.
- VAHAVA, O., MORELL, R., LYNCH, E. D., WEISS, S., KAGAN, M. E., AHITUV, N.,
 MORROW, J. E., LEE, M. K., SKVORAK, A. B., MORTON, C. C., BLUMENFELD,
 A., FRYDMAN, M., FRIEDMAN, T. B., KING, M. C. & AVRAHAM, K. B. 1998.
- Mutation in transcription factor POU4F3 associated with inherited progressive hearing loss in humans. *Science*, 279, 1950-1954.

- WATSON, G. M., MIRE, P. & HUDSON, R. R. 1997. Hair bundles of sea anemones as a model system for vertebrate hair bundles. *Hearing Research*, 107, 53-66.
- WATSON, G. M., MIRE, P. & KINLER, K. M. 2009. Mechanosensitivity in the model sea anemone Nematostella vectensis. *Marine Biology (Berlin)*, 156, 2129-2137.
- WATSON, G. M., PHAM, L., GRAUGNARD, E. M. & MIRE, P. 2008. Cadherin 23-like
 polypeptide in hair bundle mechanoreceptors of sea anemones. *Journal of Comparative Physiology A Sensory Neural and Behavioral Physiology*, 194, 811-820.
- WATSON, G. M. & ROBERTS, J. 1995. Chemoreceptor-Mediated Polymerization and Depolymerization of Actin in Hair Bundles of Sea-Anemones. *Cell Motility and the Cytoskeleton*, 30, 208-220.
- WESTFALL, J. A. 2004. Neural pathways and innervation of cnidocytes in tentacles of sea anemones. *Hydrobiologia*, 530-, 117-121.
- WOLENSKI, F. S., BRADHAM, C. A., FINNERTY, J. R. & GILMORE, T. D. 2013. NF-kappa B is required for cnidocyte development in the sea anemone Nematostella vectensis. Developmental Biology, 373, 205-215.
- XIANG, M., GAN, L., LI, D., CHEN, Z. Y., ZHOU, L., O'MALLEY, B. W., JR., KLEIN, W. &
 NATHANS, J. 1997a. Essential role of POU-domain factor Brn-3c in auditory and
 vestibular hair cell development. *Proc Natl Acad Sci U S A*, 94, 9445-50.
- XIANG, M., GAN, L., LI, D., ZHOU, L., CHEN, Z. Y., WAGNER, D., O'MALLEY, B. W., JR.,
 KLEIN, W. & NATHANS, J. 1997b. Role of the Brn-3 family of POU-domain genes in
 the development of the auditory/vestibular, somatosensory, and visual systems. *Cold* Spring Harb Symp Quant Biol, 62, 325-36.

1797 1798

1799

1800

1801

1802

1803

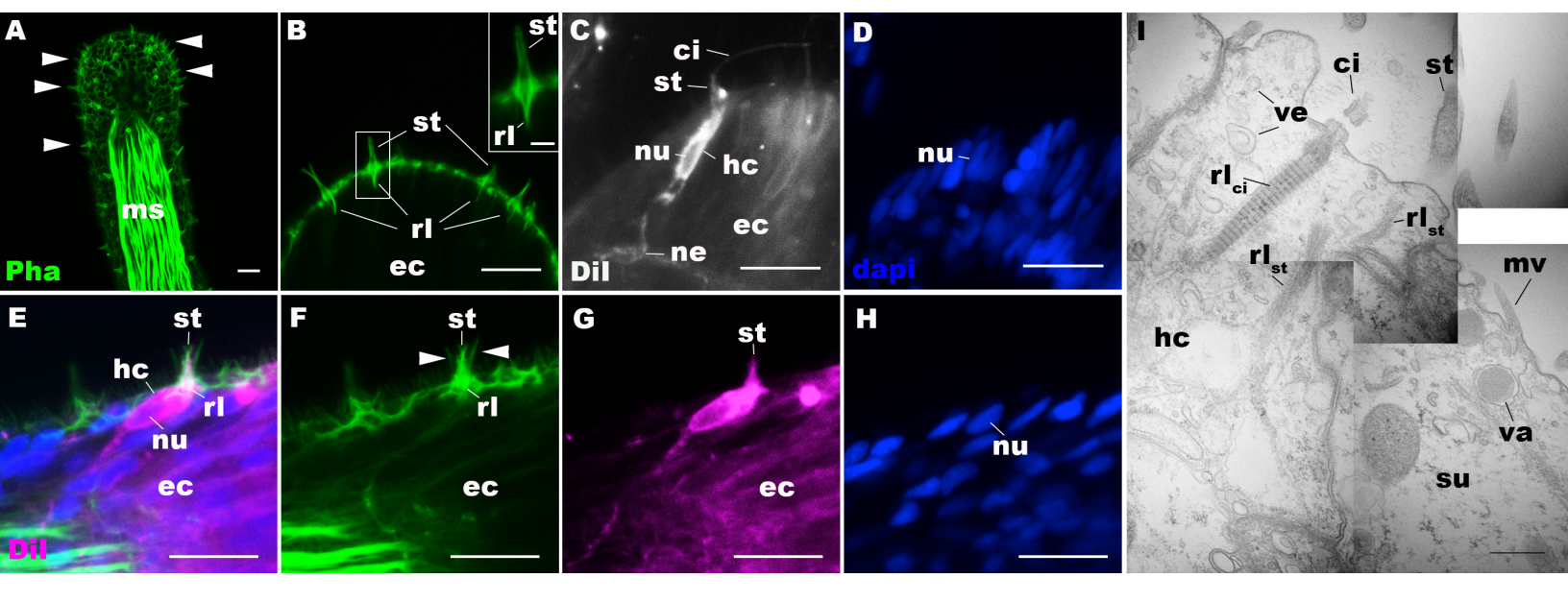
1804

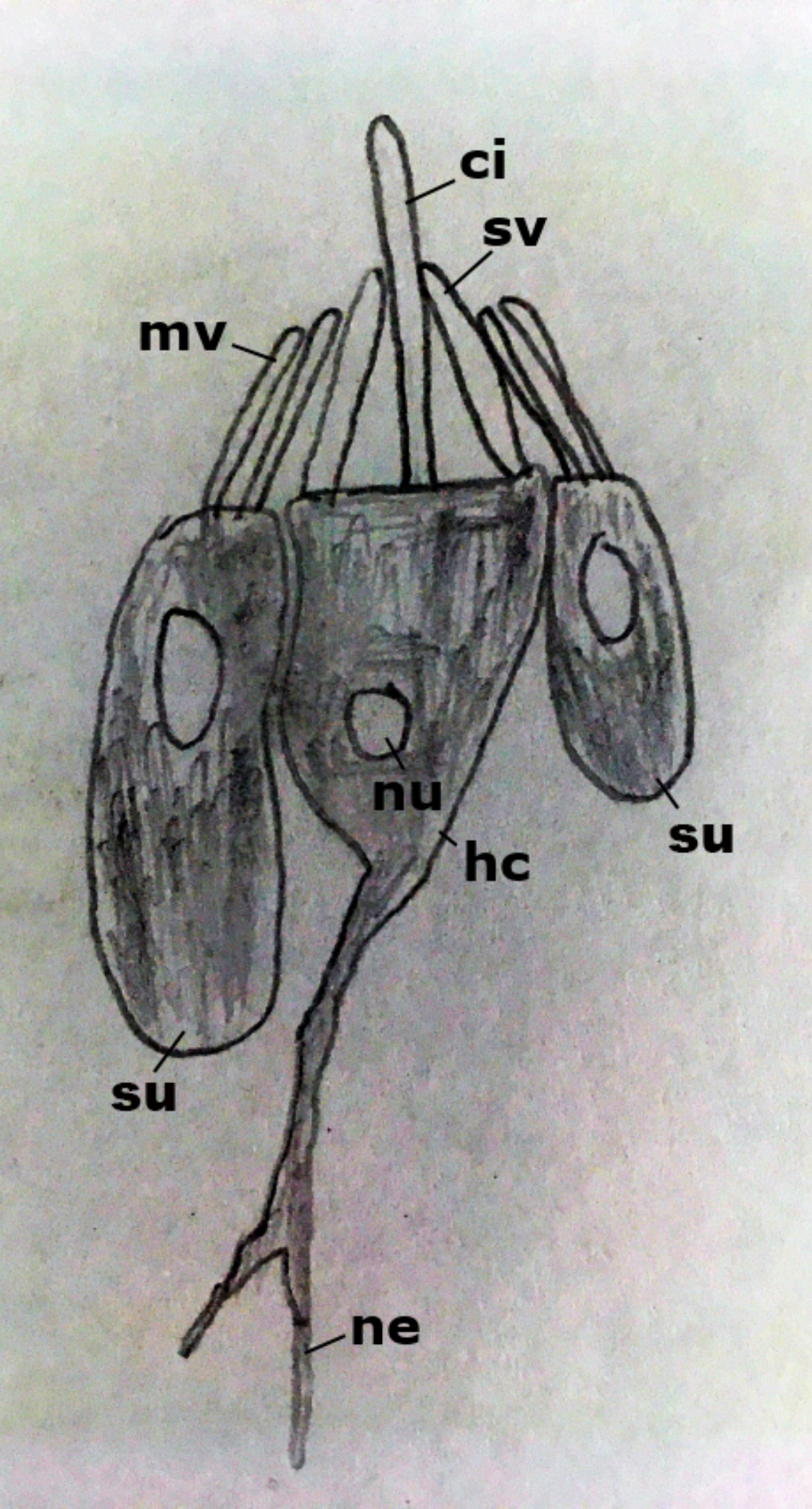
1805

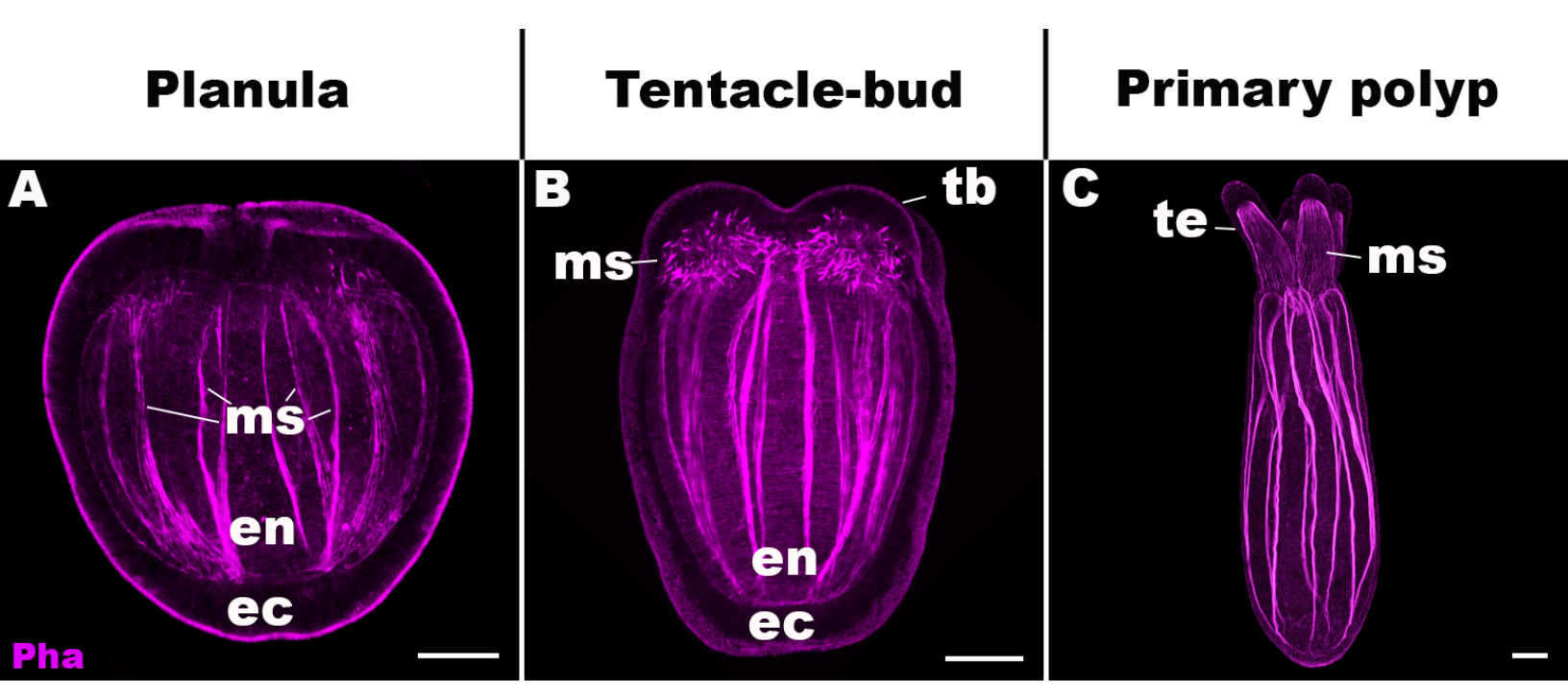
1806

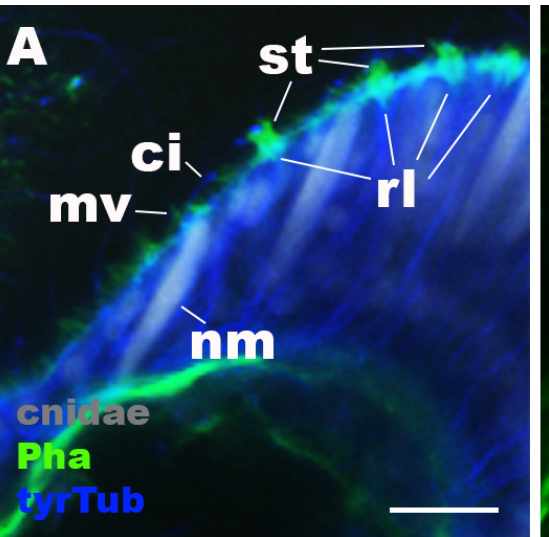
- XIANG, M. Q., GAN, L., ZHOU, L. J., KLEIN, W. H. & NATHANS, J. 1996. Targeted deletion of the mouse POU domain gene Brn-3a causes a selective loss of neurons in the brainstem and trigeminal ganglion, uncoordinated limb movement, and impaired suckling. *Proceedings of the National Academy of Sciences of the United States of America*, 93, 11950-11955.
- XIANG, M. Q., GAO, W. Q., HASSON, T. & SHIN, J. J. 1998. Requirement for Brn-3c in maturation and survival, but not in fate determination of inner ear hair cells. *Development*, 125, 3935-3946.
- YU, H. Z. V., TAO, L. T., LLAMAS, J., WANG, X. Z., NGUYEN, J. D., TRECEK, T. & SEGIL, N. 2021. POU4F3 pioneer activity enables ATOH1 to drive diverse mechanoreceptor differentiation through a feed-forward epigenetic mechanism. *Proceedings of the National Academy of Sciences of the United States of America*, 118.
- ZAPATA, F., GOETZ, F. E., SMITH, S. A., HOWISON, M., SIEBERT, S., CHURCH, S. H.,
 SANDERS, S. M., AMES, C. L., MCFADDEN, C. S., FRANCE, S. C., DALY, M.,
 COLLINS, A. G., HADDOCK, S. H. D., DUNN, C. W. & CARTWRIGHT, P. 2015.
 Phylogenomic Analyses Support Traditional Relationships within Cnidaria. *Plos One*, 10.
- ZENKERT, C., TAKAHASHI, T., DIESNER, M. O. & OZBEK, S. 2011. Morphological and Molecular Analysis of the Nematostella vectensis Cnidom. *Plos One*, 6.
- ZHANG, Y., LIU, T., MEYER, C. A., EECKHOUTE, J., JOHNSON, D. S., BERNSTEIN, B. E.,
 NUSSBAUM, C., MYERS, R. M., BROWN, M., LI, W. & LIU, X. S. 2008. Model based Analysis of ChIP-Seq (MACS). *Genome Biology*, 9.
- ZHU, A. Q., IBRAHIM, J. G. & LOVE, M. I. 2019. Heavy-tailed prior distributions for sequence count data: removing the noise and preserving large differences. *Bioinformatics*, 35, 2084-2092.

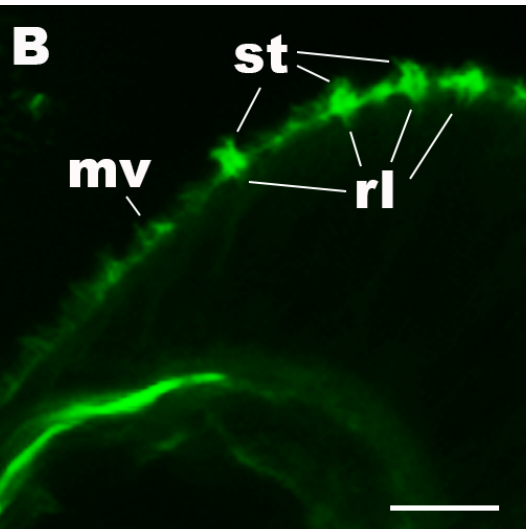
- 1820
- 1821 Supplementary Files:
- Supplementary File 1: List of 4,188 candidate POU-IV downstream target genes.
- 1823 Supplementary File 2: List of 577 genes significantly downregulated in NvPOU4 mutants
- relative to their siblings.
- 1825 Supplementary File 3: List of 657 genes significantly upregulated in NvPOU4 mutants
- relative to their siblings.
- 1827 Supplementary File 4: List of Gene Ontology terms overrepresented in genes
- downregulated in NvPOU4 mutants relative to their siblings.
- 1829 Supplementary File 5: List of Gene Ontology terms overrepresented in genes upregulated
- in NvPOU4 mutants relative to their siblings.
- 1831 Supplementary File 6: List of 293 POU-IV-activated genes.
- 1832 Supplementary File 7: List of 178 POU-IV-repressed genes.
- 1833 Supplementary File 8: List of Gene Ontology terms overrepresented in POU-IV-activated
- 1834 **genes.**
- Supplementary File 9: List of POU-IV downstream target genes represented in the adult
- 1836 metacell c79 (hair cell).
- Supplementary File 10: List of Gene Ontology terms overrepresented in POU-IV-activated
- genes represented in the adult metacell c79 (hair cell).
- 1839 Supplementary File 11: List of POU-IV downstream target genes represented in the
- 1840 cnidocyte metacell c8.
- Supplementary File 12: List of Gene Ontology terms overrepresented in POU-IV-repressed
- genes represented in the cnidocyte metacell c8.
- 1843 Supplementary File 13: Lists of POU-IV downstream target genes represented in POU-IV
- positive adult metacells c63, c64, c65, c66, c75, c76, c100, c101 and c102.
- Supplementary File 14: List of GPCR-encoding genes in the adult metacell c79 (hair cell).
- Supplementary File 15: List of gene specific primer sequences used to amplify *polycystin 1*
- 1847 **cDNA**.

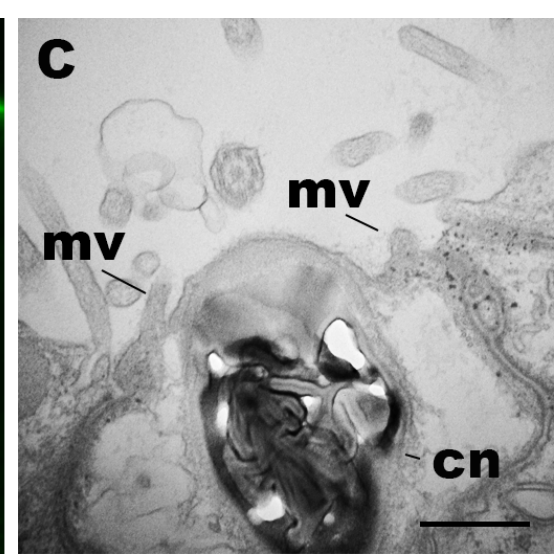












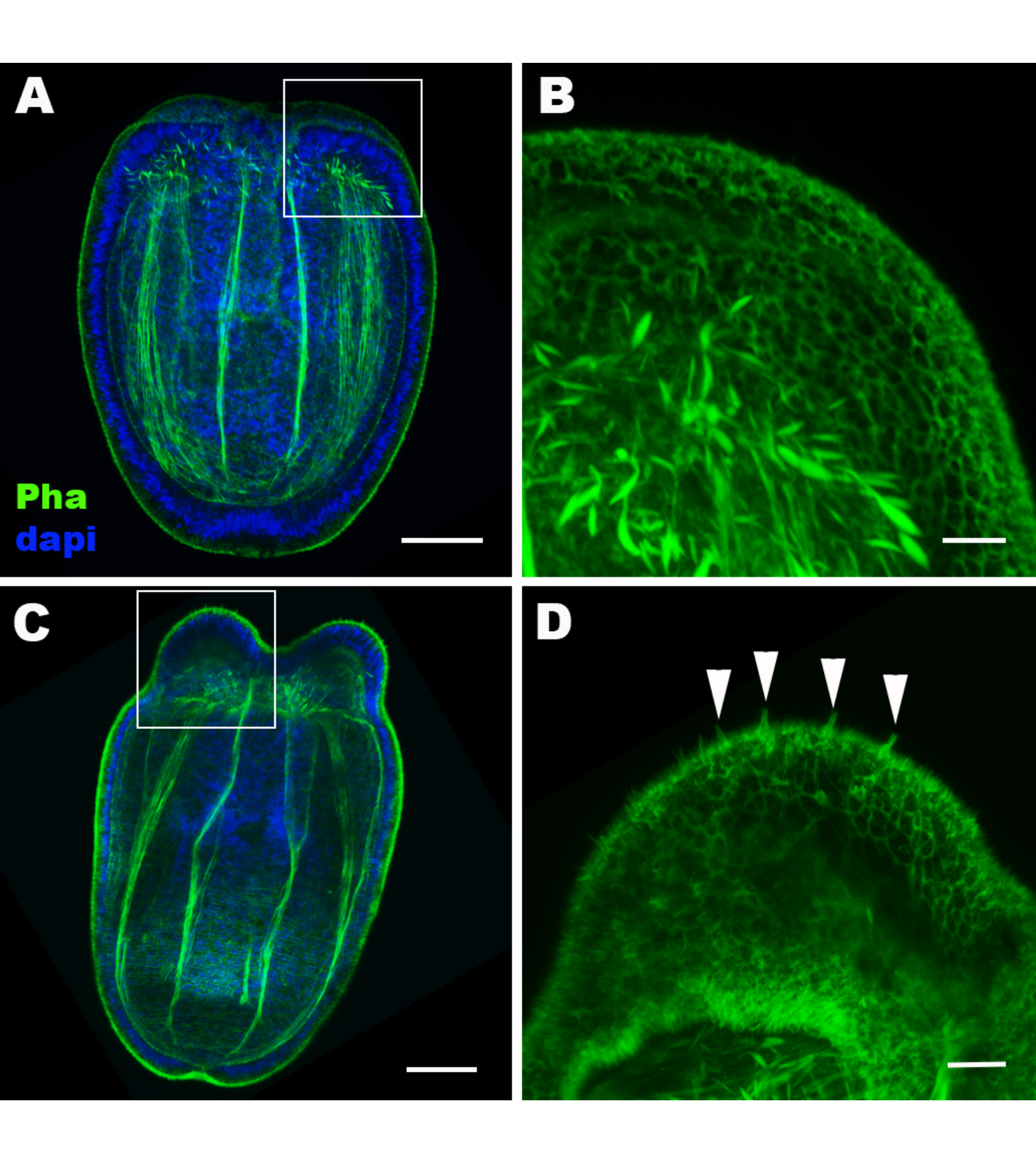
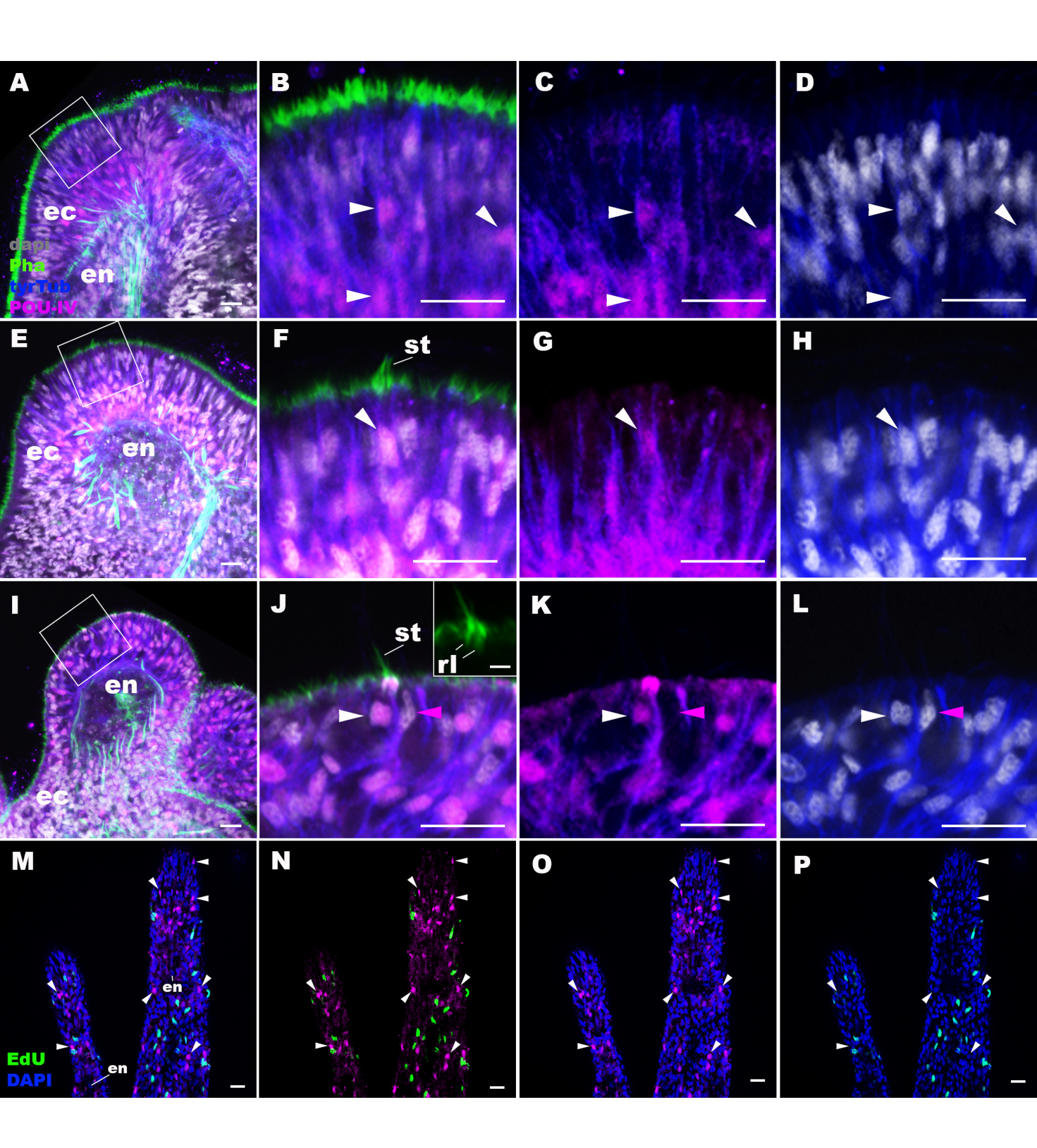
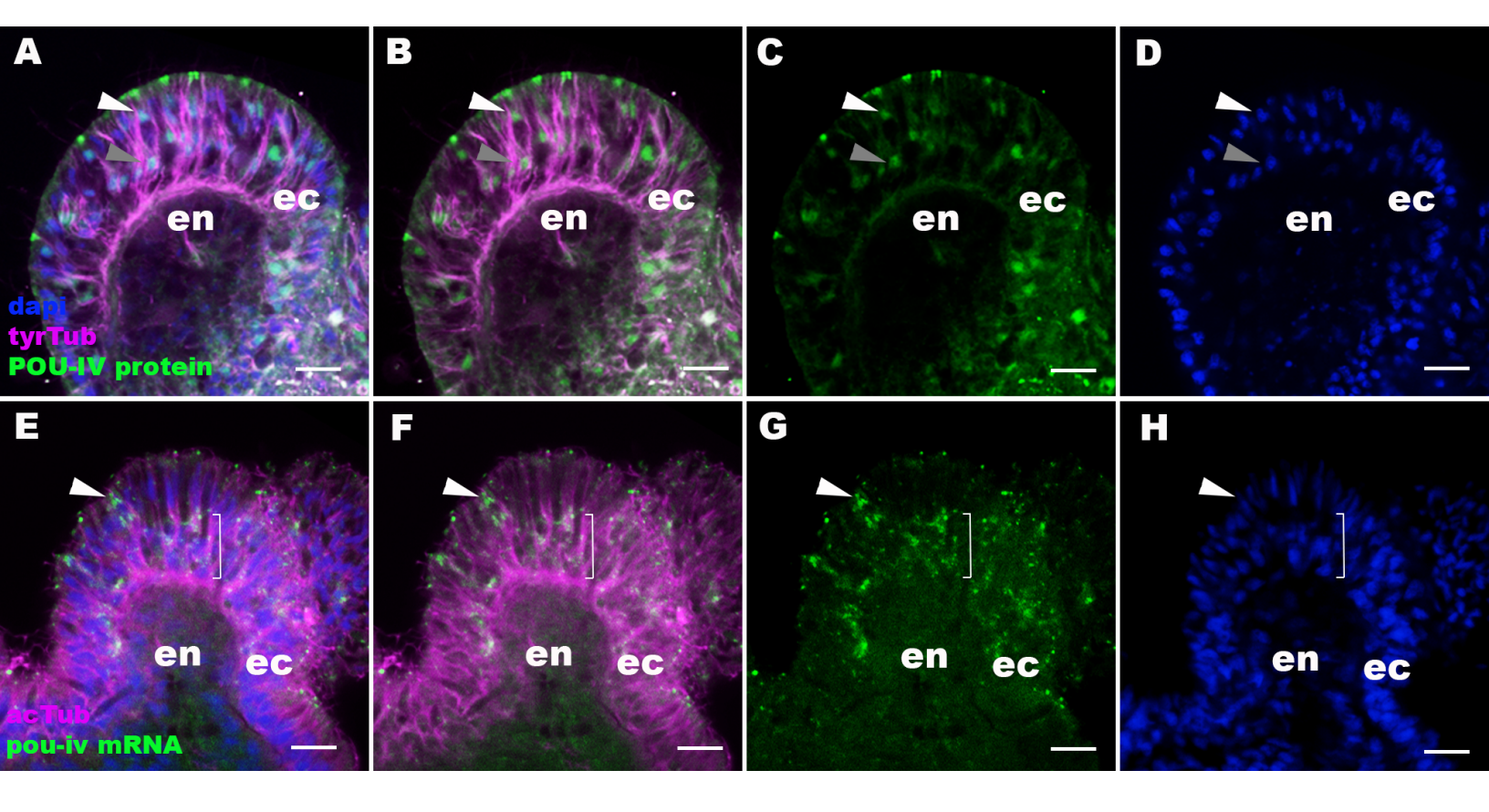
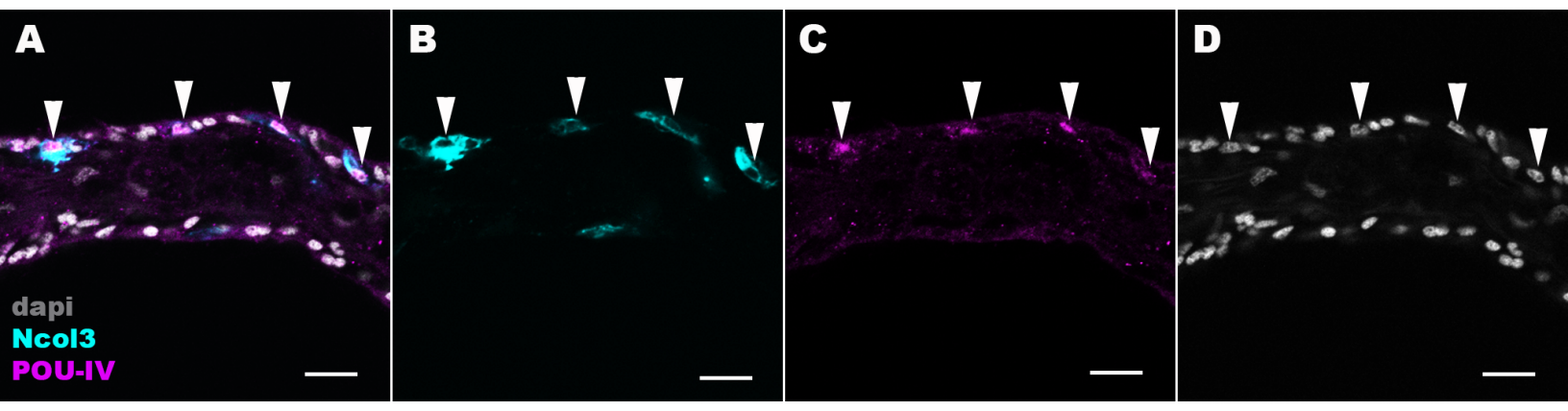
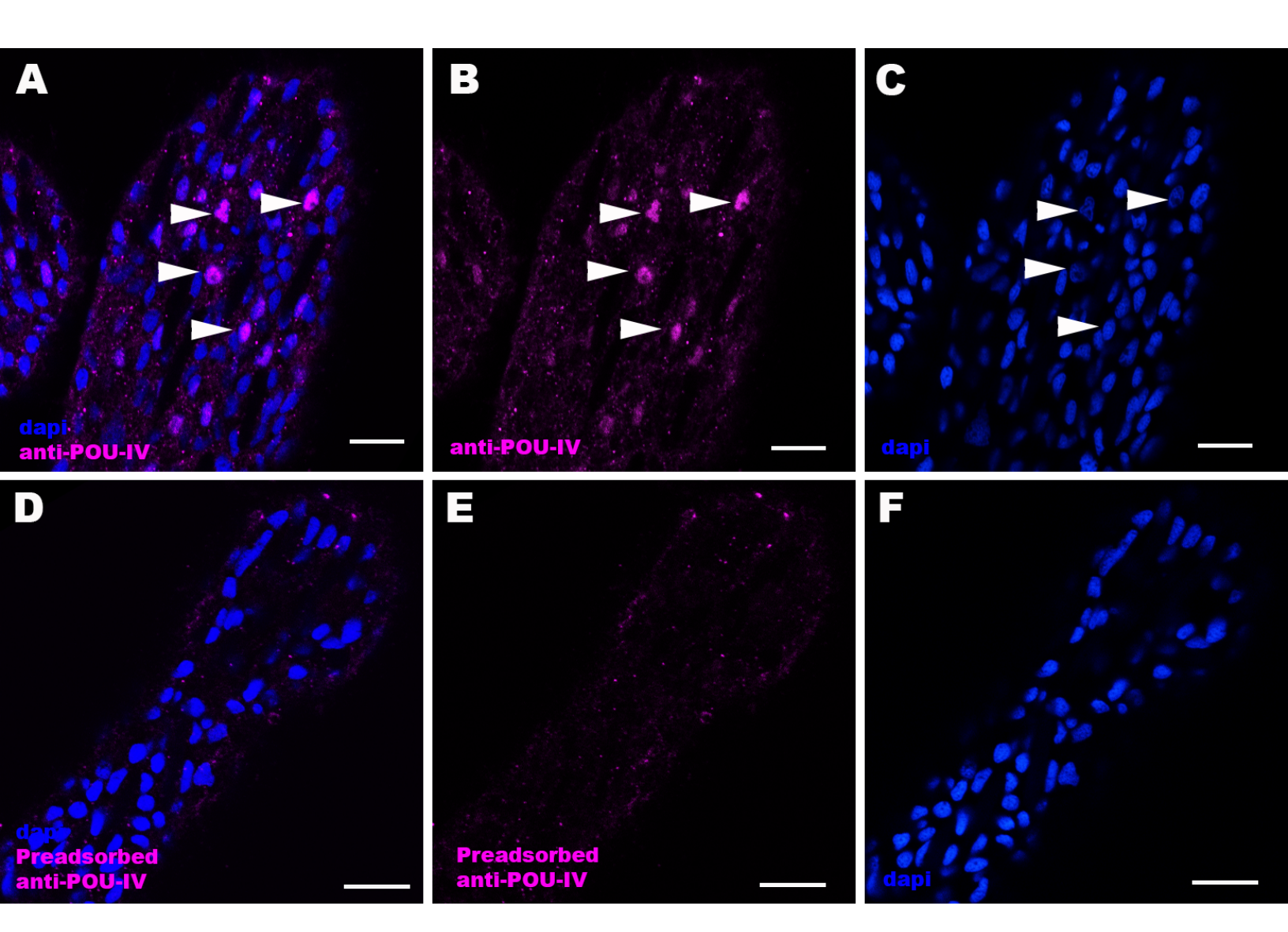


Figure 2

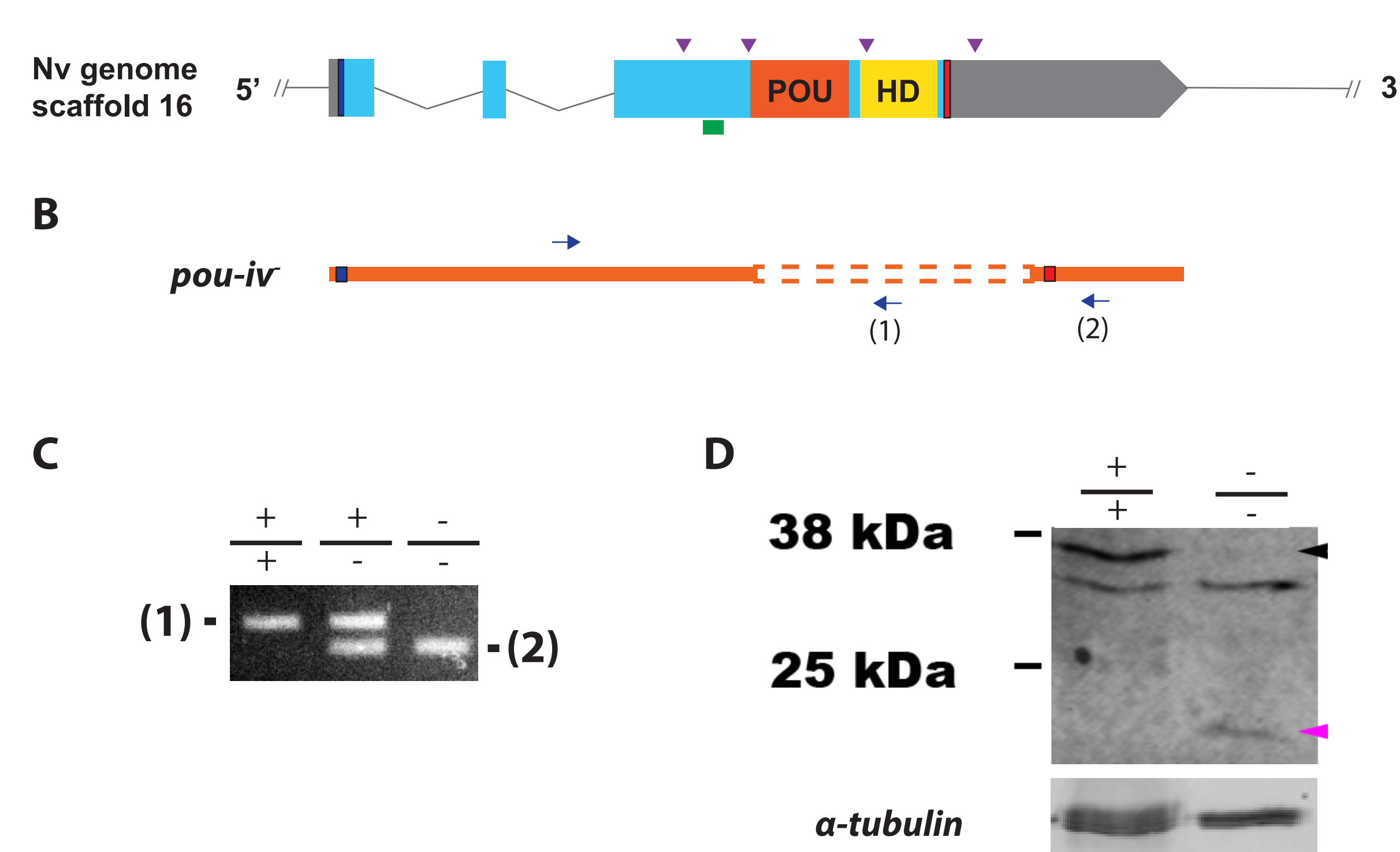


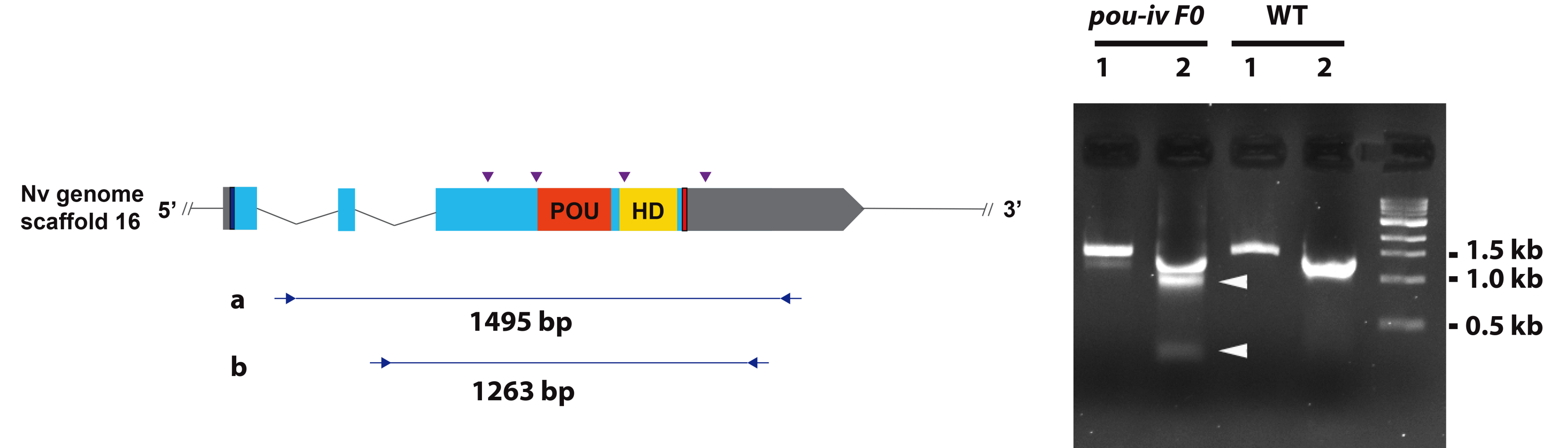




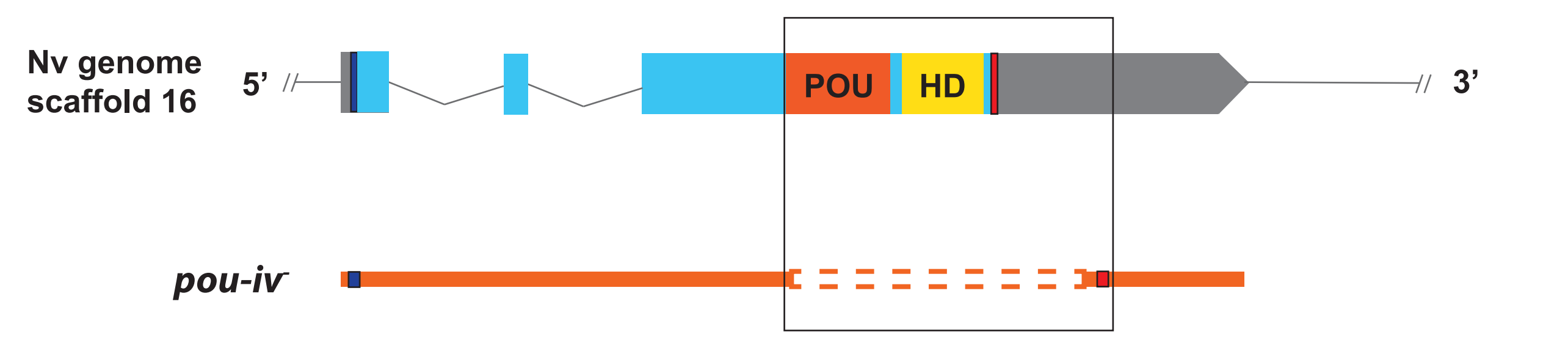


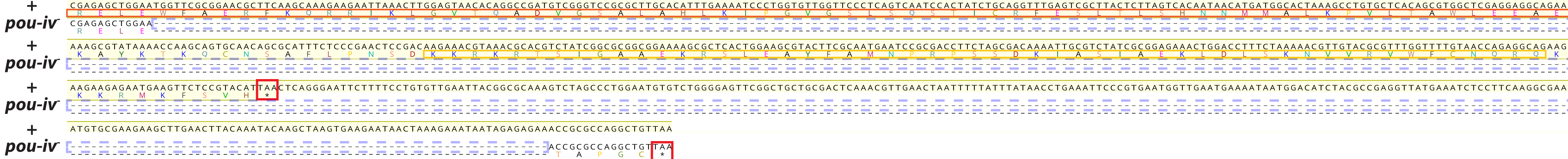
A

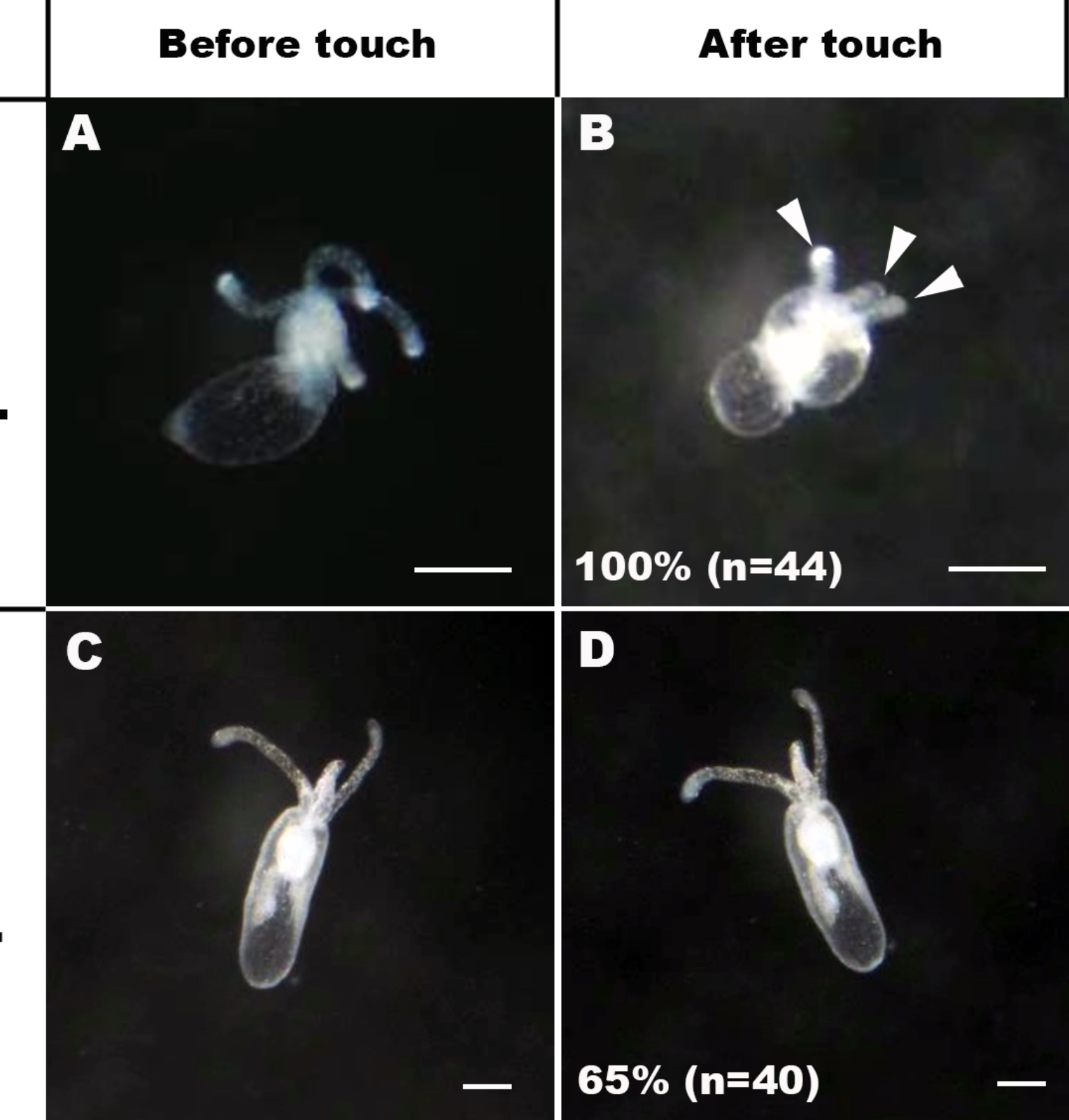


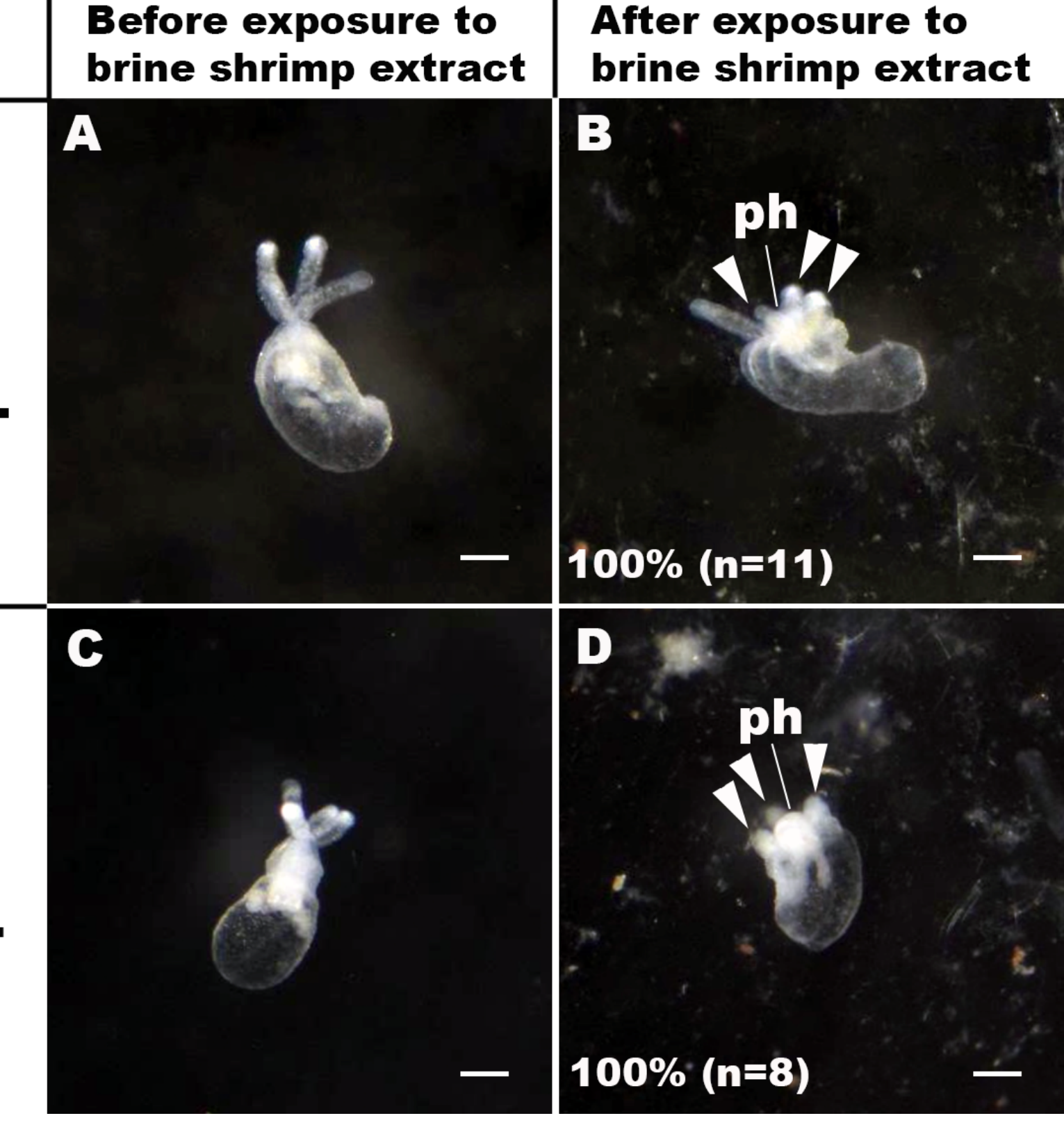


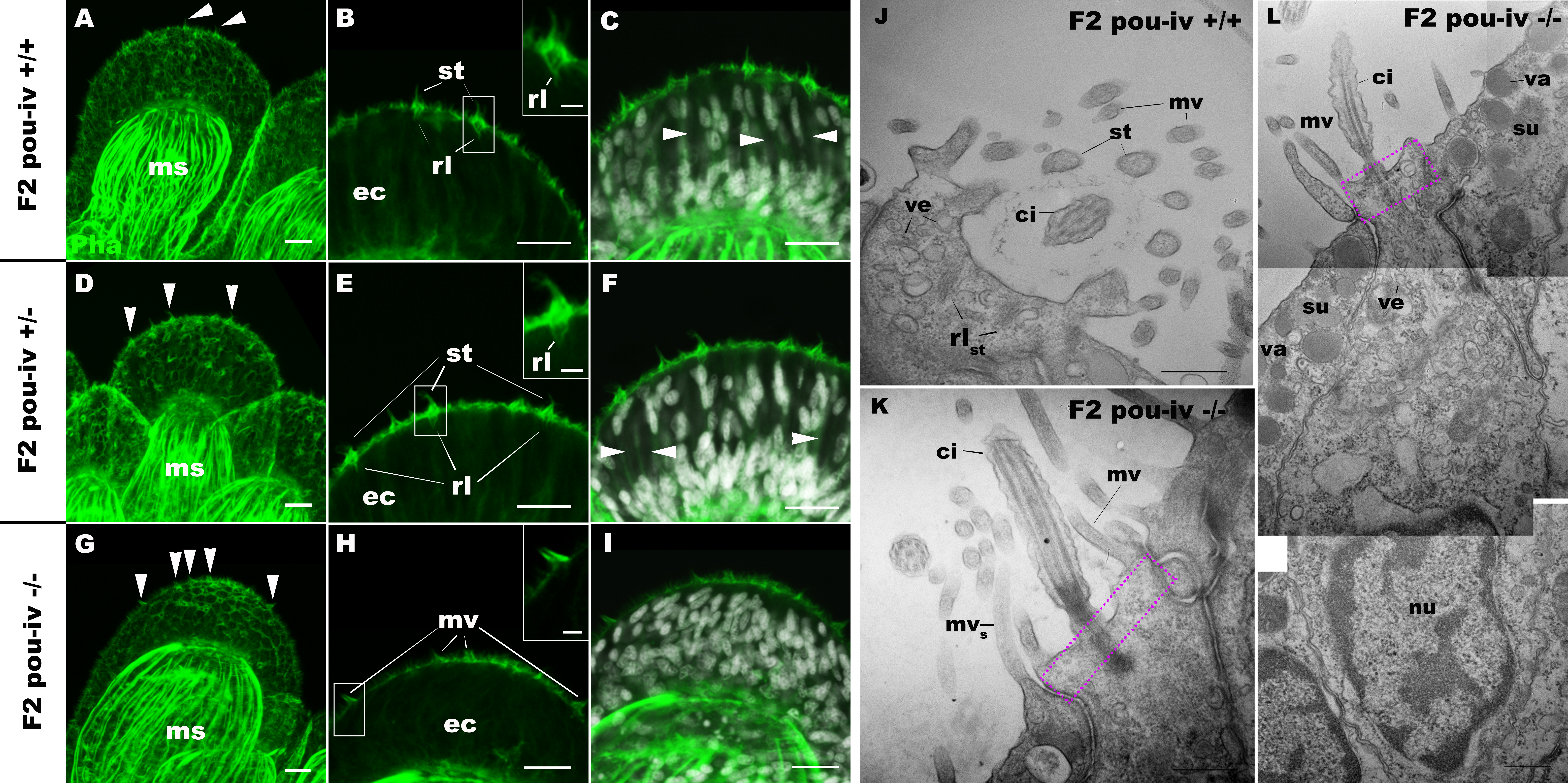












F2 pou-iv +/+

B

nu

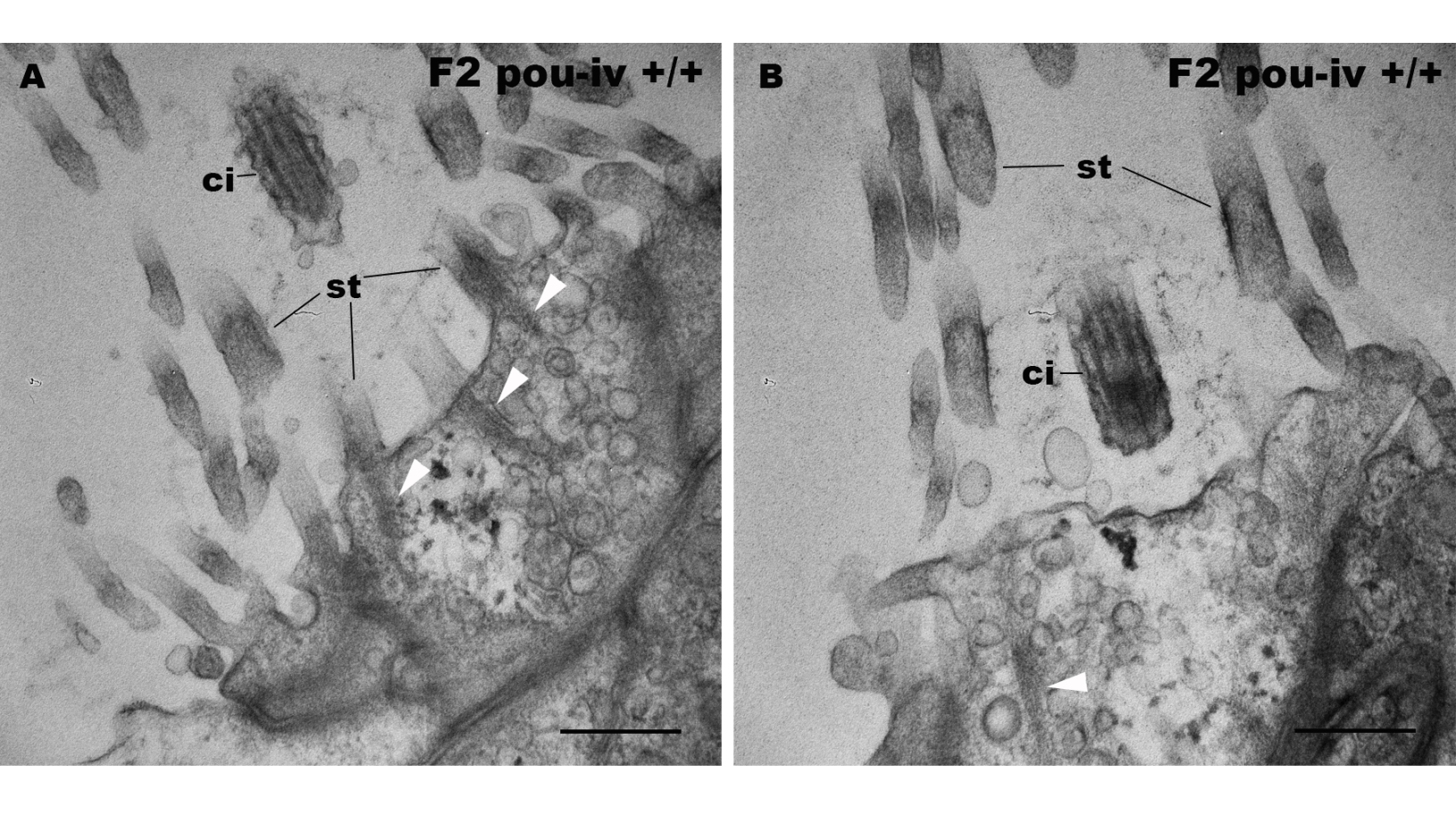
ec

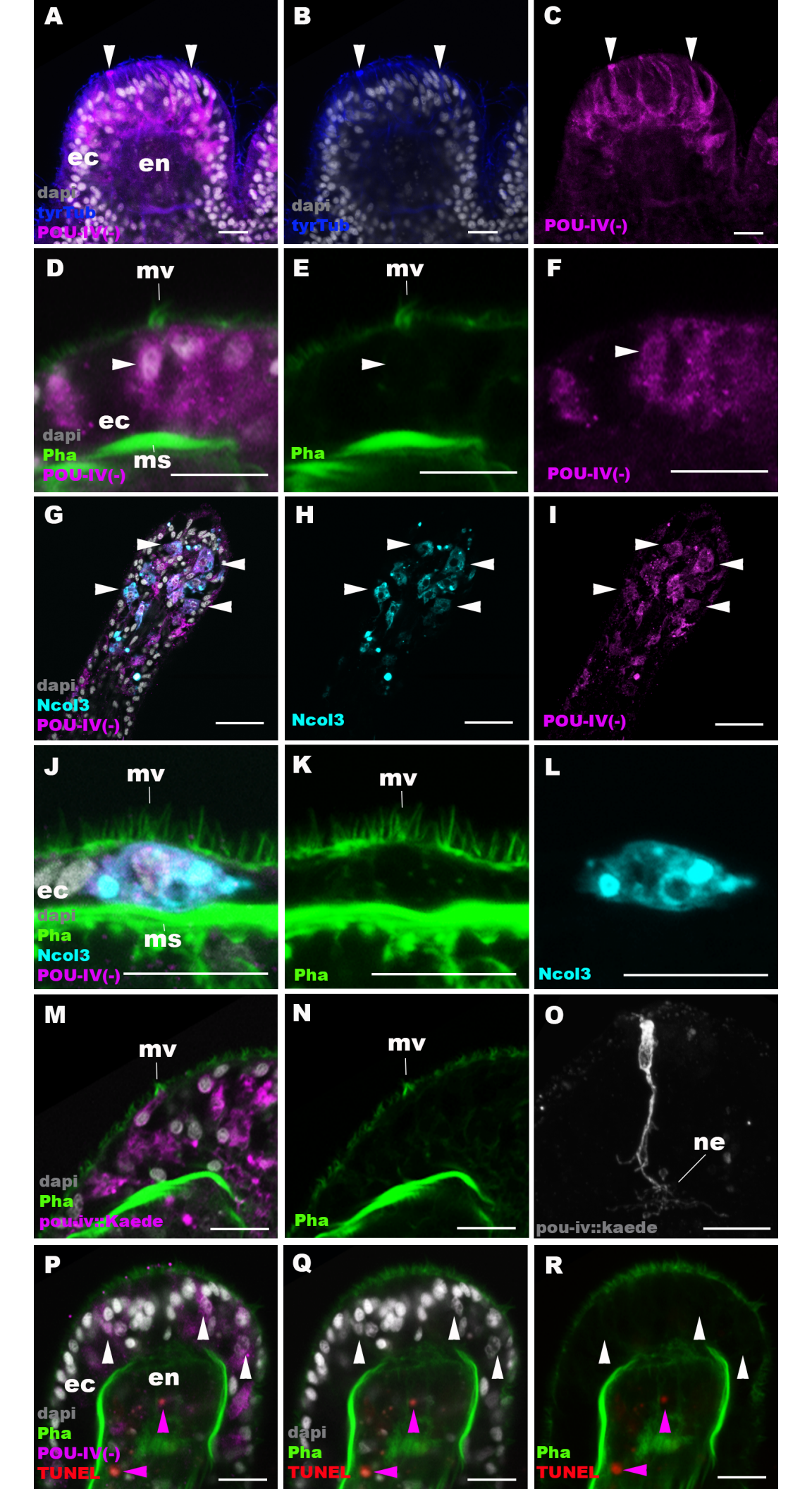
nu

ms

mg

mg







nv

ve

rl

